# IMPACT OF CLIMATE CHANGE ON FLOW REGIME IN HIMALAYAN BASINS, NEPAL



A THESIS SUBMITTED TO THE

## CENTRAL DEPARTMENT OF HYDROLOGY AND METEOROLOGY

## INSTITUTE OF SCIENCE AND TECHNOLOGY

## TRIBHUVAN UNIVERSITY

NEPAL

### FOR THE AWARD OF

### DOCTOR OF PHILOSOPHY

### IN HYDROLOGY AND METEOROLOGY

BY

## TIRTHA RAJ ADHIKARI

## JULY, 2014

## DECLARATION

This thesis entitled " **IMPACT OF CLIMATE CHANGE ON FLOW REGIME IN HIMALAYAN BASINS, NEPAL** " which is being submitted by me to the Central Department of Hydrology and Meteorology, Institute of Science and Technology (IOST), Tribhuvan University, Nepal for the award of the degree of Doctor of Philosophy (Ph.D.), is a research work carried out by me under the supervision of Prof. Dr. Lochan Prasad Devkota, Central Department of Hydrology and Meteorology, Tribhuvan University. This research is original and has not been submitted earlier in part or full in this or any university or institute, here or elsewhere for the award of any degree.

San Allockana

Tirtha Raj Adhikari (Researcher)

## RECOMMENDATION

This is to recommend that **Mr. Tirtha Raj Adhikari** has carried out research entitled "**IMPACT OF CLIMATE CHANGE ON FLOW REGIME IN HIMALAYAN BASINS, NEPAL**" for the award of Doctor of Philosophy (Ph.D.) in **Hydro-Meteorology** under my supervision. To my knowledge this work has not been submitted for any other degree.

He has fulfilled all the requirement laid down by the Institute of Science and Technology (IOST), Tribhuvan University, Kirtipur for the submission of the thesis for the award of Ph.D. degree.



### Prof. Dr. Lochan Prasad Devkota

### Supervisor

### (Head)

Central Department of Hydrology and Meteorology

Tribhuvan University

Kirtipur, Kathmandu,

Nepal

JULY, 2014

## **LETTER OF APPROVAL**

Date: 07/07/2014

On the recommendation of **Prof. Dr. Lochan Prasad Devkota**, this Ph.D. thesis submitted by **Mr. Tirtha Raj Adhikari** entitled "**IMPACT OF CLIMATE CHANGE ON FLOW REGIME IN HIMALAYAN BASINS, NEPAL**" is forwarded by Central Department Research Committee (CDCR) to the Dean, Institute of Science and Technology, Tribhuvan University, Nepal.



**Prof. Dr. Lochan Prasad Devkota** Head Central Department of Hydrology and Meteorology Tribhuvan University Kirtipur, Kathmandu, Nepal

### ACKNOWLEDGEMENTS

I express my gratitude to Professor Lochan Prasad Devkota, my Supervisor and Head of the Central Department of Hydrology and Meteorology (CDHM) for his continuous support, encouragement and guidance in both technical and analytical part of my research work. I would like to acknowledge Swami Shivalingam Kiran Sankar Yogacharya, the former Director General of Department of Hydrology and Meteorology (DHM), Nepal for his valuable suggestions during my research work. I am also thankful to Dr. Dilip Kumar Gautam from Regional Integrated Multi-Hazard Early Warning System (RIMES) Thailand, Mr. Om Ratna Bajracharya former joint secretary (DHM) and Dr. Sushil Khatiwada for editing this thesis. I would also like to heartily acknowledge Dr. Jan Seibert and the Uppsala University's Department of Earth Hydrology for supporting the software HBV- Light 3.0. I would like to acknowledge the Data Access Integration (DAI, see http://quebec.ccsn.ca/DAI/) Team for providing the data and technical support. The DAI data download gateway is the collaboration among the Global Environmental and Climate Change Centre (GEC3), the Adaptation and Impacts Research Division (AIRD) of Environment Canada, and the Drought Research Initiative (DRI). Similarly, I deeply appreciate the help from Dr. Rishi Ram Sharma Director General of DHM, Government of Nepal for providing necessary hydrological and meteorological data. I would like to acknowledge Mr. Deo Raj Gurung (Remote Sensing Expert) from ICIMOD-MENRIS for providing glacier data presented in this study. I really want to thank Nepal Academy of Science Technology (NAST) for providing me research grant on conducting this research. Finally, I would like to express thanks to Dr. Madan Sigdel Lecturer, Mr. Damodar Bagale Lecturer, Head of the Administration, Mr. Subash Chandra Kandel, Mr. Madan Shrestha of CDHM, Mr. Suresh Chand Pradhan, Hydrologist DHM, Mr. Achut Parajuli and Mr. Bikash Chandra Bhattari for supporting me in different ways in this research work. Without the support from faculty members and staffs of CDHM, I couldn't have successfully completed this research work in time.

The Rockson

(Tirtha Raj Adhikari) July, 2014

### ABSTRACT

This research studied the hydrological regime of three glacierized river basins in Khumbu, Langtang and Annapurna regions of Nepal using the Hydraologiska Byrans Vattenbalansavde (HBV), HVB-light 3.0 model. Future scenario of discharge is also studied using downscaled climate data derived from statistical downscaling method. General Circulation Models (GCMs) successfully simulate future climate variability and climate change on a global scale; however, poor spatial resolution constrains their application for impact studies at a regional or a local level. The dynamically downscaled precipitation and temperature data from Coupled Global Circulation Model 3 (CGCM3) was used for the climate projection, under A2 and A1B SRES scenarios. In addition, the observed historical temperature, precipitation and discharge data were collected from 14 different hydro-metrological locations for the implementation of this studies, which include watershed and hydro-meteorological characteristics, trends analysis and water balance computation. The simulated precipitation and temperature were corrected for bias before implementing in the HVB-light 3.0 conceptual rainfall-runoff model to predict the flow regime, in which Groups Algorithms Programming (GAP) optimization approach and then calibration were used to obtain several parameter sets which were finally reproduced as observed stream flow. Except in summer, the analysis showed that the increasing trends in annual as well as seasonal precipitations during the period 2001 - 2060 for both A2 and A1B scenarios over three basins under investigation. In these river basins, the model projected warmer days in every seasons of entire period from 2001 to 2060 for both A1B and A2 scenarios. These warming trends are higher in maximum than in minimum temperatures throughout the year, indicating increasing trend of daily temperature range due to recent global warming phenomenon. Furthermore, there are decreasing trends in summer discharge in Langtang Khola (Langtang region) which is increasing in Modi Khola (Annapurna region) as well as Dudh Koshi (Khumbu region) river basin. The flow regime is more pronounced during later parts of the future decades than during earlier parts in all basins. The annual water surplus of 1419 mm, 177 mm and 49 mm are observed in Annapurna, Langtang and Khumbu region, respectively.

KEYWORDS: Temperature, Precipitation, Water discharge, Water balance and global warming.

## LIST OF ACRONYMS AND ABBREVIATIONS

%	Percentage
°C	Degree Celsius
AM	Analogue Downscaling Method
amsl	Average Mean Sea Level
ArcGIS	Arc Geographical Information System
ArcSWAT	The Arcmap Integrated SWAT Hydrological Model
ASD	Automated Statistical Downscaling
BCAS	Bangladesh Centre for Advance Studies
BETA	Parameter that determines the relative contribution to runoff from rain
	or snowmelt
CBS	Central Bureau of Statistics
CCCM	Canadian Climate Centre Model
CGCM3	Coupled Global Climate Model
CMIP5	Coupled Model Intercomparison Project Phase 5
CNRC	Children's Nutrition Research Center
CNRCC	China National Report on Climate Change
DEM	Digital Elevation Map
DHM	Department Of Hydrology and Meteorology
DJF	December January February
DRO	Direct Runoff
EA	Actual Evaporation
EI	Evapo transpiration
EL	Lake Evaporation
ENSO	El Nino Southern Oscillation
EP	Potential Evaporation
FAO	Food and Agriculture Organization (of the United Nations)
FC	Maximum Soil Moisture Storage
GAP	Groups Algorithms Programming
GCM	General Circulation Model
GEN	Glaciological Expedition in Nepal
GFDL	Geophysical Fluid Dynamics Laboratory

GLOF	Glacial Lake Outburst Flood
HadCM3	Hadley Centre Coupled Model
HBV	Hydraologiska Byrans Vattenbalansavde
HEC-HMS	Hydrologic Engineering Center - Hydrological Modeling System
HFAM	Hydrocomp Forecast and Analysis Modeling
НКН	Hindu Kush Himalayan Region
hPa	Hectopascal
HSPF	Hydrologic Simulation Program-FORTRAN
HVB	Hydrologiska Byrans Vattenbalansavdelning
HYSIM	Hydrological Simulation Model
ICIMOD	International Center for Integrated Mountain Development
IHACRES	Identification of Unit Hydrograph And Component Flows from
	Rainfalls Evaporation and Stream flow data
IHMS	Integrated Hydrological Modeling System
IN	In Infiltration
IPCC	Intergovernmental Panel on Climate Change
ISMH	Swedish Meteorological and Hydrological Institute
JJAS	June July August September
Κ	Storage coefficient
Ki	Recession coefficient (Day-1)
km	kilometer
km <sup>2</sup>	square kilometer
km <sup>3</sup>	cubic kilometer
LOCI	local intensity scaling
LP	Soil moisture value above ET
LZ	Lower Zone reservoir
m	meter
m/year	meter per year
m <sup>3</sup> /s	cubic meter per second
MAM	March April May
Met	Meteorology
mm	millimeter
mm Day <sup>-1</sup>	millimeter per day
mm $y^{-1}$	millimeter per year Day

MOFRCB	Multi-Objective Fuzzy-Rule-Based Classification
MOS	Model Output Statistics
Ν	North
NCAR	National Center for Atmospheric Research
NCEP	National Center for Atmospheric Prediction
NOPEX	Northern hemisphere climate-Processes land-surface Experiment
ON	October November
PDD	Positive Degree Day
PER Max	Percolation to lower zone (Mm Day-1)
PERC	Percapacity
PET	Potential Evapo-transpiration
PRECIS	Providing Regional Climates for Impacts Studies
PRMS	Precipitation-Runoff Modeling System
Q	Outflow
Q filled	Filled discharge
Q obs	Observed discharge
Q sim	Simulated discharge
Q1	Base flow lower
Qi	Runoff component (Mm Day-1)
Qo	Direct runoff from upper reservoir
R	Seepage
RCMs	Regional Climatic Models
RF	Rainfall
RO	Runoff
ROtotal	computed total monthly runoff ROtotal
S	South
S	storage
SCA	Snow Covered Area
SDSM	Statistical Downscaling Model
SF	Snow Fall
SLZ	Storage in Lower Zone (Mm)
SM	Compound Soil Moisture Routine
SMHI	Swedish Meteorological and Hydrological Institute
SRM	Snow Melt Runoff

SRM	Snow Melt Runoff Model
SRTM	Shuttle Radar Topography Mission
SSARR	Stream flow Synthesis and Reservoir Regulation
S <sub>sm</sub>	Computed Soil Moisture Storage
SUZ	Storage in Upper Zone (Mm) and Has No Upper Limit
SVD	Singular Value Decomposition
SWAT	Soil and Water Assessment Tool
SWAT	Soil and Water assessment Tool)
SWMM	Strom Water Management Model)
Т	Time
Tmax	Maximum Temperature
Tmean	Mean Temperature
Tmin	Minimum Temperature
TRMM	Tropical Rainfall Measuring Mission
TT	Threshold Temperature
UBC	University of British Columbia
UK	United Kingdom
UNDP	United Nations Development Programme
UNEP	United Nations Environment Programme
UNFCCC	United Nations Framework Convention on Climate Change
UZ	Upper Zone Reservoir
UZL	Threshold P
WATBAL	Water balance Previously CLIRUN
WATFLOOD	Waterloo Hydrological and Flood Forecasting System
WMO	World Meteorological Organization
WRI	World Resources Institute
WWF	World Wildlife Fund

## LIST OF TABLES

<b>Table 3.3-1</b> Collection of daily Hydrological and meteorological data
<b>Table 3.3-2</b> Data Consistency and Homogeneity checking
<b>Table 3.4-1</b> Comparisons of average annual precipitation in three basins
<b>Table 3.4-2</b> The value of Coefficient of determination R <sup>2</sup> 41
Table 3.4-3 Predictors used in this research
<b>Table 3.5-1</b> HBV-Light-3.0 Model Calibration and Validation of three study area45
<b>Table 3.6-1</b> Statistically significant trends of hydrological stations         46
<b>Table 3.7-1</b> Scatter plot between observed discharge verses model discharge
<b>Table 3.8-1</b> Comparison of potential evapotranspiration in three stations
<b>Table 3.8-2</b> Comparison AE, WD and WS in three stations of Nepal Himalaya58
<b>Table 4.1-1</b> Precipitation distribution of the three river basins
<b>Table 4.2-1</b> Annual average precipitation trends with elevation
<b>Table 4.3-1</b> Observed significance and trend of temperature record
<b>Table 4.5-1</b> Yearly trend of observed discharge data
<b>Table 5.1-1</b> Base line temperature trend for calibration period
<b>Table 5.1-2</b> Base line temperature trend for A2 scenario    73
<b>Table 5.1-3</b> Maximum temperature trend for A2 scenario
<b>Table 5.1</b> -4 Minimum temperature trend for A2 scenario         Scenario         74
<b>Table 5.1-5</b> Mean temperature trend for A2 scenario    74
<b>Table 5.1-6</b> Maximum temperature trend for A1B Scenario    75
<b>Table 5.1-7</b> Minimum temperature trend for A1B scenario
<b>Table 5.1-8</b> Mean temperature trend for A1B scenario    76
<b>Table 5.1-9</b> Baseline precipitation trend for NCEP and A2 scenario         76
<b>Table 5.1-10</b> Precipitation trend for A2 scenario (CGCM3:2001-2060)77
Table 5.1-11 Precipitation trends for A1B scenario (CGCM3:2001-2060)77
Table 5.1-12 Maximum and minimum discharge trend for base line
Table 5.1-13 Maximum and minimum discharge trend for A2 scenario
Table 5.1-14 Mean discharge trend for base line and A2 scenario       79
Table 5.1-15 Maximum discharge trend for A1B scenario
Table 5.1-16 Minimum discharge trend for A1B scenario    80
Table 5.1-17 Mean discharge trend for A1B scenario    81

Table 5.1-18 Maximum discharge trend for A2 scenario	81
Table 5.1-19 Minimum discharge trend forA2 scenarios	82
Table 5.1-20 Mean discharge trend forA2 scenario	83
Table 5.1-21 Comparisons of climatic water balance in three stations	86

## LIST OF FIGURES

Figure 3.1.1 Study area	25
Figure 3.2.1 Major river system of Nepal	28
Figure 3.2.2 Glacier area and elevation of Modi Khola river basin	28
Figure 3.2.3 Glacier area and elevation of Langtang Khola river basin	29
Figure 3.2.4 Glacier area and elevation of Dudh Koshi river basin	29
Figure 3.3.1 Homogeneity test by Rainbow software	33
Figure 3.4.1 Schematic illustrating the general approach to downscaling	39
Figure 3.7.1 Structure of HVB- <i>light 3.0</i> hydrological model	47
Figure 3.7.2 Schematic Model Structure	49
Figure 3.7.3 Soil Moisture Routine	51
Figure 3.7.4 Realization of a single linear reservoir is a box with a porous outlet	51
Figure 3.7.5 Response function and Response routine of the HBV model	52
Figure 3.7.6 Schematic shape of recession in relation to the different parameter	53
Figure 3.7.7 The transformation function (IHMS, 2006)	53
Figure 4.1.1 Precipitation distribution of Modi Khola River Basin	60
Figure 4.1.2 Precipitation distribution of Dudh Koshi River	60
Figure 4.1.3 Precipitation distribution of Langtang Khola River Basin	60
Figure 4.2.1 Precipitation trend of study stations	61
Figure 4.2.2 Variation of precipitation with elevation (1988-2009)	62
Figure 4.3.1 Observed Tmax trend	63
Figure 4.3.2 Observed Tmin trend	63
Figure 4.3.3 Observed Tmean trend	64
Figure 4.4.1 Monthly flow regime of Modi Khola river basin	65
Figure 4.4.2 Monthly flow regime of Langtang Khola river basin	65
Figure 4.4.3 Monthly flow regime of Dudhkoshi river basin	65
Figure 4.4.4 Corrected monthly flow regime of Dudhkoshi river basin	66
Figure 4.5.1 Observed discharge trend analysis of Modi Khola river basin	68
Figure 4.5.2 Observed discharge trend analysis of Langtang Khola river basin	68
Figure 4.5.3 Observed discharge trend analysis of Dudhkoshi river basin	68
Figure 4.5.4 Comparisons of average discharge of three basins	69
Figure 4.5.5 Daily average discharge of Dudhkoshi river basin	69

Figure 4.5.6 Corrected daily average	discharge of Dudhkoshi river basin	69
Figure 4.6.1 Modi Khola , Langtang	Khola, Dudhkoshi flow duration curve	70

## **TABLE OF CONTENTS**

Declaration	ii
Recommendation	iii
Letter of Approval	iv
Acknowledgments	V
Abstract	vi
List of Abbreviations	vii-x
List of Tables	xi-xii
List of Figure	xiii-xiv

CH	APT	ER 1	.1
1.	1	Introduction	. 1
1.	2	Rational of the study	.4
1.	3	Objectives of the study	.6
CH	APT	ER 2 LITERATURE REVIEW	.7
2.	1	Literature Review	.7
2.	2	Statement of the problems	12
2.	3	Impact of climate change in hydrology and water resources	13
2.	4	Climate Change Impact on Snow and Glacier	14
2.	5	Flow regime	16
2.	6	Flow regimes and the water balance	17
2.	7	Flow regimes of extremes – low flows and floods	17
2.	8	Snow and Glacier research in the Himalayas	18
2.	9	Selection of Precipitation and Runoff Models	20
	2.9.	1 Lumped Model	21
	2.9.	2 Semi-distributed Model	22
	2.9.	3 Distributed Model	22

2.10	Gei	neral Circulation Model (GCM)	.23
2.11	Ru	noff Generation	. 24
CHAP	ГER	3 MATERIALS AND METHODS	. 25
3.1	Stu	dy Area	. 25
3.1	.1	Modi Khola River Basin	.26
3.1	.2	Langtang Khola River Basin	.26
3.1	.3	Dudhkoshi River Basin	. 27
3.2	Wa	tershed characteristics of the three basins	. 27
3.3	Res	search Methodology	. 29
3.3	.1	Collection of daily Hydro- Meteorological data	. 30
3.3	.2	Data quality control	.31
3.3	.3	Trend Analysis	.36
3.4	Dat	ta collection Methodology	. 37
3.4	.1	Meteorological data	. 38
3.4	.2	SDSM modeling	. 38
3.4	.3	SDSM Calibration and validation	.40
3.4	.4	Bias correction methodology	.42
3.4	.5	SDSM Application	.43
3.5	Cat	chment Data	.45
3.6	Hy	drological Data	.46
3.7	ΗV	B-light 3.0 Hydrological Model and its Structure	.46
3.7	.1	Schematic Model Structure	.49
3.7	.2	Snow Routine	.49
3.7	.3	Soil Moisture Routine	. 50
3.7	.4	Response Routine	.51
3.7	.5	Routing Routine and Transformation Function	. 53
3.7	.6	HVB-light 3.0 Model Data	. 53

	3.7.7	History of HVB-light 3.0 for discharge modeling	54
	3.7.8	HVB-light 3.0 Methodology for Model Calibration and Validation	54
	3.7.9	Scatter plot observation and simulation	56
	3.7.10	Model performance	57
3.8	8 W	ater surplus/deficit in the three studied basins	57
	3.8.1	Potential Evapo-transpiration (PET)	57
	3.8.2	Actual Evapo-transpiration (AE)	58
СНА	PTER	A RESULT AND ANALYSIS	59
4.1	Se	asonal and monthly precipitation of three basins	59
4.2	2 Ye	early precipitation trend of observed data	61
4.3	8 Ye	early temperature trend of observed data	62
4.4	H Me	onthly flow regime analysis of three river basins	64
4.5	5 Ye	early discharge (flow regime) trend of observed data	66
4.6	5 Flo	ow-duration curve of three basins	70
CHA	PTER	<b>5 SUMMARY AND CONCLUSION</b>	72
5.1	Su	mmary	72
4	5.1.1	Temperature scenario	72
4	5.1.2	Precipitation scenario	76
4	5.1.3	Discharge scenario	77
4	5.1.4	Impact of climate change on flow regime	83
4	5.1.5	Scenario analysis	83
4	5.1.6	Water Balance of the study basin	86
5.2	2 Co	nclusion	87
5.3	8 Re	commendation for future work	89
RF	EFERH	ENCES	91

### APPENDIX

Appendix (I) Table 1, A1B decadal scenarios of maximum (Tmax), max	ninimum (Tmin)
and mean (Tmean) temperatures from 2001 to 2060	109

Appendix (I) Table 4, A2 decadal scenarios of maximum (Tmax), minimum (Tmin)
and mean (Tmean) temperatures from 1961 to 2000110

Appendix (I) Table 5, Observed decadal precipitation (mm) of the three regions...111

Appendix (I) Table 9, A1B and A2 decadal scenario of discharge (m<sup>3</sup>/s) from maximum, minimum and mean temperatures (<sup>0</sup>C) and precipitation (2001-2060)...113

Appendix (I) Table 10, Observed instantaneous maximum and minimum discharge	•
of Dudhkoshi river basin1	14
Appendix (II) Figure 1- 24, Study Area, Watershed characteristics of three	
basins115-1	135
Appendix (III) Figure 1 to Figure 9, calibration, validation and seasonal bias	
correction of three basins	.37
Appendix (IV) Figure 3.3.1 to Figure 3.3.18, calibration and validation of	
meteorological data	40
Appendix (V) Figure 2.4.8 (a) to Figure 2.4.8 (i) Calibration and validation of	
Appendix (V) Figure 3.4.8 (a) to Figure 3.4.8, (i) Calibration and validation of	
Hydrological data	.44
Appendix (VI) Figure 3.4.14(a) to Figure 3.4.14 (h), Simulated and observed	
	140
discharge of three basins145-1	.48

### **CHAPTER 1**

### 1.1 Introduction

This research focuses on a comparative study of the impact of climate change on flow regime within three perennial monsoon dominated river basins of Nepal Himalayas. The studied basins are Modi Khola river basin in Annapurna region, Langtang Khola river basin in Langtang region and Dudhkoshi river basin in Khumbu region. In this study, four software are employed which are (i) Statistical Down Scale Model (SDSM) version 4.2.2 for climate simulation (ii) HVB-*light 3.0* hydrological model for discharge simulations (iii) CROPWAT 8 model for Evapo-transpiration estimation and (iv) Thornthwaite model (2010) for water balance computation.

#### Background

Nepal is situated in the middle of the Hindu-Kush Himalayan region. The country is extended between 26° 22' to 30° 27' N in latitudes and 80° 40' to 88° 12' E in longitudes, which is surrounded by India to the east, south, west, and China to the north. The length of the country is about 885 km from east to west and the north-south width varies from 145 km to 241 km. Within this range, the altitudinal variations is from about 60m above mean sea level in the southern plain (called Terai) to the Mount Everest (8848 m) in the northeast. Out of 147,181 Km<sup>2</sup> total area of the country, about 86 % area comprises of hilly and mountainous regions and remaining 14% are flatlands.

In general, the country is divided into five major physiographic zones. They are Terai, Siwalik, Hill, Middle Mountain and High Mountain. The higher elevated northern most part of the high mountain is also called Himalayas/Tibetan Plateau. The Terai, a long narrow belt of fertile agricultural flatland, is the part of alluvial Gangetic Plains and has altitudinal variations ranging from 60 m to 300 m. The Terai lies between the Indian boarder in the south and the first outer foothills of Nepal in the north. The Siwalik range, 600 m to 1500 m in elevations, lies in the north of Terai region. To the north of Siwalik is a zone of discontinuous valleys (also called 'Dun'). The intensive cultivation and decrease forest cover in combination has been causing a serious

problem of soil erosion in these valleys. To the north of these valleys is the Mahavarat Range (2700 m-3700 m), which in terms of formation and elevation, is well developed in eastern and central Nepal and underdeveloped in western Nepal. To the northern most parts of Nepal is a snowy mountainous regions (Himalayas), lies above 4000 m in elevation and stretches from east to the west of the country.

Nepal is predominantly an agricultural country. Agricultural production in the country is carried out by more than two million of farm families and the livelihood of 81 % of the people depends on agriculture CBS (2011). This sector also serves as the backbone of the national economy. The agricultural sector alone contributes to about 30 % of the GDP, and provides employment to nearly 65 % of the entire population. The percentage of the total land area used for agriculture are 9.3 % in the mountains, 43.1 % in the hills and 47.6 % in the Terai. It is estimated that about 986,898 ha of the land area (6.5% of the country's total land area) are still available for agricultural production Adhikari 2008). Forest and shrub covers 39.6 % of the total area of the country FAO (2009). On an average about 65 per cent of the total cultivated land is rain fed which is adversely affected by the loss of top fertile soil, due to soil erosion, landslide and flood (MOPE, 2001).

Rapid changes in the altitude and aspect along the latitudes have made existence of wide range of climatic conditions in Nepal (Nayava, 1974). Therefore, within a span of less than 200 km Nepal captures almost all types of climates, subtropical to alpine/arctic. Physically, this is more apparent that the country has been home of diverse habitats, vegetation and fauna.

Temperature in Nepal varies mainly with topographic variations along south-north direction. Normally, the average temperature decreases by 6 <sup>o</sup>C for every successive gain in altitude by 1000 m (Jha, 1992). Eighty percent of the precipitation that falls in Nepal comes in the form of summer monsoon rain. Winter rains are more common in the western hills. The average annual rainfall in Nepal is about 1600 mm, with large variations between eco-climatic zones. Climate of Nepal is, thus, characterized mainly by altitude, topography, and by the seasonal precipitation induced by the monsoon system. In addition, aspect has an important influence particularly on vegetations at lower altitudes. In general, moisture is retained more on north and west faces than on

south and east faces. The south and east faces are drier because of the long expose to the sun.

The Himalayan region comprises of sub-alpine and alpine climate with the existence of summer grazing pastures in the lower elevations. The Himalayan range at above 5,500m is normally covered with perpetual snow/ice without vegetation. Above 6,000m of this region is defined as an arctic desert or the nival zone. The major perennial river systems of South Asia originate from this region. As Nepal located in the central portion of the Himalayas, it lies in the transitional zone between the eastern and western Himalayas.

In Asian region, the frequency of extreme events such as floods, droughts including forest fires and tropical cyclones has increased in recent years. Increase in intensity of rainfall would increase flood risks in temperate and tropical Asia. Likewise, combined influence of Climate change and population pressure would exacerbate threats to biodiversity due to land-use and land-cover changes. Northward movement of the southern boundary of the permafrost zones would result in a change of thermokarst and thermal erosion with negative impacts on social infrastructure and industries Lee et. al. (2008). Locally, the effects of climate change in Nepal are large flash floods, frequent flooding, prolonged drought, increase in vector borne diseases and rapid glacier melt (Bajracharya et al. 2008). In Nepal increases in temperature have been greater in the uplands than the lowlands (Shrestha et al. 1999). Such regional changes in climate have already affected diverse physical and biological systems in many parts of the world. Shrinkage of glaciers, thawing of permafrost, late freezing and earlier break-up of ice on rivers and lakes, pole-ward and altitudinal shifts of plant and animal species, declines of some plant and animal populations, and earlier emergence of insects have been observed (IPCC, 2001). The IPCC (2007a), report also concludes that the warming is expected to be greatest over land and at most high northern latitudes, where snow cover is projected to contract and it is very likely that hot extremes, heat waves, and heavy precipitation events will continue to become more frequent. The spatial variation in observed and projected climate is large and mountain ranges and their downstream areas are particularly vulnerable for several reasons. Firstly, the rate of warming in the lower troposphere increases with altitude, i.e. temperatures will increase more in high mountains than at low altitudes

(Rangwala et al. 2013). Secondly, mountain areas exhibit a large spatial variation in climate zones due to large differences in altitude over small horizontal distances (Beniston et al. 1997). Finally, mountains play an important role in the water supply of downstream areas. More than one sixth of the global population depends on water supplied by mountains; and changes in hydrology and water availability are expected to be large in mountain basins (Barnett et al. 2005, Viviroli et al. 2007). Especially the diminishing role of snow and ice as a natural store for water supply will have a tremendous impact. In addition, snow cover extent in the Himalayas and on the Tibetan–Qinghai plateau could influence water availability of the Himalaya region through change in the strength of the monsoon.

The analysis of impact of climate change on the hydrology of high altitude glacierized catchments in the Himalayas is a complex problem due to various region. The high variability in climate, lack of data, large uncertainties in climate change projection by models and uncertainty about the response of glaciers are some of the complexities. Present study tries to use different models to assess the future change in the glaciers and the runoff within three catchment areas in Nepal Himalayas. The analysis projects that both temperature and precipitation will keep increasing, resulting in a steady decline of the glacier area. Climate change analysis using downscaled data from 5 different GCMs shows that temperatures are projected to increase by 0.06 °C y-1 and precipitation by 1.9 mm y-1. The analysis also reveals a large variability among the different GCMs in particular for precipitation (Immerzeel et al. 2011).

This study attempts to downscale GCM simulated high resolution gridded data through statistical algorithm to point data using SDSM 4.2.2. The products of scenario generated by CGCM3 climate model, temperature and precipitation data were utilized for running HVB-*light 3.0* hydrological model for the computation of future discharge scenario.

### **1.2** Rational of the study

This study focuses mainly on climate change and associated flow regime. Study is based on preprocessing and spatial analysis of the Digital Elevation Model (DEM) for the automatic delineation of watershed and processing of satellite images for mapping of glaciers in rugged and inaccessible terrain. Hydro meteorological data of Modi Khola river basin (Annapurna region), Langtang Khola river basin (Langtang region) and Dudhkoshi river basin (Khumbu region) of Nepal Himalaya are analyzed by hydrological model (HVB-*light 3.0*). The analysis provides information about the climatic water balance and future trends which are helpful for future water-resource planning in hydropower, irrigation and drinking water etc. The results are also useful for water resources systems analysis, watershed hydrology, flood management, water sustainability, adaptation planning and sustainable management of water resources in other similar conditions in the Himalaya region.

**Limitations of study:** Rapid change of climate parameters in short distance or with the altitudinal difference in rugged mountain region, influences temperature and precipitation pattern and hence the available meteorological stations cannot sufficiently represent the whole study area in study basins.

Long term temperature, precipitation, and river flow data are available mostly at the lower levels. So the obtaining trend of the weather parameters at higher altitudes is rather complicated.

Other influencing weather parameters, such as solar radiation, wind speed, and atmospheric pressure are not considered due to study limitation and unavailability of data.

One day temperature missing value in daily series is reconstructed from the observed historical average and linear interpolation method from the adjacent intervals (Boakye, 1993).

All data are considered as the representative for the whole river basins considered. The weather data and hydrological observations are available only after 1988, with number of missing values.

### **1.3** Objectives of the study

Hypothetically, it has been observed that there is an increasing temperature and precipitation trends in Himalayan basins resulting in shrinking of snow and glacier area in the recent years (Immerzeel et al. 2011). As a consequence the flow regime and runoff generation are increasing. The main objective of the study is, therefore, to assess the impact of climate change in flow generation on three high Himalayan river basins of Nepal. In addition, following specific objectives are targeted in this research;

- To characterize watershed of three basins.
- To analyze the hydro-meteorological characters in three basins.
- To apply hydro-meteorological models in Himalayan basins to estimate the impact of climate change on flow regime.
- To compare the water balance of three basins.

### **CHAPTER 2 LITERATURE REVIEW**

#### 2.1 Literature Review

Water is fundamental to human life. It is required for agriculture, industry, ecosystems, energy, transportation, recreation and waste disposal (Frederick and Gleick, 1999). Therefore any changes in the hydrological system and water resources could have a direct effect on the society, environment and economy. Climatic processes influence the hydrological processes, vegetation, soils and water demands (Kaczmarek et al. 1996). Precipitation is the main driver of variability in the water balance over space and time. Change in precipitation could have very important implications for hydrology and water resources (IPCC, 2001b). Floods and droughts primarily occur as a result of too much or too little precipitation. Changes in precipitation and evaporation have a direct effect on the ground water recharge, which is the major source of water across much of the world. More intense precipitation and longer drought periods are considered to be expected impacts of climate change for most of the land areas of the world (IPCC, 2001a), which could cause reduced ground water recharge. Less ground water recharge means reduction in water availability in these areas (IPCC, 2001b).

The average surface temperature of the earth has increased by 0.3 °C to 0.6 °C over the past hundred years; and the increase in global temperature is predicted to continue rising during the 21<sup>st</sup> century. During the same period, on the Indian subcontinent, surface temperatures is predicted to increase between 3.5 and 5.5 °C (IPCC, 2001a) and an even greater increase is predicted for the Tibetan Plateau (Lal, 2002). In the Himalayas, climate change is causing the net shrinkage and retreat of glaciers as well as the increase in size and number of glacial lakes. Recent studies showd that the recession rate of glaciers has increased with rising temperature. For example, with the temperatures rising by 1 °C, alpine glaciers have shrunk by 40 % in area and by more than 50 % in volume since 1850 (IPCC, 2001b and CSE, 2002). Climate has changed considerably throughout the history of the earth due to change in its forcing components, whether natural or anthropogenic. There has been an unprecedented warming trend during the 20<sup>th</sup> century mainly due to anthropogenic global warming concentrations (IPCC, 2007). Temperatures of the last half century were unusual in comparison with those of previous 1300 years. The current average global surface temperature of 15 °C is nearly 0.6 °C higher than it was 100 years ago and 0.56 °C to 0.92 °C higher over the past 50 years (1906 – 2005). These numbers indicate that there is rapid warming of global surface temperature (IPCC, 2008). Climate change is projected to compound the pressure on natural resources and the environment associated with rapid urbanization, industrialization and economic development (Eriksson et al. 2009).

The Fourth Assessment Report of the Inter Governmental Panel on Climate Change IPCC, compiled current knowledge on various aspects of climate change, including the key indicators, based on research conducted in the previous years (IPCC, 2007). One of the most visible impacts of climate change in the Himalayan region is the retreat of glaciers (WWF, 2005), which are the reliable sources of freshwater to many people living downstream to meet their needs for water supply, irrigation, hydropower and navigation. Himalayan glaciers cover about 17 % of the global mountain i.e. around 33,000 sq.km (Eriksson et al., 2009), and store about 12,000 cu. km of fresh water (Thompson and Gyawali, 2007). There are about 3,252 glaciers with coverage of 5,323 sq. km areas and an estimated ice reserve of 481 km<sup>3</sup> in Nepal (Mool et al. 2001a).

Although regional differences exist, growing evidence shows that the glaciers of the Himalaya are receding faster than the world average (Thompson and Gyawali, 2007) and are thinning by 0.3-1 m/year (Dyurgerov and Meier 2005). In the last half century, 82 % of the glaciers in western China have retreated (Liu et al. 2006). On the Tibetan Plateau, the glacial area has decreased by 4.5 % over the last twenty years and by 7 % over the last forty years (CNRCC, 2007).

The rapid shrinkage of Himalayan glaciers due to climate change is likely to threaten water availability seriously in the region, particularly during lean flow seasons when melt water contribution is crucial to sustain the river flow which supports human activities and ecosystem services in these areas and downstream (IPCC, 2008). As the contribution of snow and glacial melt to the major rivers in the HKH region ranges from less than 5 % to more than 45 % of the average flow (Alford, 1992), changing temperatures have impacts on the melting of glaciers and snow in the mountains as

well as the snowmelt contribution and river discharge (Kattelmann 1987; Singh and Bengtsson 2004). IPCC (2007) predicts the annual river discharge will increase until around 2030 and then decrease thereafter because of rapid melting of snow and glacier until 2030 which will substantially decrease available snow and glacier mass thereafter. In most areas snow cover responses to both temperature and precipitation exhibits a strong negative correlation with air temperature. As the climate warms, snow cover is projected to shrink, and glaciers and ice caps to lose mass as a consequence of the increase in summer melting being greater than the increase in winter snowfall. Widespread increase in thaw depth over much of the permafrost regions are projected to occur in response to warming (IPCC, 2008). Consequently, snow cover has decreased in most regions, especially in spring and summer. Satellite observations of Northern hemisphere snow cover over the 1966 to 2005 period showed decrease in every month except November and December, with a stepwise drop of 5 % in the annual mean in the late 1980s (IPCC, 2008).

Singh and Kumal, (2001) reported that the earth's average surface temperature has increased between 0.3 and 0.6  $^{0}$ C over the past 100 years, and by about 0.2 to 0.3  $^{0}$ C since 1950. The mean sea level has risen between 10 and 25 cm over the same period primarily due to the thermal expansion of the oceans (0.2 to 0.7 mm/year), retreat of glaciers (0.2 to 0.4 mm /year) and other temperature-related causes, including possible melting of the Antarctic and Greenland ice sheets.

**Overview of climate of Nepal:** In Nepal average maximum temperature increase was recorded as 0.06  $^{0}$ C per year and that in Terai and Himalayas was 0.04  $^{0}$ C and 0.08  $^{\circ}$ C/year respectively (Shrestha et al. 1999). He reported maximum temperature increase of 0.06  $^{\circ}$ C to 0.12  $^{\circ}$ C per year in most of middle mountain and Himalayan regions while Siwalik and Terai region showed warming trend of less than 0.03  $^{\circ}$ C /year between 1971 - 1994.

The change of temperature is more rapid along elevation gradient than along the horizontal distances (Bajracharya et al. 2007). The Tibetan Plateau has experienced warming at the rate of 0.02  $^{\circ}$ C – 0.03  $^{\circ}$ C per year over the last 50 years (Yao et al. 2006) which is much higher than the mean global rate of 0.74  $^{\circ}$ C for the years 1906-2005 (IPCC, 2007). The rate of increase of mean temperature in Nepal, of 0.040

 $^{0}$ C/year for the year 1975 to 2005 (Baidya et al. 2007), is also much higher than the global mean. An analysis of annual mean minimum and maximum temperature for the years 1976 to 2005 by Marahatta et al. (2009) has shown higher increase in maximum temperature (0.05 °C per year) than minimum temperature (0.03 °C per year). Although the temperature data is analyzed for a relatively short period, it showed significantly high warming rate.

Most glaciers studied in Nepal are undergoing rapid de-glaciations. The reported rate of glacial retreat ranges from several meters to 20 m/year (Fujita et al.2001a; Fujita et al. 1997; Kadota et al. 1997).

The oldest temperature records available at Kathmandu and its surroundings were documented by Hamilton during his stay in Nepal from April 1802 to March 1803, but there is no information on site and equipment of measurement (Chalise, 1994). There is no continuous temperature record at all for the subsequent years up to 1921. The studies on analyses of the temperature records of Kathmandu for the period of 1921-1994 showed a similar temperature trend as that averaged over 24°- 40 °N, that is a general warming trend till 1940s, a cooling trend during 1940s-1970s and a rapid warming after the mid-1970s (Shrestha et al. 2000; Shrestha et al. 1999). Sharma et al. (2000a) indicated that the increasing trend of average temperatures during the period 1940s-1970s was primarily due to the increasing trend of maximum temperatures and there was no increasing trend of minimum temperatures. The temperature trends during the periods of 1971-1994 was analyzed by Shrestha et al. (1999) and found wide variation among the geographical regions and seasons in Nepal. Average annual temperatures in the Terai regions of Nepal increased by about 0.04 °C/year, whereas those in the middle mountain areas in the north increased by about 0.08 °C/year (Shrestha et al. 1999). Similarly, the pre-monsoon season (March-May) showed the lowest warming rate of 0.03 °C/year, while the post-monsoon season (October-November) showed the highest of 0.08 °C/year (Shrestha, 2001).

Precipitation over land generally increased over the  $20^{\text{th}}$  century between 30  $^{0}$ N and 85  $^{0}$ N, but notable decrease have occurred in the past 30 to 40 years from 10  $^{0}$ S to 30  $^{0}$ N (IPCC, 2008). however, even though Nepal lies between 26 to 30  $^{0}$ N, precipitation has increased (analysis from 1978 to 2001) at the rate of 0.6 % annually (Chaulagain,

2003). Although the precipitation fluctuation in Nepal is not the same as the all-India precipitation trend, it is well related with rainfall variations over northern India (Shrestha et al. 2000; Kripalani et al. 1996).

Nepal has a wide variation of climates from subtropical in the south, warm and cool in the hills and cold in the mountains within a horizontal distance of less than 200km (UNEP, 2001; Shankar and Shrestha, 1985; Chalise, 1994). The amount of precipitation varies considerably from place to place because of the non-uniform rugged terrain (Shankar and Shrestha, 1985). The length of the regular and systematic observations of climatological and hydrological data in Nepal is only about 50 years (Mool et al. 2001b). The longest systematic temperature and precipitation data have been available for Kathmandu since 1921 recorded by Indian Embassy under British rule (Shrestha et al. 1999). The existing climatological and hydrological stations are generally located at the lower elevations. The high mountain areas with very low population density and negligible economic activities are mostly without any hydrological and meteorological stations. The meteorological observations in high mountain areas were only initiated in 1987 after the establishment of the Snow and Glacier Hydrology Section in the Department of Hydrology and Meteorology of Nepal (Mool et al. 2001a).

About 10 % of the total precipitation in Nepal falls as snow (UNEP, 2001). About 23 % of Nepal's total areas lie above the permanent snowline of 5000 m (MOPE, 2004). Presently, about 3.6 % of Nepal's total areas are covered by glaciers (Mool et al. 2001b). A new inventory of glacial lakes was published by ICIMOD in 2011 based on an analysis of Landsat satellite images from 2005/6; 1,466 lakes were identified with a total area of 65 km<sup>2</sup> (ICIMOD, 2011). One of the widely studied glacier AX010 in the eastern Nepal Himalayas retreated by 160m in 1978-1999 and has shrunk by 26 % in 21 years, from 0.57 km<sup>2</sup> in 1978 to 0.42 km<sup>2</sup> in 1999 (Fujita et al., 2001a).

Nepal Himalayas are considered highly sensitive to the changing climate. Several studies in the Himalayas reveal that glaciers in this region have retreated remarkably, in the past two decades (Fujita et al., 2006). Although it is still ambiguous which climatic parameter is playing a key role in the glaciers retreat in this region, Ren et al., (2004 and 2006) reported that the current glacier retreat in the central Himalayas is

due to the combined effect of reduced precipitation and warmer temperature. The study warned that if prevailing climatic conditions continue, the glacier retreat in this region will accelerate further. The lives and properties in the downstream side of the Himalayas are obviously threatened by glaciers retreat.

Temperature is the most sensitive parameters to the PDDM and shows an increase in  $2^{0}$ C in temperature will raise the discharge by 31.9% (Niraj et al. 2014). The previous study (Fukushima et al. 1987) showed that the runoff variation between 0.51 and 13.1 mm/day and winter discharge of Langtang valley constitute 4 % of the annual discharge (Motoyama et al. 1987). Mean daily discharges of central and western Himalayan glaciers were well correlated with the glaciered area (Puri et al. 1995). In contrast, changing precipitation characteristics, mainly lowering of winter snow cover extent and duration could reduce the headwater river flow drastically, while the glacier component sustains the low flow. A sharp runoff decline of 45 % was observed during the short duration of three years demonstrating the stress which the Himalayan cryosphere experiences in a climate change regime. The result also suggest that the lower reaches of the Himalayan headwater rivers could expect larger annual runoff variations in future, as buffering efficiency of shrinking glaciers reduce further.

Continuing climate change is predicted to lead to major changes in the strength and timing of the Asian monsoon, inner Asian high pressure systems, and winter westerly, the main systems affecting the climate of the Himalayan region. The impacts on river flows, ground water recharge and natural hazards could be dramatic, although not the same in terms of rate, intensity or direction in all parts of the region. Given the current state of knowledge about climate change, determining diversity of impacts is a challenge, and risk assessment is needed to guide future action.

### 2.2 Statement of the problems

The effect of the global warming on the glaciers and ice reserves of Nepal has serious implications for the fresh water reserve and consequently for low flows. Any significant change in glacier mass and ground water storage will impact water resource in a regional scale. Increase in temperature and precipitation in Himalayas

accelerates the process of ice/snow melting as well as enhances flooding event from direct runoff whereas dry season discharge (base flow) decreases. The projected changes in climatic parameters have adverse effect on water storage capacity of the Nepalese Himalayas. The major concern is rapid reduction of glaciers in much of the Himalayan region and shifting snow line upwards.

In the past, many attempts were made to study climate change impact on flow regime. Most of these have focused on the extreme events like flood and drought. Whereas, climate change studies in Himalayan regions have focused mainly on the glacier melting, retreating, Glacial Lake Outburst Flood (GLOF), and its trend. However, this study is carried out to investigate the contribution of snow and glacier melt in stream flow of glacier-fed river and impact of climate change on flow regime.

### 2.3 Impact of climate change in hydrology and water resources

In recent years, numerous studies have investigated the impact of climate change on hydrology and water resources in many regions (Arnell and Reynard, 1996; Bergstrom et al. 2001; Middelkoop et al. 2001; Gao et al. 2002; Menzel and Burger, 2002; Pilling and Jones, 2002; Arnell et al. 2003 and Christensen et al. 2004). Charlton et al. (2006) investigated the impact of climate change on water supplies and flood hazard in Ireland using a grid-based approach, the HYSIM model (Manley, 1993) with statistically downscaled climate data from the Hadley Centre Climate Model, HadCM3 (Gordon et al. 2000). Murphy et al. (2006a) employed similar downscaled data to force HYSIM Model, modeling individual basins rather than a gridded domain. As discussed in Murphy et al. (2006b), parameter uncertainty is addressed by employing the GLUE methodology (Beven and Binley, 1992) with Latin-Hypercube sampling (McKay et al. 1979) as an alternative to Monte- Carlo simulations. There are some key differences between the study of Charlton et al. and Murphy et al. and Sibert's on calculating the parameter uncertainty. Charlton et al. (2006), and Murphy et al. (2006a) used dynamical rather than statistical downscaled climate data in the HVB-light 3.0 hydrology model whereas Seibert (2005) used Monte-Carlo simulations. Regional climate model is used to produce dynamically downscaled precipitation and temperature data which are required by the HVB-light 3.0 conceptual rainfall-runoff model.

#### 2.4 Climate Change Impact on Snow and Glacier

According to the World Resources Institute (WRI), the total size of the world's glaciers has declined by about 12 % in the twentieth century (Anthwal et al., 2006). Combes et al., 2004 reported that since the early 1960s, mountain glaciers worldwide have experienced an estimated net loss of over 4,000 km<sup>3</sup> of water. This loss was more than twice as fast in the 1990s than during previous decades. Projected climate change over the next century will further increase the rate at which glaciers melt. Average global temperatures are expected to rise by 1.1 to 6.4 <sup>o</sup>C by the end of the 21<sup>st</sup> century (IPCC, 2007). Simulation by Combes et al. (2004) projects that 4 <sup>o</sup>C rise in temperature would eliminate nearly all of the world's glaciers.

Glaciers are the world's water towers (Thompson, 2006) and the origin and lifeline of the major river systems. They represent valuable natural reservoirs of water exerting a strong control on drainage characteristics of alpine catchments. Hence, storage and release of water from glaciers are important for various practical and scientific fields including hydroelectric power, flood forecasting, sea level fluctuations, glacier dynamics, sediment transportation and formation of landforms (Jansson et al., 2003). Global warming is melting the glaciers in every region of the world. The loss of glaciers threatens the water resources of many parts of the world and will directly affect millions of people who depend on water released from glaciers during the dry season (Thompson, 2006). Besides, continued-widespread melting of glaciers during the coming century will lead to severe floods and sea level rise threatening and destroying the coastal communities and habitats.

Global sea level rose at an average rate of 1.80 ( $\pm 0.50$ ) mm per year over 1961-2004, with an estimated contribution of 0.50 ( $\pm 0.18$ ) mm per year from melting glaciers. The projected sea level rise at the end of the 21st century ranges from 0.18 to 0.59 mm per year under the different emission scenarios (IPCC, 2007). This trend of sea level rise will affect coastal regions throughout the world causing flooding, erosion and salt water intrusion into aquifer and fresh water habitants. Thus, even those who live far from the mountains will have to face the consequences of melting glaciers (Hall and Fagre, 2003).

Climate change can greatly alter the water resources in mountain environments with substantial snow and ice-cover areas (Garr and Fitzharris, 1994). Daily and seasonal fluctuations in temperature and precipitation have a significant impact on the seasonal distribution of snow storage and runoff. Changes in the snowfall pattern have been observed in the Himalayas in the past decades. Consequently, almost 67 % of the glaciers in the Himalayas have retreated in the past decade (IPCC, 2001b). Increasing temperature would lead to reduction in snow and glacier volume and thereby reduction in water availability in the Himalayas.

The hydrological cycle of the HKH region is influence by the Asian monsoon, the globe indicate that the stream flow regime in snowmelt dominated river basin is most sensitive to wintertime increase in temperature (Stewart et al. 2004, Nijssen et al. 2001). In the regions where the land surface hydrology is dominated by winter snow accumulation and spring melt, the performance of water management systems such as reservoirs, designed on the basis of the timing of runoff, is relative among the global models as to the magnitude (and even direction of) precipitation changes regionally (Giorgi et al. 2001, Giorgi et al. 2005, Ruiz et al. 2003 and Dia A. 2003).

The Himalayan Rivers are expected to be very vulnerable to climate change because snow and glacier melt water make a substantial contribution to their runoff (Singh, 1998). However, the degree of sensitivity may vary among the river systems. The magnitudes of snowmelt floods are determined by the volume of snow, the rate at which the snow melts and the amount of rain that falls during the melt period (IPCC, 1996b). A runoff sensitivity analysis (Mirza and Dixit 1997) showed that a 2 °C rise in temperature would cause a 4 % decrease in runoff, while a 5 °C rise in temperature and 10 % decrease in precipitation would cause a 41 % decrease in the runoff of the Ganges River near New Delhi. There will be decrease in runoff in dry seasons and increase in runoff in monsoon season under the doubled  $CO_2$  scenario using the Canadian Climate Centre Model (CCCM) and Geophysical Fluid Dynamics Laboratory (GFDL) models (Gurung, 1997).

According to the various studies done all over the world current demands for water in many parts of the world will not be met under plausible future climate conditions. The

other key factor affecting water availability is lack of enough reservoir storage to manage a shift in the seasonal cycle of runoff (Barnett et al. 2005).

On an annual time scale, the water that flows from a glacierized catchment is the sum of the precipitation and the melted snow and ice (minus some negligible evaporation). Both contributions can have a pronounced seasonality (e.g. spring-time snow melt, glacier melt in summer, highest precipitation in autumn) and will strongly vary by region and degree of glacierization. On a decadal time scale, a change in the long-term reservoirs will also have an impact on runoff characteristics, as a diminishing glacier cover will produce less melt-water (UNEP, 2010). Rapid shrinkage of glaciers in the Nepal Himalayas has been observed during recent decades by analyzing air temperature records. However, it is still not known how global warming affects the mountains in Nepal, since long-term meteorological records for high elevations (more than 4000 amsl) are few (Fujita et al., 2006).

### 2.5 Flow regime

In general, the term regime refers to any system of control. In science, regime refers to a particular state of affairs where a particular physical phenomenon or boundary condition is significant, such as "the super-fluid regime" or "the steady state regime". In hydrology, regime refers to the seasonal patterns of runoff which is consistent with the more general notion in science at large, as the regimes reflect classes of processes not known in exact detail that do differ in important aspects. In other words, a river flow regime describes the average seasonal behavior of flow and reflects the climatic and physiographic conditions in a basin. Differences in the regularity of the seasonal patterns reflect different dimensionality of the flow regimes, which can change due to changes in climate conditions. Krasovskaia and Gottschalk (2002) mention that, the river flow regimes reflect the climate conditions and, naturally, are bound to respond to a climatic forcing (such as global warming, for example). Considering the irregular character of many river flow regimes, it is hardly adequate to predict only some average seasonal patterns in the future caused by, for example, climate change. One should rather refer to the changed frequencies of occurrence of different seasonal flow patterns during each individual year in the future.

### 2.6 Flow regimes and the water balance

The task of hydrology is to solve the water balance equation at various space and time scales. As such, an assessment of hydrological processes in catchments needs to start with an analysis of the water balance components. Merz and Bloschl (2004) and Parajka et al. (2004) estimated the water balance components for a large number of Austrian catchments using climatic inputs, runoff data, and snow depth data, based on a conceptual catchment model. Estimates of the hydrological catchment scale fluxes (precipitation, evapo-transpiration, runoff) and storage terms (soil moisture and snow water equivalent) clearly highlight the reasons for the seasonal patterns of runoff. This type of information complements the descriptive regime type approach as it provides quantitative estimates of the relative role of the water balance components, their average seasonal patterns and variability between years as well as their spatial patterns at the regional scale.

### 2.7 Flow regimes of extremes – low flows and floods

Similar to the water balance, more detailed analyses can provide insight into the main driving processes at the extreme ends of the runoff spectrum, i.e. low flows and floods. In the case of low flows, Laaha and Bloschl (2004) used seasonality to tag processes, and allowed them to unravel process controls of the Q95 low flow discharges in Austria. The ratio of summer and winter low flows pointed to regions where either summer evaporation or alpine snow packs controlled the presence of low flows. In the case of floods, the analyses of Merz and Bloschl (2003) were more involved and included process indicators such as the spatial coherence of floods, snow conditions and the moisture state of catchments that were used to classify 12,000 annual floods into "flood types" (long rain floods, short rain floods, flash floods, rain on snow floods, snow melt floods). For Austrian conditions, north of the Alps. Rain on snow floods were most frequent north of the Danube.

An important issue in global warming is its impact on the environment, and water resources in particular. During the last three decades many studies have been devoted to this latter problem (Nemec and Schaake, 1982; Arnell et al. 1990; Jones, 1999; Beltaos and Prowse, 2001). The majority investigated the effects of eventual climate

change on water resources in terms of water volumes and only a few have yet taken up its effect on seasonality of flow, i.e. river flow regimes (Krasovskaia and Gottschalk, 1992; Krasovskaia and Gottschalk, 1995; Krasovskaia and Saelthun, 1997). The IPCC Third Assessment Report (IPCC, 2001) draws attention to changes in the timing of stream flow caused by global warming and the increasing interest in the temporal changes of the river flow regimes is manifested by many quite recent studies on this topic (Westmacott and Burn, 1997; Bouraoui et al. 1999; Leblois, 2001; Middelkoop et al. 2001). Different flow regime patterns can be treated as some "preferred states" of the runoff system, which are more or less stable. Under the influence of changing climatic conditions, a flow regime might destabilize and turn over to another one with sometimes quite different seasonal patterns of high and low water, thus disturbing the established hydro-ecological conditions and water uses. The importance of such a change will clearly depend on the sensitivity of a certain regime pattern to the changing climate. In order to identify a change in any pattern (whatever the reason), it is necessary first of all to adequately describe its initial state. There are diverse pattern recognition methods, and both supervised and non-supervised approaches have been applied to describe the flow regime patterns (Parde, 1933; Lvovich, 1938; Gottschalk, 1985; Haines et al. 1988; Krasovskaia et al. 1994). In the supervised approach a couple of indicators (flow regime types) are defined first and the patterns consistent with the defined ones are then searched in long-term mean monthly runoff data. In a non supervised approach (in this context most often clustering) no such indicators are available and the task is to identify the types indicated by the data structure. Whatever approach is chosen for the initial pattern identification, it will affect the analyses of its eventual changes in time. Paradoxically, a too precise definition of the "indicator type" may lead to exaggerated sensitivity to a climatic variation and vice versa, while with the non-supervised approach the selected degree of consistency in the identified groups ("the stopping rule") may also affect the result. Thus, it is reasonable to avoid a rigid framework of pre-defined flow regime types, at the same time preserving information about seasonal behavior of river flow.

#### 2.8 Snow and Glacier research in the Himalayas

Rango and Martinec (1997) examined the influence of changes in temperature and precipitation on the snow cover using SRM. Singh and Kumar (1997b) used

University of British Columbia (UBC) watershed model (Quick and Pipes, 1977) for similar study on a high altitude river. Singh and Bengtsson (2004) used a conceptual snowmelt model to assess the impact of global climate changes in Sutlej River basin. The study showed that when the aerial extent of glaciers decreases due to higher melt rate on long term, the water availability from the complex basins will be reduced but increased in glacier fed river basins.

Jordan et al., (2005) analyzed the impact of climate change in Simulation Control Area (SCA) by using aerial photographs of the Cotopaxi Volcano ice cap dating from 1956 to 1976 and found that the loss of surface area by about 30 % between 1976 and 1997. Slope exposure did not seem to have significant effect since all the glaciers of the volcano retreated in the same proportion. In accordance with specific measurement performed on 15 glaciers nearby Antizana, it was suggested the strong recession observed after 1976 was associated with increasing melting conditions which have occurred repeatedly during the intense duration of warm ENSO phases.

Several models and empirical relations have been used to study Himalayan glaciers from simple system model to conceptual to more physical based model. For example, empirical relations to calculate glacier ablation by Agata and Higuchi (1984), a simplified model for estimating glacier ablation under debris layer by Nakawo and Takahashi (1982), and Rana et al. (1996) and energy balance modeling or glacier mass balance on Glacier AX010 by Kayastha et al. (1999). Direct field observations are very difficult to carry out in the Himalayas because of rugged and remote mountain terrain. So, the model and method to predict snow and ice melt should be simple with a minimum field data requirement. Following this concept of simplicity, Kayastha et al. (2000) used the "positive degree-day factors" in Khumbu Glacier, Nepal for the ablation under various debris thickness were found and a practical relationship between debris layer. Similarly, Fukushima et al. (1991) used a conceptual runoff model called HYCYMODEL in Langtang River Basin, using method developed by Agata and Higuchi (1984), which gives empirical relation to calculate snow and ice melt without consideration of effect of debris on glacier surface. Braun et al. (1993) applied the conceptual precipitation-runoff model in the same basin (Langtang basin) for better understanding of hydrological process and efficient planning and operation of water resources.

Arnold et al. (1996) is the pioneer on using digital elevation model (DEM) to study the mass balance of the glaciers. The study developed and tested the surface energy balance model for calculation of snow melt with help of DEM along with topography and meteorological data from site in front of the glacier and determined the hourly or daily energy balance components and calculated the snow melt on a spatial resolution of 20m by 20m. This type of energy balance concepts to calculate ablation have been used in IMJA glacier by Shrestha (2008) and Kayastha et al. (1999) used the same mass balance model based on energy balance at the snow or ice surface in the small glacier, AX010 in Nepalese Himalayas, considering the process that affected absorption of radiation.

Because of simplicity and reasonably good results, the degree day concept has been used by many authors. Laumanna and Reeh (1993) and Johnnesson et al. (1995) also applied the degree day method for estimating melts rates on different glaciers in Iceland, Norway, and Greenland. Similarly, Braithwaite and Zhang (2000) and Hock (1999) used PDD method for sensitivity analysis of Swiss and Swedish small glaciers. Kayastha et al. (2005) used the classical degree day method to estimate snow and ice melt in Langtang and Lirung Khola in Nepalese Himalayas. Annual discharges were calculated using positive degree day with monthly mean air temperature and monthly total precipitation in consideration of types and depth of debris layer too.

### 2.9 Selection of Precipitation and Runoff Models

The result of runoff from the glacier fed streams, the melting portion of snow or ice from glacier, as discussed above, is then added to precipitation over the region is calculate. There are many Rainfall (Precipitation)-Runoff model to transform the precipitation to runoff, ranging from black box i.e. simple system method (Unit hydrograph, regression, transformation model etc.) to conceptual model (Crawford, tank, SRM, HEC models etc.) and then to more rigorous i.e. physical model (SHE Model, IHDM). Conceptual models use some physical process like infiltration, evaporation, snow melt etc. and calculate calibration parameter for the input output relationship. Physically based models such as: lumped, semi distributed and distributed models are more rigorous and based on physical processes and equations for mass and energy transfer in the catchment with minimum measurable catchments characteristics. In lumped model, the whole catchment is assumed as one unit and a relationship between observed inputs and output are determined without considering any physics and spatial variability in the catchment. In distributed model, the catchments are divided into small segments called grid cells and consider all spatial and temporal variability in catchment as well as employing physically consistent formulation and parameters. The major drawback in lumped model is requiring extensive data, physics and equations and expertise. Semi distributed model is a bridge between these two extremes, i.e. distributed and lumped model. These models utilize the conceptual relationship for hydrological process with some simple equations. Nevertheless, snow and glacier melt should be added to the effective precipitation component in using the simple rainfall model in glacierized catchment basins as such models calculate runoff from rainfall data only. The models are described in detail in the following subsections.

#### 2.9.1 Lumped Model

Parameters of lumped hydrological models do not vary spatially within the basin and thus, basin response is evaluated only at the outlet without explicitly accounting for the response of individual sub basins. Parameters of lumped models often do not represent physical features of hydrologic process and usually involve certain degree of empiricism. The impact of spatial variability of model parameters is evaluated by using certain procedures for calculating effective values for the entire basin. The most commonly employed procedure is area weighted average (Haan et al. 1982). The representation of hydrologic process in lumped hydrologic models is usually very simplified; however they can often lead to satisfactory results, especially if the interest is in the discharge prediction only. They are capable of modeling the potential climate change impact on river basin water balance or seasonal snow accumulation and melt, for example IHACRES (Identification of unit Hydrograph and component flows from Rainfalls, Evaporation and Stream flow data), SRM (Snow Melt Runoff), WATBAL (Water balance Previously CLIRUN).

#### 2.9.2 Semi-distributed Model

There are two main types of semi-distributed model: a) Kinematic wave theory models (KW models), such as Hydrologic Engineering Center-Hydrologic Modeling System (HEC-HMS), and b) probability distributed models (PD models, such as TOPMODEL). The KW models are simplified versions of the surface and/or subsurface flow equation of physically based hydrologic models. In the PD models spatial resolution is accounted for by using probability distributed model is that their structure is more physically based than the structure of the lumped models, and that they are less demanding on input data than the fully distributed models. Some of such models are HBV-96 (Hydrologiska Byrans Vattenbalansavedelning), HEC-HMS, HFAM (Hydrocomp Forecast and Analysis Modeling), HSPF (Hydrologic Simulation Program-Fortran), PRMS (Precipitation-Runoff Modeling System), SSARR (Streamflow Synthesis and Reservoir Regulation), SWAT (Soil and Water assessment Tool), SWMM (Strom Water Management Model), TOPMODEL etc.

#### 2.9.3 Distributed Model

Parameters of distributed models are fully allowed to vary in space at a resolution usually chosen by the user. Distributed modeling approach attempts to incorporate data concerning the spatial distribution of parameter variations together with computational algorithms to evaluate the influence of this distribution on simulated precipitation- runoff behaviors. Distributed models generally require large amount of (often unavailable) data for parameterization in each grid cell. However, the governing physical processes are modeled in detail, and if properly applied, they can provide the highest degree of accuracy. Some examples of distributed models are CASC2D, CEQUEAU, GAWSER/GRIFFS, HYDROTEL, MIKE SHE, Waterloo Hydrological and Flood Forecasting System (WATFLOOD), TOPKAPI, Vflo etc.

There are numerous methodologies to simulate snowmelt runoff. These vary from the simple index methods to complex energy balance approaches. Among the various index methods, the temperature index models are the most frequently used in operational studies. In temperature index models, mean air temperature is used commonly to estimate the snowmelt runoff because air temperature data are readily

available climatologically as well as from operational hydro-meteorological networks. Furthermore, it stores most of climatic information and climate change pattern and it is probably the best single index to represent aerial snow cover change. The other main components of melt i.e. short wave radiation as well as sensible and latent heat have large variations due to topography and vegetation cover, and it is hard to obtain these data where hydro-meteorological measurements are scarce, as in Himalayan region. Additionally, the factors that determine the melt process are correlated with temperature or, in other words, the air temperature contains information on the major energy sources like net radiation, i.e. incoming long wave radiation which transfers information of air temperature to surface (Ohamura, 2001). The popularity of temperature index models also arises from the fact that they "give melt estimate that are comparable to those determined from a detailed evaluation of various terms in the energy equation" (Male and Gray 1981).

The SRM is a degree-day based temperature index model. It computes water production from snowmelt and rainfall, superimposes the value on the calculated recession flow, and transforms all together into daily discharge values (Martinec et al. 2007). The SRM has been used worldwide for over 100 basins in 25 countries in snow melt hydrological studies. Exponential relationship between the Snow Covered Area (SCA) values and the Cumulative Mean Daily Air Temperature (CMAT) (starting from melting season) for interpolating the SCA in period of no satellite imagery and the importance of dating of satellite images can be generated. Despite the simplicity of the degree-day method, the reported studies prove its utility for simulation or forecasting of river discharges induced from snowmelt (Singh and Kumar, 2001; Martinec et al. 2007).

#### 2.10 General Circulation Model (GCM)

These are used to simulate changes in temperature, precipitation and other climate variables at the global and regional scales as a function of increasing greenhouse gas concentrations and other drivers. These model results are used to project future changes under the alternative scenarios (i.e., different assumptions about future greenhouse gas emissions). While GCMs are valuable for modeling climate change at such scales, they are too coarse to capture factors that influence climate at the scale of

individual countries. Hence downscale product are implied for point or small scale studies (Detail in 3.4.2)

#### 2.11 Runoff Generation

Catchment runoff is the best measured water balance component. However, runoff generation is yet not fully understood. There is still scientific debate on the role of overland, subsurface and groundwater flows in runoff generation and its mechanisms. Disastrous floods can be caused by unusual combinations of hydro-meteorological factors and river basin conditions that have not been observed during a long observation period. Physically-based models of runoff generation enable one to find dangerous possible combinations of hydro meteorological factors and to estimate the risk of extreme floods discharge that may be from snowmelt or rainfall depending on the river basin area and the runoff generation mechanism. Monthly water-balance models have been used as a means to examine the various components of the hydrologic cycle (for example, precipitation, evapo-transpiration, and runoff). The water-balance model analyzed the allocation of water among various components of the hydrologic system using a monthly accounting procedure based on the methodology originally presented by Thornthwaite (Thornthwaite, 1948; Mather, 1978, 1979; McCabe and Wolock, 1999; Wolock and McCabe, 1999).

# **CHAPTER 3 MATERIALS AND METHODS**

## 3.1 Study Area

Three watershed areas are selected for comparing the impact of climate change on flow regime. They are;

- 1. Modi Khola River Basin (Annapurna region)
- 2. Langtang Khola River Basin (Langtang region)
- 3. Dudhkoshi River Basin (Khumbu region)

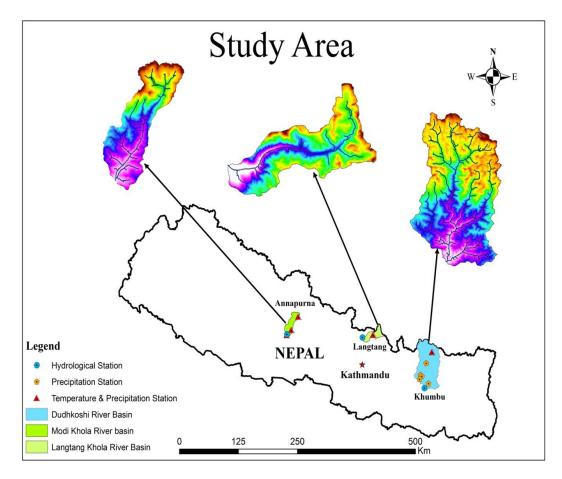


Figure 3.1.1 Study area

#### 3.1.1 Modi Khola River Basin

Modi Khola river basin is located in the Annapurna region in Gandaki zone of Western Development region of Nepal. Modi Khola river is one of the major tributaries of Kaligandaki river basin. It is bordered by Mardi and Seti rivers in the east, by Marshayangdi basin in the north and by Kaligandaki basin in the west and south. The Modi Khola river basin of area 676.8 km<sup>2</sup> extends up to Kaligandati confluence. However, only about 640.79 km<sup>2</sup> of the watershed is considered in this study. The upper part of the basin attracts tourism while lower part is endowed with extensive agricultural land and hydropower projects. Glacier starts at 4130 meter and is characterized mainly by debris cover. Study area covers the lateral moraine ridge of the Annapurna South Glacier and extends up to Machapuchhre base camp where the end moraine is located.

In this study, data from Modi Khola river basin hydrological station at latitude 28.12 N and Longitude 83.42 E and meteorological stations (Table 3.3-1) at latitude 28.13 N to 28.31 N and Longitude 83.42 E to 83.57 E are used (Figure 3.1.1 and Appendix II, Figure 1).

#### 3.1.2 Langtang Khola River Basin

The Langtang Khola river basin has area of 583.41 km<sup>2</sup> and is located approximately 100 km north of Kathmandu. The elevation of study area ranges from Syaprubesi 1434 masl up to the peak of Langtang Lirung at 7234 masl with an average altitude of 4334 masl. In total, 26 % (153.14 km<sup>2</sup>) of the catchment is glacierized. The glacier tongues below 5200 masl is 32 km<sup>2</sup> and are generally debris covered (Immerzeel et. al, 2011). The main valley is divided by the Langtang Khola River and it is typically U-shaped. In the Langtang Khola catchment, about 78 % of annual precipitation of 634 mm y<sup>-1</sup> falls during monsoon season.

In this study, data from Syaprubesi hydrological station at latitude 28.16 N and Longitude 85.35 E and Langtang Kyanging meteorological station (Table 3.3-1) at latitude 28.22 N and Longitude 85.62 E are used (Figure 3.1.1 and Appendix II, Figure 2).

#### 3.1.3 Dudhkoshi River Basin

Dudhkoshi river basin has an area of  $3710.30 \text{ km}^2$  and is situated in the Khumbu area in Eastern region of Nepal, which covers three districts viz. Khotang, Okhaldhunga and Solukhumbu. Basin elevation ranges from 439 amsl to 8848 amsl and 415.09 km<sup>2</sup> area is glacier covered, which is 11.18 % of the total area of the basin. Within the basin, the glacier area ranges from 4347 amsl to 8136 amsl. Dudhkoshi river basin is the main tributary of Saptakoshi river basin, which has seven major tributaries, namely: Sunkoshi, Tamakoshi, Dudhkoshi, Indrawati, Arun, Likhu and Tamur rivers. The Dudhkoshi river joins Sunkoshi river at Harkapur and then Sunkoshi river joins Arun and Tamur rivers at Tribeni, downstream of which is called Saptakoshi. At Barahchhetra, it descends from mountain and then called simply Koshi River. These tributaries encircle Mount Everest from all the sides and are fed by one of the world's highest glaciers, Khumbu Glacier. Further downstream, at Tribeni the river cuts a deep gorge across the Lesser Himalayan Range of the Mahabharat Lekh and then passes through a plain near Chatara. After flowing for another 58 km it enters North Bihar plains of India near Bhimnagar and after another 260 km, inters into the Ganges. The river travels a distance of 729 km from its source to its confluence into the Ganges (Rao, 1975).

In this study, data from Rabuwa Bazar hydrological station at latitude 27.16 N longitude 86.65 E and Khumbu region meteorological stations (Table 3.3-1) latitude 27.21 N to 27.89 N and longitude 86.45 E to 86.83 E are used (Figure 3.1.1 and Appendix II, Figure 3).

#### **3.2** Watershed characteristics of the three basins

Watershed characteristics depend upon the peak discharge, time variation of runoff (hydrograph), stage versus discharge, total volume of runoff, frequency of runoff (statistics and return period). However, in this study, flow regime of all three river basins is dependent on monsoon storms, glacier area and its melting contribution. In Nepal flow regime is divided into seven drainage basins: the Kankai Mai River Basin, the Koshi River Basin, the Bagmati River Basin, the Narayani River Basin, the West Rapti River Basin, the Karnali River Basin, and the Mahakali River Basin Figure 3.2.1. Among them only three sub river basins viz; Modi Khola, Langtang Khola and

Dudhkoshi river basins are considered for this study. In the Modi Khola river basin, highest glacier area was found in between 2550 m to 5750 m (Figure 3.2.2). The highest glacier area in the Langtang Khola river basin was found in-between 5434 m to 5934 m (Figure 3.2.3). Finally, the Dudhkoshi river basin had the highest glacier area in-between 4500 m to 5000 m 413.2 sq km (Figure 3.2.4).

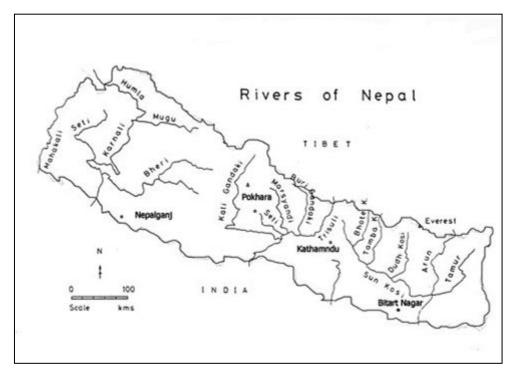


Figure 3.2.1 Major river system of Nepal

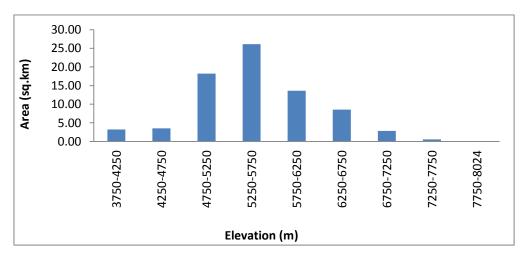


Figure 3.2.2 Glacier area and elevation of Modi Khola river basin

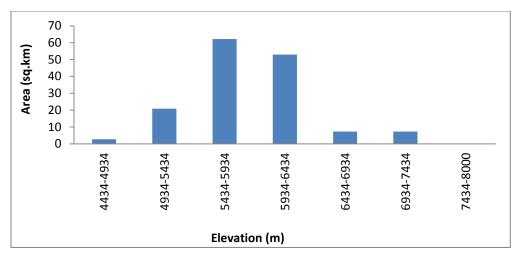


Figure 3.2.3 Glacier area and elevation of Langtang Khola river basin

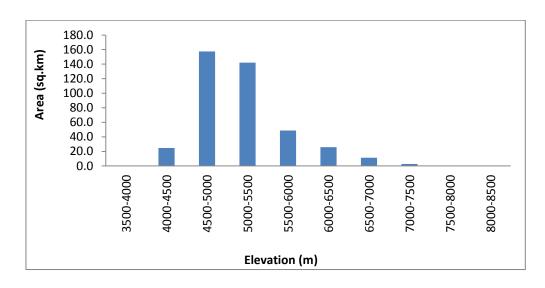


Figure 3.2.4 Glacier area and elevation of Dudh Koshi river basin

## 3.3 Research Methodology

For the protection of environment, climate and water studies play key role. Therefore, the following methods are applied for climate change flow regime analysis;

- Selection of the study basins: Modi Khola river basin (Annapurna region), Langtang Khola river basin (Langtang region) and Dudhkoshi river basin (Khumbu region) were selected for study. These selections are based on availability of relatively better Hydro-meteorological data compared to other regions of Nepal Himalayas.
- Downloading SRTM DEM data (http://www.cgiar-csi.org/data/srtm-90mdigital-elevation-database-v4-1) and separation of the study basin was done by

GIS software. The SRTM digital elevation data, produced by NASA originally, is a major breakthrough in digital mapping of the world, and provides a major advance in the accessibility of high quality elevation data for large portions of the tropics and other areas of the developing world.

- Collection of daily Hydro- Meteorological data.
- Evaluation of data quality and classification into seasons : Winter (DJF) December of the previous year to February, Spring - (MAM) March to May, Summer -(JJAS) June to September and Autumn -(ON) October to November.
- Calibration of SDSM.
- Validation of SDSM.
- Generation of temperature and rainfall scenario by SDSM.
- Comparison of the observed and modeled data.
- Bias correction.
- Hydrological modeling in HVB-light 3.0.
- Calibration of HVB-*light 3.0* model.
- Validation of HVB-*light 3.0* model.
- Generation of discharge scenario.
- Computation of seasonal trends of rainfall and discharge.
- Comparison of the seasonal trend of basins characteristics.
- Comparison of water balance of basins.

## 3.3.1 Collection of daily Hydro- Meteorological data

Data from five climatic stations, six precipitation stations and three hydrological stations were selected for this study. The lowest elevation of hydrological station considered is from Dudhkoshi river basin which is situated at 460 amsl altitude, whereas highest station is from Langtang Khola river basin at 1434 amsl. Modi Khola river basin is situated at 667 amsl. The details of these stations are presented in Table 3.3-1.

<b>Table 3.3-1</b> Conection of addry Hydrological and meteorological add								
Station name	Туре	Latitude (N)	Longitude (E)	Elevation (m)	Area (Km <sup>2</sup> )	Record Period		
Machhapuchhre	Climatic	28.31	83.57	3470		1987-2009		
Lumle*	Climatic	28.18	83.48	1740		1969-2009		
Parbat*	Precipitation	28.13	83.42	891		1969-2009		
Modi**	Hydrological	28.12	83.42	667	640.79	1991-2008		
Langtang*	Climatic	28.22	85.62	3920		1987-2010		
Sabrubasi**	Hydrological	28.16	85.35	1434	583.14	1994-2010		
Dingboche Khumbu*	Climatic	27.89	86.83	4355		1987-2009		
Chaurikhark*	Precipitation	27.42	86.43	2619		1949-2009		
Parkarns*	Precipitation	27.26	86.34	1982		1948-2009		
Aiselukhark*	Precipitation	27.21	86.45	2143		1948-2009		
Okhaldhunga*	Climatic	27.32	86.50	1720		1948-2009		
Mane Bhanjyang*	Precipitation	27.29	86.25	1576		1948-2009		
Salleri*	Precipitation	27.3	86.35	2378		1948-2009		
Dudhkoshi Rabuwa**	Hydrological	27.16	86.65	460	3710.3	1964-2008		

 Table 3.3-1 Collection of daily Hydrological and meteorological data

Meteorological Station\*, Hydrological station\*\*

#### **3.3.2 Data quality control**

The time-series data are considered to be acceptable only if they satisfy some level of quality control (WMO, 1988). For trend analysis (Section 3.3.3), the annual value was computed from daily values. In this study, annual meteorological data was kept blank if there was missing values in the series for any period, because the Sen's slope estimation method allows estimating the trend with missing values. The double-mass analysis (or sometimes called double-sum analysis) is useful method for assessing homogeneity in a weather parameter (Allen et al. 1998, Raghunath 2006, Silveira 1997). This is a useful tool for checking the consistency of climatic variable where the error is caused due to various reasons, such as change in environment (or exposure) of a station such as planting of trees or cutting of nearby forest, which affects the catch of the gauge due to change in the wind pattern or exposure. The replacement of instruments with new methods might also bring such deviation (Raghunath 2006).

**Homogeneity test:** Homogeneity tests are carried out by using Raghunath procedure for the daily data. This requires data series from two weather stations, where  $X_i$  (i = 1, 2,..., n) in a chronological data set for a given variable observed for a certain time

length at a "reference" station, and which is considered to be homogeneous. Similarly,  $Y_i$  is a dataset of the same variable, with the same time duration, observed at another station and for which homogeneity needs to be analyzed. In this technique, starting with the first observed pair of values  $X_1$  and  $Y_1$ , cumulative data sets are created by progressively summing values of  $X_i$  and  $Y_i$  to verify whether the long-term trends in variation of  $X_i$  and  $Y_i$  are the same. This is typically applied as a graphical procedure. The graphical application of the double-mass analysis is done by plotting all the coordinate points from cumulative values ( $x_i$  and  $y_i$ ). The plot is then visually analyzed to determine whether successive points of two stations follow a unique straight line, indicating the homogeneity of the data set  $Y_i$  relative to data set  $X_i$ . If there appears to be any break line or deviation in the plot of  $x_i$  and  $y_i$ , then there is a visual indication that the data series  $Y_i$  (or perhaps  $X_i$ ) is not homogeneous (Allen et al. 1998). Two reference stations (Lumle and Okhaldhunga) with relatively long time period and less or no data gaps were chosen for the test.

For the annual data, homogeneity test was conducted using a software named Rainbow. Frequency analysis of data requires the data be homogeneous and independent. The restriction of homogeneity assures that the observations are from the same population. One of the tests of homogeneity (Buishand, 1982) is based on the cumulative deviations from the mean:

$$S_k = \sum_{i=1}^{K} (X - X_{avg})$$
 K=1,..., n 3.3.1

where Xi are the records from the series  $X_1, X_2, ..., X_n$  and  $X_{avg}$  the mean. The initial value of  $S_k=0$  and last value  $S_k$  =n are equal to zero. When plotting the Sk's (also called a residual mass curve) changes in the mean are easily detected. For a record Xi above normal the  $S_k$  =i increases, while for a record below normal  $S_k$  =i decreases. For a homogenous record one may expect that the Sk 's fluctuate around zero since there is no systematic pattern in the deviations of the Xi's from their average value  $X_{avg}$ . The example of homogeneity test for observed temperature and precipitation at selected station example is shown in following Figure 3.3.1.

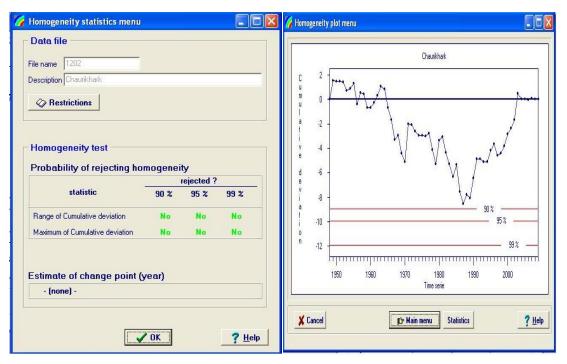


Figure 3.3.1 Homogeneity test by Rainbow software.

**Consistency test:** Mann-Kendall tests are non-parametric tests for the detection of trend in a time series. These tests are widely used in environmental science, because they are simple, robust and can cope with missing values and values below a detection limit. This test was first proposed by Mann in 1945 and by Kendall in 1975 and then afterwards in 1981 co-variances between Mann-Kendall statistics were proposed by Dietz and Kileen (1981). In 1982 Hirsch and Slack extended it to include seasonality. Similarly, the slope of a linear trend can be estimated with the nonparametric Sen's method (Gilbert, 1987). This method has advantage of not being greatly affected by single data errors or outliers. Mann-Kendall test and Sen's slope estimator are used in its original form.

Mann-Kendall test: The univariate MK statistic for a time series  $\{Zk, k = 1, 2, ..., n\}$  of data is defined as

$$S = \sum_{j < i} \operatorname{sgn}(Z_i - Z_j)$$
3.3.2

where

$$sgn(x) = \begin{cases} 1, & if \ x > 0\\ 0, & if \ x = 0\\ -1, & if \ x < 0 \end{cases}$$

Ho, i.e. the observations  $Z_i$  are randomly ordered in time, against the alternative hypothesis, H1, where there is an increasing or decreasing monotonic trend. For time series with less than 10 data points the S value is directly used, and for time series with 10 or more data points the normal approximation is used. However, if there are several tied values (i.e. equal values) in the time series, it may reduce the validity of the normal approximation when the number of data values is close to 10. The statistic S is approximately normally distributed with

$$E(S) = 0 \qquad Var[S] = \frac{n(n-1)(2n+5) - \sum_{p=1}^{q} t_p(t_p-1)(2t_p+5)}{18} \qquad 3.3.3$$

Where q is the number of tied groups and  $t_p$  is the size of the p<sup>th</sup> tied group. The values of S and VAR(S) are used to compute the normal standardized test statistic Z as follows:

$$z = \frac{s+1}{\sqrt{VAR(S)}}$$
 if  $s > 0$  3.3.4

z=0 if s=0

$$z = \frac{s+1}{\sqrt{VAR(S)}}$$
 if  $s < 0$  3.3.5

The presence of a statistically significant trend is evaluated using the Z value. To test for either an upward or downward monotone trend (a one-tailed test) at  $\alpha$  level of significance, H<sub>0</sub> (no trend) is rejected if the absolute value of Z is greater than Z<sub>1- $\alpha$ </sub>, where Z<sub>1- $\alpha$ </sub> is obtained from the standard normal cumulative distribution tables.

**Sen's method**: If a linear trend is present in a time series, then the true slope (change per unit time) can be estimated by using a simple nonparametric procedure developed by Sen (1968). This means that linear model f (t) can be described as

$$f(t) = Qt + B$$
 3.3.6

Where Q is the slope and B is a constant. To derive an estimate of the slope Q, the slopes of all data pairs are calculated.

$$Q_{i} = \frac{Z_{j}-Z_{k}}{(j-k)} \text{ where } j > k$$

$$3.3.7$$

If there are n values  $Z_j$  in the time series we get as many as N = n(n-1)/2 slope estimates  $Q_i$ . The Sen's estimator of slope is the median of these N values of  $Q_i$ . The N values of  $Q_i$  are ranked from the smallest to the largest and the Sen's estimator is

$$Q = \begin{cases} \frac{Q_{N+1}}{2} \text{ if N is odd} \\ \frac{1}{2} \left\{ Q_{\frac{N}{2}} + Q_{\frac{N+2}{2}} \right\} \text{ if N is even} \end{cases}$$
 3.3.8

Above equations were used for Mann Kendall test and Sen's slope estimation in this study. The normal variate statistics (Z) and Sen's slope were obtained from the calculation for each month and also for annual time series. The presence of a statistical significance of trend was evaluated using the Z value.

To test for either an upward or downward monotone trend (a one-tailed test) at  $\alpha$  level of significance, H<sub>0</sub> (no trend) was rejected if the absolute value of Z is greater than Z<sub>1- $\alpha$ </sub> where Z<sub>1- $\alpha$ </sub> was obtained from the standard normal cumulative distribution tables. The significance level 0.05 means that there is a 5 % probability that the values Z<sub>i</sub> are from a random distribution and with that probability we make a mistake when rejecting H<sub>0</sub> of no trend. Sen's slope is available as average change per year; negative value indicates negative trend and positive value positive trend shown in Table 3.3-2.

Station name	Consistency test	Homogeneity test	Accept Or Reject	Data record length	Data reject Year
Macapuchhre	ok	ok	Accept	1987-2009	No
Lumle	ok	ok	Accept	1969-2009	No
Parbat	ok	ok	Accept	1969-2009	No
Modi	ok	ok	Accept	1991-2008	No
Langtang	ok	ok	Accept	1987-2010	No
Sabrubasi	ok	ok	Accept	1994-2010	No
Dingboche Khumbu	ok	ok	Accept	1887-2009	No
Chaurikhark	ok	ok	Accept	1949-2009	1952 missing
Parkarns	ok	Not	Reject	1948-2009	No
Aiselukhark	ok	ok	Accept	1948-2009	No
Okhaldhunga	ok	ok	Accept	1948-2009	1958 missing
Mane Bhanjyang	ok	Not	Reject	1948-2009	No
Salleri	ok	ok	Accept	1948-2009	1962-1972 missing
Dudhkoshi	ok	ok	Accept	1964-2008	No

Table 3.3-2 Data Consistency and Homogeneity checking

### 3.3.3 Trend Analysis

To test the hypothesis of whether or not a long-term trend in time series data exists, the trend analysis is broadly divided into parametric and non-parametric. There are several methods available in both these categories which are well described by Helsel and Hirsch (1992). The parametric method is a simple linear trend which can be computed using a linear equation and assumes that the data follows normal distribution. In this study, the non-parametric rank-based Mann-Kendall (MK) test (Mann 1945, Kendall, 1975) has been chosen. The non-parametric test for trend makes no assumption about the distribution of the data. Therefore, distribution free test is useful for monotonic trend detection. MK test is based on sign differences rather than value, and is robust against the effect of extreme values and outliers (Helsel and Hirsch, 2002). Many researchers have found the MK test as an excellent tool in similar applications (Gemmer et al. 2004, Hamed 2008, Sharma et al. 2000b). MK test is based on the difference ( $x_i - x_j$ ) between successive years of data for a given period. A test statistic (S) is estimated as the summation of signs:

$$S = \sum_{i=1}^{n-1} \sum_{j=i+1}^{n} Sign(xi - xj)$$
 3.3.9

A Z value is then computed to estimate the significance level of the trend. The significance level increases with number of identical successive signs. Three different significance levels are used to test the annual trends of precipitation, temperature and discharge as shown below:

 $\alpha = 0.001$  or 99.9 percent confidence level (\*\*\*),  $\alpha = 0.01$  or 99 percent confidence level (\*\*) and  $\alpha = 0.05$  or 95 percent confidence level (\*)

The significance level 0.001 means that there is a 0.1 percent probability that the values xi are from a random distribution and with that probability we make mistake when rejecting  $H_0$  of no trend. Thus the significance level 0.001 means that the existence of a monotonic trend is very likely (Helsel and Hirsch, 1992).

To estimate the true slope of an existing trend (as change per year), the nonparametric Sen's method (Sen 1968) was used. This method calculates the median of all possible pairwise slopes. This procedure is particularly useful since missing values are allowed during the analysis. The Sen's method can be used in cases where the trend can be assumed to be linear.

#### **3.4 Data collection Methodology**

Observed meteorological (maximum and minimum temperatures, precipitation and evaporation) and hydrological (water level and discharge) data for Modi Khola, Langtang Khola and Dudhkoshi (1948 to 2010) were collected from DHM, government of Nepal, the detail of which is shown in Table 3.3-1. The glacier coverage data of these basins were collected from ICIMOD.

#### 3.4.1 Meteorological data

In this study, observed Hydro-Meteorological information is necessary as an input in hydrological model development as well as in the performance evaluation (verification) of the model outputs. To fulfill these objectives, Meteorological data from 1961-2009 was used in which the number of meteorological variables collected varies from station to station depending on their types. Some stations contain only rainfall data whereas some stations include maximum and minimum temperatures and evaporation data. Monthly mean of potential evapo-transpiration required to run the model was calculated by using Penman method CROPWAT 8.

#### 3.4.2 SDSM modeling

General Circulation Models (GCMs) indicate that rising concentrations of global warming will have significant implications for climate at global and regional scales. Unfortunately, GCMs are restricted in their usefulness for local impact studies by their coarse spatial resolution (typically of the order 50,000 km<sup>2</sup>) and inability to resolve important sub–grid scale features such as clouds and topography. As a consequence, two sets of techniques have emerged as a means of deriving local–scale surface weather from regional–scale atmospheric predictor variables (Figure 3.4.1). Firstly, statistical downscaling is analogous to the "model output statistics" (MOS) and "perfect prog" approaches used for short–range numerical weather prediction Lu et al. (2007). Secondly, Regional Climate Models (RCMs) simulate sub–GCM grid scale climate features dynamically using time–varying atmospheric conditions supplied by a GCM bounding a specified domain. Both approaches will continue to play a significant role in the assessment of potential climate change impacts arising from future increases in greenhouse–gas concentrations.

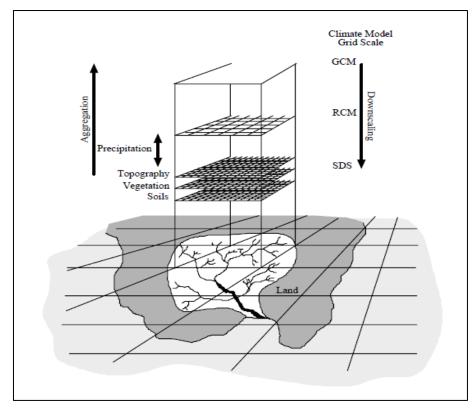


Figure 3.4.1 Schematic illustrating the general approach to downscaling

### (Source: Wilby and Dawson, 2007)

Statistical Downscaling method has several practical advantages over dynamical downscaling approach. In situations where low–cost, rapid assessments of localized climate change impacts are required, statistical downscaling represents the more promising option at present. Statistical downscaling methodology enables the construction of climate change scenarios for individual sites at daily time–scales, using grid resolution GCM output. In addition, this method has also advantage of filling up the missing data for temperature and precipitation. The software used is SDSM (Statistical Down Scaling Model) and is coded in Visual Basic 6.0. (Wilby and Dawson, 2007).

The GCM data are available from the NCEP/NCAR reanalysis product. The NCEP/NCAR reanalysis products Kalnay et al. (1996) and Kistler et al. (2001) have been interpolated onto the CGCM3 Gaussian Grid, and made available for the calibration procedure of statistical downscaling models. The NCEP/NCAR reanalysis use a T62 (~ 209 km) global spectral model to consistently collect observational data from a wide variety of observed sources. All the data included are of quality 'A' or

'B', which means that they are influenced directly (to some extent) by observational data. Details of the reanalysis project and this categorization scheme can be found in Kalnay et al. (1996). All NCEP/NCAR data has been averaged on a daily basis from 6 hourly data, before being linearly interpolated to match the CGCM3 data.

#### 3.4.3 SDSM Calibration and validation

Observed daily precipitation data are available for the period 1987 to 2009 in Annapurna (Machapuchhre), Langtang (Kyaging) and Khumbu (Dingboche). Consequently, observed and CGCM3 data from 1987 to 1995 were utilized for SDSM calibration and data from 1996 to 2003 were used for its validation (NCEP data were available only up to 2003). Statistical Downscaling Model (SDSM 4.2.2), a decision support tool for the assessment of regional climate change impact, which is a hybrid of the stochastic weather generator and transfer function methods and developed by Robert L. Wilby and Christian W. Dawson (2007) in the United Kingdom, is chosen for developing daily climate scenario study.

In Annapurna, Langtang and Khumbu only three high Himalaya stations have observed daily precipitation data (1987-2009). These data are used for SDSM downscaling Table 3.4-1. Hence, observed precipitation and NCEP predictor data are utilized for SDSM calibration (1987-1996) and validation (1996 -2003). The model captures the annual cycles well.

Observed temperature and precipitation data are plotted against modeled output to calculate coefficient of determination ( $R^2$ ) as shown in the Appendix (IV), from Figure 3.3.2 to Figure 3.3.19. The  $R^2$  value greater than 0.90 is very highly significant, 0.70 to 0.89 is highly significant, 0.50 to 0.69 is moderately significant, 0.30 to 0.49 is low significant and less than 0.20 cannot be considered as significant. The plotted result obtained from SDSM (model) and observed temperature and precipitation data ( $R^2$ ) is shown in Table 3.4-2.

Study area	Year	Observed	Down scale CGCM3 Model	Obs GRID (DHM)	Projected PRECIS HadCM3	TRMM
Modi Khola river basin	1990-2008	2459	2434	1734	3308	1958
Langtang Khola river basin	1990-2008	670	652	938	2616	1455
Dudhkoshi river basin	1990-2008	494	507	1694	2212	1398

Table 3.4-1 Comparisons of average annual precipitation in three basins

Figure No	Region	Downscaled Parameters	Calibration R <sup>2</sup>	Validation R <sup>2</sup>
3.3.2	Annapurna	Maximum Temperature (Tmax)	0.96	
3.3.3	Annapurna	Maximum Temperature (Tmax)		0.87
3.3.4	Annapurna	Minimum Temperature (Tmin)	0.98	
3.3.5	Annapurna	Minimum Temperature (Tmin)		0.97
3.3.6	Langtang	Maximum Temperature (Tmax)	0.83	
3.3.7	Langtang	Maximum Temperature (Tmax)		0.62
3.3.8	Langtang	Minimum Temperature (Tmin)	0.92	
3.3.9	Langtang	Minimum Temperature (Tmin)		0.80
3.3.10	Khumbu	Maximum Temperature (Tmax)	0.64	
3.3.11	Khumbu	Maximum Temperature (Tmax)		0.59
3.3.12	Khumbu	Minimum Temperature (Tmin)	0.89	
3.3.13	Khumbu	Minimum Temperature (Tmin)		0.82
3.3.14	Annapurna	Precipitation (PPT)	0.92	
3.3.15	Annapurna	Precipitation (PPT)		0.94
3.3.16	Langtang	Precipitation (PPT)	0.68	
3.3.17	Langtang	Precipitation (PPT)		0.82
3.3.18	Khumbu	Precipitation (PPT)	0.77	
3.3.19	Khumbu	Precipitation (PPT)		0.87

*Table 3.4-2* The value of Coefficient of determination  $R^2$ 

#### 3.4.4 Bias correction methodology

The results from GCMs and RCMs always show some degree of biases for both temperature and precipitation data. The reasons for such biases include systematic model errors cause by imperfect conceptualization, discretization and spatial averaging within the grids. The bias correction approach is used to eliminate the biases from the daily time series of downscaled data (Salzmann et al. 2007). In this study, equations 3.4.1 and 3.4.2 are used to de-bias daily temperature and precipitation data (Mahmood et.al. 2012).

$$T_{deb} = T_{SCEN} - \overline{(T_{CONT} - \overline{T_{obs}})}$$
 3.4.1

$$P_{deb} = P_{SCEN} \times \left(\frac{\overline{P_{obs}}}{\overline{P_{CONT}}}\right)$$
 3.4.2

Where,  $T_{deb}$  and  $P_{deb}$  are bias corrected daily temperature and precipitation respectively.  $T_{SCEN}$  and  $P_{SCEN}$  are daily temperature and precipitation obtained from downscale data (SDSM).  $\overline{T_{obs}}$  and  $\overline{P_{obs}}$  are long term monthly mean of observed temperature and precipitation respectively, while  $\overline{T_{CONT}}$  and  $\overline{P_{CONT}}$  are long term monthly mean of temperature and precipitation simulated using SDSM for observed period.

Several methods of bias corrections have been proposed to improve the quality of **GCM** data for hydrological analysis purposes, such as linear scaling of precipitation and temperature, local intensity scaling (**LOCI**) of precipitation, power transformation of precipitation, variance scaling of temperature, distribution mapping of precipitation and temperature and delta-change correction of precipitation & temperature (Teutschbin et al. 2012). Both precipitation and temperature output obtained by statistical downscaling SDSM data were bias corrected for the calibration period 1988 to 1996 and validation period 1996 to 2003. The validation of the bias corrected temperature and precipitation data is shown in Appendix (IV), (Figure 1 to Figure 9).

#### 3.4.5 SDSM Application

GCMs simulated climate predictors are the basis for developing future climate scenarios at a given location using statistical downscaling method. Results using the climate change predictors from different GCMSs or from the same GCMS with different emission scenarios can be very different. It is thus suggested that predictors from a few different climate change scenarios be used in order to incorporate the uncertainties. In this study, source of daily observed predictor variables was the National Centre for Environmental Prediction (NCEP) reanalysis data set. (Wave site detail can be refer: http://www.cics.uvic.ca/scenarios/index.cgi?Scenarios OR http://loki.qc.ec.gc.ca/DAI/gcm\_CGCM3-e.html). Various steps involved in the application of SDSM for downscaling of GCM products are data preparation, screening of predictor variables, model calibration, weather and scenarios generation and statistical analysis. NCEP predictors were considered as the independent variables for multiple regression analysis and climate observation as the dependent variable. Significant predictors were selected, which is shown in Table 3.4-3.

Finally, optimization of the model was completed by applying ordinary least squares method. In above analyses, observed and NCEP data sets have year length of 365 (366 in leap years) days. Meteorological data used in this study include daily precipitation, daily maximum temperature and daily minimum temperature of Annapurna, Langtang and Khumbu.

Parameters	Annapurna	Langtang	Khumbu	
	<b>P</b>	8		
Maximum	Mean sea level	500 hPa	Surface vorticity,	
temperature	pressure and	geopotential height	500 hPa divergence	
(Tmax)	850 hPa	and 850 hPa	and 850 hPa	
	geopotential height	geopotential height	geopotential height	
	geopotential height			
Minimum	Mean sea level	500 hPa	Mean sea level	
temperature (Tmin)	pressure, 500 hPa	geopotential height	pressure, Surface	
	meriodional	and 850 hPa	velocity, 500 hpa	
	velocity, 500 hpa	geopotential heigh	geopotential height	
	geopotential height		and 850 hPa	
	and 850 hPa		geopotential height	
	geopotential height			
Mean temperature	Mean sea level	500 hPa	Mean sea level	
(Tmean)	pressure, 500 hPa	geopotential height	pressure, 500 hPa	
	meriodional	and 850 hPa	geopotential height	
	velocity, 500 hpa	geopotential heigh	and 850 hPa	
	geopotential height		geopotential height	
	and 850 hPa			
	geopotential height			
		5001D	50010	
Precipitation (PPT)	Surface meridional	500 hPa	500 hPa	
	velocity, 500 hPa	geopotential height	geopotential height	
	geopotential height	and 850 hPa	and 850 hPa	
	and 850 hPa	geopotential heigh	geopotential heigh.	
	geopotential heigh.			

.

Table 3.4-3 Predictors used in this research

#### **3.5** Catchment Data

The catchment data was generated from ArcGIS 9.3 by available SRTM DEM. The area was delineated after generation of catchment for the determination of catchment area. Elevation zones were generated in three river basins (Table 3.5-1) from the available data by the reclassification process.

Name of Study area	Elevation Range (m)	Drainage Area (Km <sup>2</sup> )	Calibration period	Validation period	No of Elevation Zone
Modi Khola river basin	750-7750	640.79	1991-1999	2000-2008	15
Langtang river basin	1434-7434	583.14	2002-2005	2006-2009	13
Dudhkoshi river basin	500-8848	4123.6	1965-1970	1970-1979	17
Dudhkoshi river basin	500-8848	4123.6	1980-1989	1990-2008	17

Table 3.5-1 HBV-Light-3.0 Model Calibration and Validation of three study area

The reclassified data was converted into the feature by raster conversion. The converted feature was then dissolved into fifteen elevation in Modi Khola river basin, thirteen elevation in Langtang Khola river basin and seventeen elevation in Dudhkoshi river basin and finally all the elevation zones were masked by the SRTM DEM data. The first procedure was repeated after masking the aspect map preparation for each of the elevation zone. The aspect were then reclassified and converted into feature in order to calculate area. Finally aspects were divided into three parts viz. North, South and East/West and area of each elevation with respect to aspect was generated. The same procedure was again carried out by ArcGIS 9.3 software, but this time for glacier and the catchment areas delineation. The detail characteristics of study area, DEM, elevation map, aspect and glacier areas are depicted in Appendix (II), Figures 1 to Figure 21.

Watershed delineation is the first step in HVB-*light 3.0* Hydrological Model and is followed by digitization of the catchment into hydrologic response units. Elevation zones were considered as primary hydrological units of the catchment and were divided into different vegetation zones. The version of HVB-*light 3.0* model used for this study allows dividing the catchment up to 20 elevation zones and into three

vegetation zones per elevation zone (Seibert, 2010). These zonings were done based on elevation and land cover data of the study areas using ArcGIS.

## 3.6 Hydrological Data

The daily stream flow data are essential to calibrate and validate the HVB-*light 3.0* Hydrological Model. The stream flow data (1991 to 2009) located at Naipaul representing Modi Khola river basin, data located at Syaprubesi (1994 to 2010) representing Langtang Khola river basin and data located at Rabuwa bazar (1964-2008) representing Dudhkoshi river basin were collected from the DHM. These data ware checked by several methods such as personal judgments, homogeneity test, significance test etc for errors. Small (one day) gaps of temperature and discharge data were filled by interpolation methods whereas longer gaps in daily temperature data were filled by SDSM output and large gap for daily discharge data was filled after the hydrological model simulation.

Table 3.6-1, summarize the statistically significant long-term trends of the stations data. Both increasing and decreasing trends can be observed. The Langtang Khola hydrological station at Syaprubesi showed a statistically significant trend with higher than 95 percent confidence level. However, the gauging stations at Modi Khola and Dudhkoshi hydrological stations are shows a statistically insignificant decreasing negative trend.

Time series	Data Record Iength	Trend (m <sup>3</sup> /sec/year)	Significant	Qmin99	Qmax99	Qmin95	Qmax95
Modi Khola	1991-2010	-0.30		-0.70	0.21	-0.52	0.06
Langtang	1994-2010	-0.38	**	-0.78	-0.06	-0.72	-0.25
Dudh Koshi	1991-2010	1.95		-1.88	6.84	-0.83	5.47

Table 3.6-1 Statistically significant trends of hydrological stations

 $\alpha = 0.01$  or 99 percent confidence level (\*\*)

## 3.7 HVB-light 3.0 Hydrological Model and its Structure

The HVB-*light 3.0* model is a conceptual hydrological model for continuous simulation of runoff. It was originally developed at the Swedish Meteorological and Hydrological Institute (SMHI) in the early 70s to assist hydropower operations

(Bergstrom and Graham, 1998) by providing hydrological forecasts. The model was named after the abbreviation of Hydrologiska Byråns Vattenbalans-avdelning (Hydrological Bureau Water balance-section). The HVB-*light 3.0* model simulates daily discharge using daily rainfall and temperature, and monthly estimates of potential evaporation.

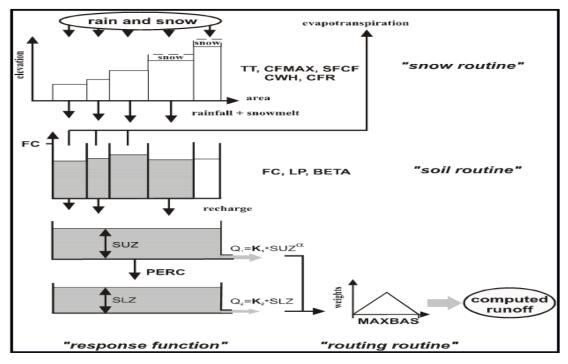


Figure 3.7.1 Structure of HVB-light 3.0 hydrological model.

The model consists of subroutines for snow accumulation and melt, soil moisture accounting procedure where groundwater recharge and actual Evapo transpiration are coupled, routines for response and transformation function for runoff generation and finally, a simple routing procedure. Further descriptions of the model can be found elsewhere (Bergstrom, 1992). The version of the model used in this study, "HVB-*light 3.0*" (Seibert, 1997), corresponds to the version HBV-96 described by (Bergstrom, 1992). The model simulates daily discharge using daily rainfall, temperature and potential evaporation as input. Precipitation is simulated to be either snow or rain depending on whether the temperature is above or below a threshold temperature, **TT** [°C]. All precipitation simulated to be snow, i.e. falling when the temperature is bellow **TT**, is multiplied by a snowfall correction factor, **SFCF** [-].

Snowmelt is calculated with the degree-day method by Equation 3.7.1. Melt water and rainfall is retained within the snowpack until it exceeds a certain fraction, CWH [-], of the water equivalent of the snow. Liquid water within the snowpack refreezes according to Equation 3.7.2. Rainfall and snowmelt (P) are divided into water filling the soil box and groundwater recharge depending on the relation between water content of the soil box (SM [mm]) and its largest value (FC [mm]), Equation 3.7. 3. Actual evaporation from the soil box equals the potential evaporation if SM/FC is above LP [-] while a linear reduction is used when SM/FC is below LP in Equation 3.7.4. Groundwater recharge is added to the upper groundwater box (SUZ [mm]). **PERC** [mm d<sup>-1</sup>] defines the maximum percolation rate from the upper to the lower groundwater box (SLZ [mm]). Runoff from the groundwater boxes is computed as the sum of two or three linear outflow equations depending on whether SUZ is above a threshold value, UZL [mm]Equation 3.7.5. This runoff is finally transformed by a triangular weighting function defined by the parameter MAXBAS from Equation 3.7.6 to give the simulated runoff  $[mm d^{-1}]$ . If different elevation zones are used the changes in precipitation and temperature with elevation are calculated using the two parameters PCALT [ %/100 m] and TCALT [ °C / 100 m] in Equations 3.7.7 and 3.7.8. The long-term mean of the potential evaporation,  $E_{pot,M}$  for a certain day of the year can be corrected to its value at day t,  $E_{pot}(t)$ , by using the deviations of the temperature, T(t), from its long-term mean,  $T_M$ , and a correction factor,  $C_{ET}$  [°C<sup>-1</sup>] (Equation 3.7.9).

$$melt = CFMAX(T(t) - TT)$$
3.7.1

$$Refreezing = CFR \ CFMAX(TT - T(t))$$
3.7.2

$$\frac{recharge}{P(t)} = \left(\frac{SM(t)}{FC}\right)^{BETA}$$
 3.7.3

$$E_{act} = E_{pot} \min\left(\frac{SM(t)}{FC.LP}, 1\right)$$
3.7.4

$$Q_{GW}(t) = K_2 SLZ + K_1 SUZ + K_0 \max(SUZ - UZL, 0)$$
 3.7.5

$$Q_{sim}(t) = \sum_{i=1}^{MAXBAS} c(i) Qw (t-i+1)$$

Where,

$$c(i) = \int_{i-1}^{i} \frac{2}{MAXBAS} - \left| u - \frac{MAXBAS}{2} \right| \frac{4}{MAXBAS} du \qquad 3.7.6$$

$$P(h) = P_0 \left( 1 + \frac{PCALT (h - h_0)}{10000} \right)$$
 3.7.7

$$T(h) = T_0 - \frac{TCALT(h-h_0)}{100}$$
3.7.8

$$E_{pot}(t) = (1 + C_{ET}) (T(t) - T_M))^{E_{pot}}, M$$

$$but \ 0 \le E_{pot} \ (t) \le 2E_{pot}, M \tag{3.7.9}$$

# 3.7.1 Schematic Model Structure

The Figure 3.7.2 to Figure 3.7.5 below gives an overview of the structure of the different routines within the model.

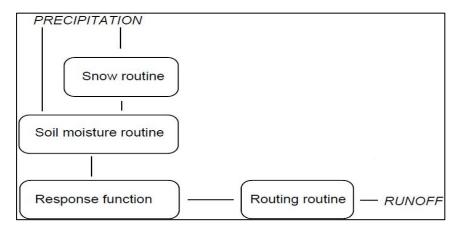


Figure 3.7.2 Schematic Model Structure

# 3.7.2 Snow Routine

The snow and glacier factor is controlled by snow routine which generates the snow melt and snow pack contributing runoff. The input data for the snow routine is precipitation and temperature and the output data is snow pack and snow melt. The detailed description of this routine is given below which includes parameter and its function.

 $CFMAX = degree-day factor (mm °C^{-1} day^{-1})$ 

CFR= refreezing coefficient

TT= threshold temperature (°C), Accumulation of precipitation as snow if temperature  $< T_T (T_T \text{ is normally close to 0 °C })$ 

Melt of snow starts if temperatures are above  $T_T$  calculated with a simple degree-day method.

melt water =  $C_{FMAX}$  (T-T<sub>T</sub>) (mm day<sup>-1</sup>)

 $C_{FMAX}$  varies normally between 1.5 and 4 mm  $^{\circ}C^{-1}$  day<sup>-1</sup> (in Sweden), with lower values for forested areas. As approximation, the values 2 and 3.5 can be used for  $C_{FMAX}$  in forested and open landscape respectively.

The snow pack retains melt water until the amount exceeds a certain portion (CWH, usually 0.1) of the water equivalent of the snow pack. When temperatures decrease below  $T_T$  this melt water refreezes again.

## Refreezing melt water = CFRCFMAX $(T_T-T)$

It has to be noted that all precipitation that is simulated to be snow is multiplied by a correction factor, SFCF. These calculations are carried out separately for each elevation and vegetation zone.

#### 3.7.3 Soil Moisture Routine

The soil moisture accounting routine is the main part controlling runoff formation. This routine is based on the three parameters:

- FC = maximum soil moisture storage (mm),
- LP = soil moisture value above which ET <sub>act</sub> reaches ET <sub>pot</sub>
- BETA= parameter that determines the relative contribution to runoff from rain or snowmelt (-)

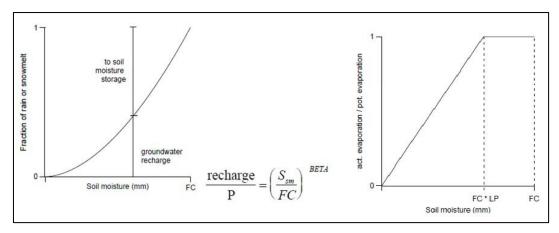


Figure 3.7.3 Soil Moisture Routine

where  $S_{sm}$  is computed soil moisture storage; and FC is a model parameter and not necessarily equal to measured values of 'field capacity'.

## 3.7.4 Response Routine

The model of a single linear reservoir is a simple description of a catchment where the runoff Q(t) at time t is supposed to be proportional to the water storage S(t).

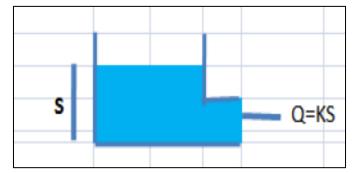


Figure 3.7.4 Realization of a single linear reservoir is a box with a porous outlet

A realization of a single linear reservoir is a box with a porous outlet, thus obtaining Equation 3.7.1 from Darcy's law.

Where S = storage (mm), Q = outflow (mm day-1), t = time (day) and k = storage (or recession) coefficient (day-1)

$$Q(t) = k \cdot S(t)$$
 3.7.10

The water balance equation of a catchment  $P(T) = E(t) + Q(t)\frac{ds(t)}{dt}$ , ignoring precipitation and evapo-transpiration, together with equation 3.7.1 differential equation gives solution function

$$Q(t) = Q(t_0) \cdot e_0^{(t_0-t)k}$$
 3.7.11

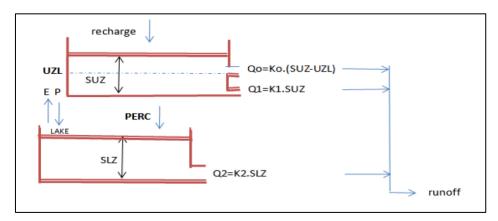


Figure 3.7.5 Response function and Response routine of the HBV model

Where,

recharge = input from soil routine (mm day<sup>-1</sup>)

SUZ = storage in upper zone (mm) and has no upper limit.

SLZ = storage in lower zone (mm)

UZL = threshold parameter (mm)

PERC = max. Percolation to lower zone (mm day<sup>-1</sup>)

 $Ki = Recession \ coefficient \ (day^{-1})$ 

 $Qi = runoff component (mm day^{-1})$ 

It has to be noted that SUZ has no upper limit, Q2 can never exceed PERC, and SLZ can never exceed PERC/K2

If ln Q is plotted against time during a dry period, the slopes of the hydrograph at different runoff values provide good first estimates of the response-function parameters.

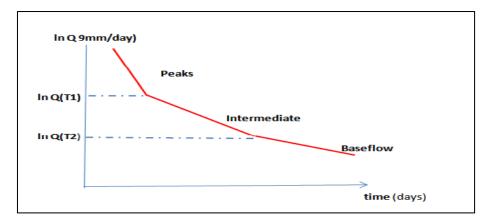


Figure 3.7.6 Schematic shape of recession in relation to the different parameter

Slope of the recession: -Peaks: K0 + K1 + K2 with thresholds  $Q(T1) \leq PERC+K1UZL$  and  $Q(T2) \leq PERC$ 

- Intermediate: K1 + K2,
- Base flow: K2

## 3.7.5 Routing Routine and Transformation Function

The generated runoff of one time step is distributed on the following days using one free parameter, MAXBAS, which determines the base in an equilateral triangular weighting function.

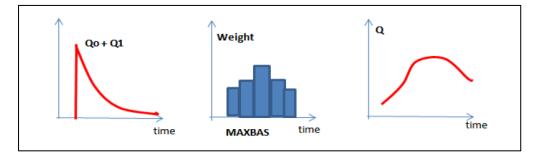


Figure 3.7.7 The transformation function (IHMS, 2006)

## 3.7.6 HVB-light 3.0 Model Data

Daily values of areal rainfall and areal temperature and potential evapo-transpiration are main input data of the model. The monthly mean potential evaporation was estimated using Penman-Monteith method to estimate PET (Allen et al. 1998) and the missing temperature was filled by using SDSM downscaling model. The glacier area is also necessary for computing output and Arc GIS version 9.3 was used for estimating aspect and area of glacier as well as vegetated area.

#### 3.7.7 History of HVB-light 3.0 for discharge modeling

More than 30 years back, the HVB model was used for the first time to simulate catchment runoff (Bergstrom, 1972). During the last decades the HBV model (Bergstrom 1976) has been further developed by the Swedish Meteorological and Hydrological Institute (SMHI) and has become widely used for runoff simulations in Sweden (Bergstrom, 1990; 1992). Moreover, the model has been applied, sometimes in modified versions, in about 30 countries. The HBV model is a conceptual, semidistributed, rainfall-runoff model. Seibert (2005) developed a new version called HBV light3.0, which is an easy to use Windows version for research and education. Seibert (2005) describe the model as follows: daily discharge is simulated by HBV light3.0 using daily rainfall, temperature and potential evaporation as input. The simulated catchment can be divided in twenty elevation and three vegetation zones. Each zone is sub-divided into three ordinate classes (north, south and east/west). Additionally this new version of the model differentiates between glacierized and non glacierized area; consists of the snow, soil, response and runoff generation (Routing) routines. The routines are applied to each HVB-light 3.0 class to generate the runoff at the outlet of the basin. The model does not require initial conditions and instead has a 'warming-up' period in which an initial state is reached.

### 3.7.8 HVB-light 3.0 Methodology for Model Calibration and Validation

Methodology: Present study builds on the work of Wang et al. (2006) to develop a methodology to be used with an ensemble of dynamically downscaled climate data to investigate the impacts of climate change on the hydrology of Irish rivers. Wang et al. (2006) used the HBV model (Bergstrom, 1992) from the Swedish Meteorological and Hydrological Institute (SMHI) which is usually calibrated using a manual trial and error approach. Here, it has been replaced by the HVB-*light 3.0* model of Seibert (2005) because its interface allows Monte-Carlo simulations. Calibration using Monte-Carlo methods yields an ensemble of simulations which allows accounting for parameter uncertainty in analysis. A Monte-Carlo approach to calibration was used, in

which the 99<sup>th</sup> percentile of an ensemble of 10,000 parameter sets were selected for use in the impact study. This approach allows the inclusion of parameter uncertainty in the study, and provides a range of possible values rather than a single value which further allows an estimation of confidence in the research outcome. The HVB-*light* 3.0 model was validated for a reference period (1961–2000) to ensure that stream flow was modeled correctly. A persistent positive bias in the downscaled precipitation was observed and removed to improve the agreement between modeled and observed stream flow. It was shown that the impact of parameter uncertainty on the validation of seasonal (winter and summer) flow was less significant than in the annual maximum daily mean flow.

To investigate the hydrological and catchment characteristics, the analysis of affecting parameter was carried out, missing dataset of temperature and precipitation was filled by statistical downscaling model and conceptual model was run several times to generate three different results by varying the parameter affecting the hydrological characteristics. Three sets of methods, one without using glacier component and another by using glacier were carried out; and finally simulation of the river discharge by HVB-*light 3.0* model was carried out by assuming the temperature increase (Konz and Merz, 2010) applied HBV model for Tamor river in order to estimate runoff at Tapethok, Taplejung in eastern Nepal. Generally, HBV model was able to correctly simulate low flow except for some sharp peaks due to isolated precipitation events (Konz and Merz, 2010). In this study, similar analysis was carried out and similar results were obtained as HBV model was able to simulate low flows well except in the case of sharp peaks.

Model HVB-*light 3.0* was calibrated for the three river basins by the study area was divided into 15 elevation zones in Modi Khola river basin, 13 elevation zones in Langtang river basin and 17 elevation zones in Dudhkoshi river basin. Two vegetation zones, namely, glacier and vegetated area for calibration period have been used and described in Table 4.5-1 Calibration of HVB-*light 3.0* model was made by trial and error technique in three study basin, the calibration and validation results are presented Appendix, (V) Figure 3.4.8(a) to Figure 3.4.8(i).

## 3.7.9 Scatter plot observation and simulation

Data obtained from hydrological model i.e. simulated data and the real observed data was plotted in the scatter diagram in order to examine the efficiency of the model for two different set of the calibrated data. Efficiency of the model is the most important factor that determines the reliability of the model and the results of the scatter diagram are also highly efficient.

Figure No	Observed discharge verses Model discharge	Calibration (R <sup>2</sup> )	Validation (R <sup>2</sup> )
3.4.14 (a)	Modi Khola river basin calibration (1991_1999)	0.77	
3.4.14 (b)	Modi Khola river basin validation (2000_2008)		0.83
3.4.14 (c)	Langtang Khola river basin calibration (2002_2005)	0.84	
3.4.14 (d)	Langtang Kola river basin validation (2006_2009)		0.86
3.4.14 (e)	Dudhkoshi river basin calibration (1965_1970)	0.78	
3.4.14 (f)	Dudhkoshi river basin validation (1970_1979)		0.78
3.4.14 (g)	Dudhkoshi river basin calibration (1980_1989)	0.75	
3.4.14 (h)	Dudhkoshi river basin validation (1990_2008)		0.67

 Table 3.7-1 Scatter plot between observed discharge verses model discharge

Best-fit models were calibrated for each set of input data based on initial parameter sets. A weakness in the model results which applies to all catchments is that the simulations have a tendency to underestimate discharge and it gives proxy value for output. Best fit line and efficiency of the model is the governing factor for validation and application of hydrological model. The observed and simulated discharge from 1991 to 1999 Modi Khola river basin, 2002 to 2003 Langtang Khola river basin and 1965 to 1970 Dudhkoshi river basin was plotted in the different graphs as shown in Appendix VI, Figure 3.4.14 (a) to 3.4.14 (h). The coefficient of determination (R<sup>2</sup>) between observed discharge verses model (explain in section 3.4.3) discharge value is shown in Table 3.7-1.

### 3.7.10 Model performance

By using the A1B and A2 scenario from CGCM3 data set and downscaling precipitation and temperature data for discharge projection, the results showed that the downscaled precipitation data is suitable for the climate change impact on flow regime study in these three glacier fed basins. The result of observed and simulated discharge obtained from HVB-*light 3.0* model is similar while comparing the performance in simulation of historical stream flow in the three river basins.

## **3.8** Water surplus/deficit in the three studied basins

In 2012, Adhikari et al. reported that in the context of water surplus and water deficit in the three basins, the water deficit is found in winter and autumn at Annapurna region. Similarly, the water deficit is found in winter, spring and autumn at Langtang region and in all seasons of the year in Khumbu region (Table 3.8-2).

### **3.8.1** Potential Evapo-transpiration (PET)

The PET is the amount of water that would be evaporated under an optimal set of conditions, including an ultimate supply of water. The highest value of PET is found in the month of May in all three stations as shown in Table 3.8-1. In Annapurna area, the PET shows quite variable trend in the modeled results (highest values of 96 mm and the lowest value of 49 mm). The PET is decreased with elevation.

Region	Jan	Feb	Mar	Apr	May	Jun	Jul	Aug	Sep	Oct	Nov	Dec	Annual (mm)
Annapurna	49	53	68	88	96	79	76	76	71	72	63	59	852
Langtang	53	55	70	87	92	76	76	75	68	72	62	58	845
Khumbu	50	49	59	71	73	62	63	70	57	59	60	59	731

Table 3.8-1 Comparison of potential evapotranspiration in three stations

### **3.8.2** Actual Evapo-transpiration (AE)

Actual evapo-transpiration in a soil water budget is the actual amount of water delivered to the atmosphere by evaporation and transpiration. AE can be visualized as "water use" that is actually evaporating and transpiring. The AE is an output of water that is dependent on moisture availability, precipitation, sunshine hour, wind, temperature, and humidity. In wet months, when precipitation exceeds potential evapo-transpiration, actual evapo-transpiration is equal to PET. In dry months, when potential evapo-transpiration exceeds precipitation, actual evapo-transpiration is equal to precipitation plus the absolute value of the change in soil moisture storage. In this study, AE was estimated by using Penman method. In Annapurna and Khumbu area PET >AE in all season, but in Langtang area PET equaled AE in summer and in other season PET >AE (Table 3.8-2). This indicates that the deficit occurs when the soil is completely dried out.

Station	Condition	Dec-Feb	Mar-May	Jun-Sep	Oct-Nov	Total
Name	Condition	(DJF)	(MAM)	(JJAS)	(ON)	(mm)
	AE	135	252	303	123	813
Annapurna	WD	27	0	0	13	40
	WS	0	294	1170	27	1491
	AE	38	90	296	71	495
Langtang	WD	129	159	0	63	351
	WS	0	0	177	0	177
	AE	20	49	232	55	356
Khumbu	WD	144	155	19	64	382
	WS	0	0	49	0	49

 Table 3.8-2 Comparison AE, WD and WS in three stations of Nepal Himalaya

# **CHAPTER 4 RESULT AND ANALYSIS**

# 4.1 Seasonal and monthly precipitation of three basins

The month of July has the highest rainfall followed by August in Modi Khola river basin and Dudhkoshi river basin. The monsoon precipitation is more pronounced in Modi Khola river basin and Dudhkoshi river basin. In case of Langtang Khola river basin, August has the highest rainfall followed by July.

The total precipitation of Modi Khola river basin during the summer (JJAS) is 2062 mm out of which 85 % rainfall is in monsoon season and the rainfall of 44 mm is found during winter (DJF). Similarly, the total precipitation of Langtang Khola river basin during the summer (JJAS) is 492 mm out of which 78 % precipitation is in monsoon season and the precipitation of 20 mm during the autumn (ON) season. The total precipitation of Dudhkoshi river basin during the summer (JJAS) is 345 mm out of which 80 % precipitation found in monsoon season and the precipitation of 2 mm found in Winter (DJF) (Table 4.1-1).

The maximum coefficient of variation exceeded in November at Modi Khola river basin and Dudhkoshi river basin. Similarly the coefficient of variation exceeded from October at Langtang Khola river basin (Figure 4.1.1 to Figure 4.1.3).

	<b>Tuble 4.1-1</b> Trecipitation distribution of the three river basins											
Season	Modi Khola	a river basin	Langtang Kl	nola river basin	Dudh Koshi river basin							
	seasonal total	seasonal %	seasonal total	seasonal %	seasonal total	seasonal %						
DJF	44	2	28	4	9	2						
MAM	220	9	94	15	57	13						
JJAS	2062	85	492	78	345	80						
ON	109	4	20	3	20	5						
Annual	2436	100	634	100	431	100						

Table 4.1-1 Precipitation distribution of the three river basins

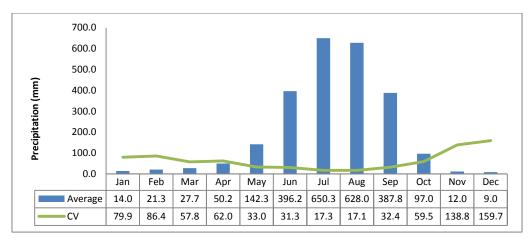


Figure 4.1.1 Precipitation distribution of Modi Khola River Basin

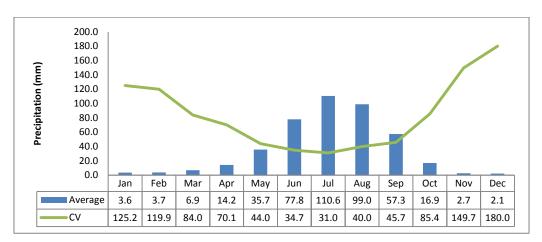


Figure 4.1.2 Precipitation distribution of Dudh Koshi River

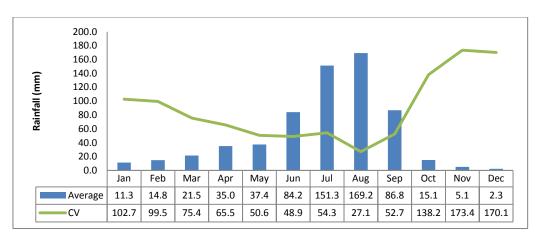


Figure 4.1.3 Precipitation distribution of Langtang Khola River Basin

# 4.2 Yearly precipitation trend of observed data

The observed **annual** precipitation trend analysis (1988-2009) is carried out in 9 stations which has given in Table 4.2-1.

		Elevation	Average Precipitation	
Station Name	Data Period	(m)	(mm)	Trends
Chaurikhark	1988-2009	2660	2116	-15.363
Salleri	1988-2009	2378	1690	13.690
Aisealukhark	1988-2009	2417	1087	4.648
Okhaldhunga	1988-2009	1720	1170	6.287
Dingboche	1988-2009	4355	452	-1.108
Langtang	1988-2009	3920	634	10.896
Annapurna	1988-2009	3470	2473	9.000
Lumle	1988-2009	1740	4083	4.056
Parbat	1988-2009	891	2580	1.820

 Table 4.2-1 Annual average precipitation trends with elevation

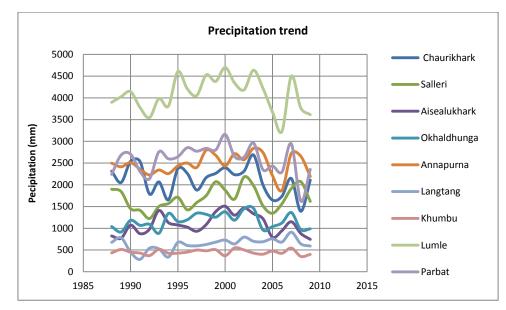


Figure 4.2.1 Precipitation trend of study stations

The highest increasing trend of 13.690 mm is found in Salleri station and highest decreasing trend of -15.363 mm in Chaurikhark, both station lies in Dudhkoshi Basin (Figure 4.2.1). The highest annual precipitation occured in Lumle station in the elevation 1740 amsl in Modi Khola basin and the lowest precipitation occured in station Dingboche 452 mm in the elevation 4355 amsl. Precipitation is found decreased with elevation at the rate of -0.5832 mm per thousand meter (Figure 4.2.2).

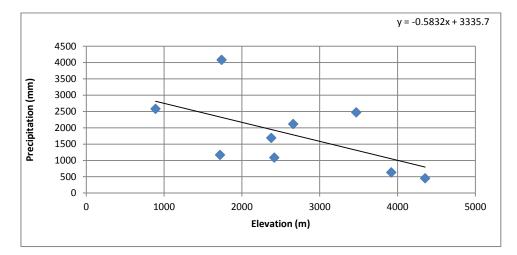


Figure 4.2.2 Variation of precipitation with elevation (1988-2009)

# 4.3 Yearly temperature trend of observed data

Five stations are included in the temperature trend analysis from the three basins discussed in Chapter 3.3.3. The temperature stations selected for the trend analysis are provided in Table 4.3-1. Results indicate that there is a high confidence in recent warming which is also statistically significant. The observed trends in selected temperature stations are shown in Figure 4.3.1, Figure 4.3.2 and Figure 4.3.3. All the stations indicate a rising trend in both maximum and mean temperature . However, the magnitude of the trend is higher in the maximum temperature than in the minimum temperature. Two of the stations, Annapurna and Lumle, showed decreasing trends of -0.004  $^{\circ}$ C/year and -0.002  $^{\circ}$ C/year for minimum temperature. The maximum increasing trend of temperature is found in Langtang area which is 0.176  $^{\circ}$ C.

Station Name	Data period	Maximum temperature statistically significant		Minimum Temperature statistically significant	Minimum Trend	Mean Temperature statistically significant	Mean Trend
Annapurna	1988-2009	*	0.089		-0.004	**	0.048
Lumle	1988-2009	*	0.097		-0.002	**	0.05
Langtang	1988-2009	**	0.176	*	0.151	*	0.129
Okhaldhunga	1988-2009	**	0.129		0.011	**	0.065
Khumbu	1988-2009	**	0.123	*	0.151	**	0.065

Table 4.3-1 Observed significance and trend of temperature record

 $\alpha = 0.01$  or 99 percent confidence level (\*\*)

 $\alpha = 0.05$  or 95 percent confidence level (\*)

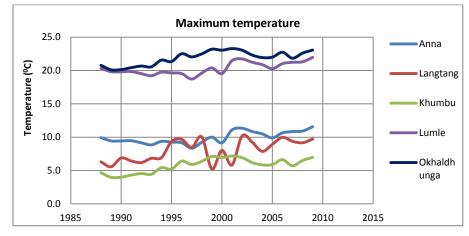


Figure 4.3.1 Observed Tmax trend

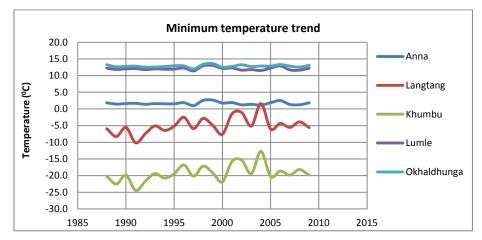


Figure 4.3.2 Observed Tmin trend

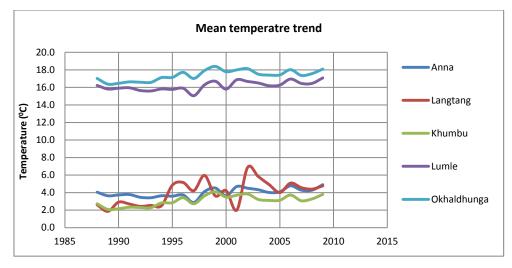


Figure 4.3.3 Observed Tmean trend

### 4.4 Monthly flow regime analysis of three river basins

A flow regime of a river is essentially a statistical summary of how flows in a river vary over time, the amount of water and the rate of flowing water in a river carries to different months. Recent research has advanced range of approaches to the analysis of flow regimes in order to define operational rules for protecting or restoring fluvial hydro-systems (Nestler and Long, 1997). In the Modi Khola Basin system the maximum discharge is found as 916  $m^3/s$  in the month of August due to the monsoonal effect, the minimum discharge is  $5.31 \text{ m}^3/\text{s}$  in the month of March. The maximum peak discharge increased to 194.0 m<sup>3</sup>/s in April due to the effect of snow melt. There is a slight decrease in observed discharge in May, but after mid-May, it is continuously increased till August (Figure 4.4.1). In the Langtang Khola Basin the snow melt effect started from March to mid of June. The observed peak discharge from snow is 101.4 m<sup>3</sup>/s and it decreased to 88 m<sup>3</sup>/s by mid-July. After the monsoonal effect the maximum discharge is  $111.4 \text{ m}^3/\text{s}$  (Figure 4.4.2). In this basin snow melt is more efficient as compared to other two basins. The minimum discharge in the month of March is similar to that in Modi Khola Basin. In Modi Khola and Langtang Khola Basins snow melt effect can be significant as compared to Dudhkoshi basin. Snow melt contribution in Dudhkoshi Basin continues supporting monsoonal discharge and they cannot be separated from each other like in Modi Khola and Langtang Khola Basin. The maximum discharge of Dudhkoshi basin is 2580 m<sup>3</sup>/s occurs in August and minimum of 13.5  $m^3/s$  in March (Figure 4.4.3 and 4.4.4).

1000.0 900.0 800.0 (% m) ab 500.0 500.0 300.0 200.0 100.0													
0.0	Jan	Feb	Mar	Apr	May	Jun	Jul	Aug	Sep	Oct	Nov	Dec	
Average	12.5	11.5	10.9	13.7	21.2	57.9	139.1	168.0	102.9	40.4	21.9	16.9	
Max	16.6	14.6         17.9         194         63.6         357         675         916         395         116         98.3         80											
Min	7.61	6.14	5.31	6.72	9.48	13.4	33.6	74	43.6	20	12.5	8.81	

Figure 4.4.1 Monthly flow regime of Modi Khola river basin

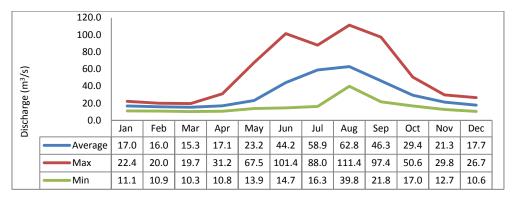


Figure 4.4.2 Monthly flow regime of Langtang Khola river basin

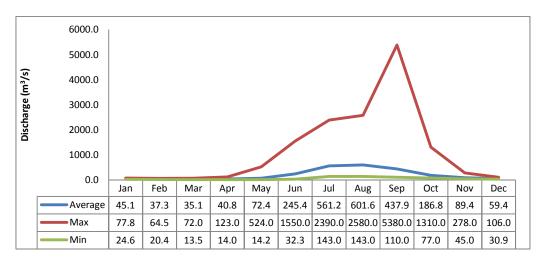


Figure 4.4.3 Monthly flow regime of Dudhkoshi river basin

00000 5000.0 00000 00000 00000 00000 00000 00000 0000								2	5	380.0		
0.0	Jan	Feb	Mar	Apr	May	Jun	Jul	Aug	Sep	Oct	Nov	Dec
Average	45.1	37.3	35.1	40.8	72.4	245.4	561.2	601.6	437.9	186.8	89.4	59.4
Max	77.8	64.5 72.0 123.0 524.0 1550.0 2390.0 2580.0 5380.0 1310.0 278.0 106.0										
Correct Max	77.8	64.5	72.0	123.0	524.0	1550.0	2390.0	2580.0	1410	887.0	278.0	106.0
Min	24.6	20.4	13.5	14.0	14.2	32.3	143.0	143.0	110.0	77.0	45.0	30.9

Figure 4.4.4 Corrected monthly flow regime of Dudhkoshi river basin

## 4.5 Yearly discharge (flow regime) trend of observed data

Three discharge stations of studied river basins are considered for the yearly flow regime analysis. These three stations are shown in Figure 4.5.1, Figure 4.5.2 and Figure 4.5.3. The flow regime analysis of the discharge data indicated significant inter-annual variability. The rising and falling trends have similar behavior among the stations.

The most notable behavior is found in Annapurna area during the year 2000-2003. There is a sudden increase in discharge due to the high precipitation fall but overall annual maximum discharge is in decreasing trend -8.779 m<sup>3</sup>/s and minimum trend is found to be -0.035 m<sup>3</sup>/s (Figure 4.5.1). In contrast, Modi Khola station is located in the downstream region where additional stream flow is contributed by the area and also by occurrence more precipitation.

Another notable behavior was found in Langtang area during the year 1999-2001 due to the heavy snow fall with a similar increasing precipitation data in 2000 (Adhikari et al. 2012). The annual maximum decreasing trend was found -0.7236  $m^3/s$  and minimum trend was found -0.1542  $m^3/s$  in Langtang area (Figure 4.5.2).

The results of the observed discharge from DHM show that, in September 3, 1998 the highest instantaneous flow was recorded with the value of 9880.0  $\text{m}^3$ /s which is

shown in Appendix (I) Table 9; and average maximum discharge was 5380.0  $m^3/s$  (Figure 4.5.3).

According to Dwivedi et al. (1999), in September 3, 1998, a GLOF event occurred in Tam Pokhari Lake of Dudhkoshi river basin. This GLOF was triggered when an ice avalanche hit the frontal lake and induced a surge wave which overtopped the end moraine dam. There is a brief report which indicates that lives were lost and that NRs 156 million (about 2 million US\$) in damage was incurred. Similarly, the most extraordinary behavior was found during the years 1998 in Dudhkoshi basin. Due to the GOLF event, the river cross section was changed according to local perception. For the actual flow regime analysis purpose, a new rating curve should be established from DHM for future study.

According to given rating curve annual maximum flow regime was found to be 19.403 m<sup>3</sup>/s, annual minimum was 0.2142 m<sup>3</sup>/s and mean was 318.3 m<sup>3</sup>/s in Dudhkoshi river basin (Figure 4.5.3). Due to monsoonal effect maximum discharge trend is high but minimum discharge trend is low due to shrinkage of glacier area. It has to be noted that most of the discharge occurred during the monsoon season in all three basin when the water level is high. Comparison of yearly observed discharge trend of three river basins along with the significant test are depicted in Table 4.5-1 and in Figure 4.5.4.

Basin Name	Elevation (m)	Trend (m <sup>3</sup> /sec/year)	Statistically Significant	Average discharge
Modi Khola river	667	-0.2984		(m <sup>3</sup> /s)
Langtang Khola river	1362	-0.3799	**	31
Dudhkoshi river	460	1.9531		197

Table 4.5-1 Yearly trend of observed discharge data

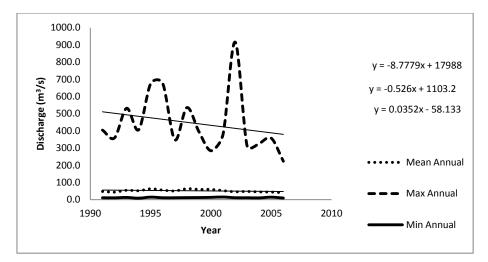


Figure 4.5.1 Observed discharge trend analysis of Modi Khola river basin

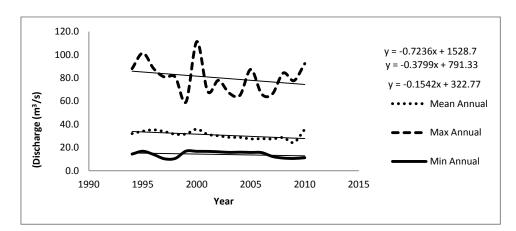


Figure 4.5.2 Observed discharge trend analysis of Langtang Khola river basin

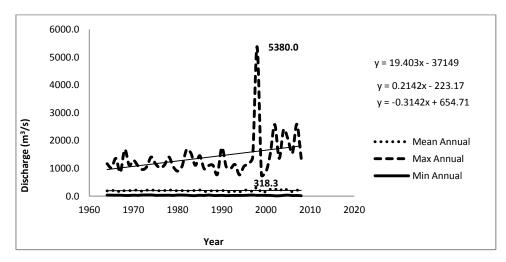


Figure 4.5.3 Observed discharge trend analysis of Dudhkoshi river basin

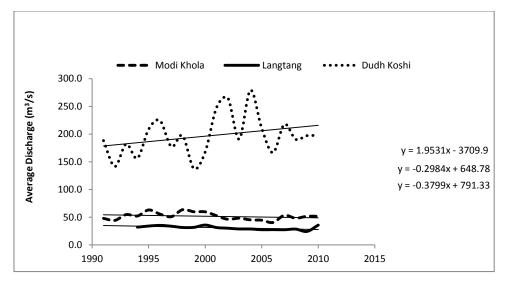


Figure 4.5.4 Comparisons of average discharge of three basins

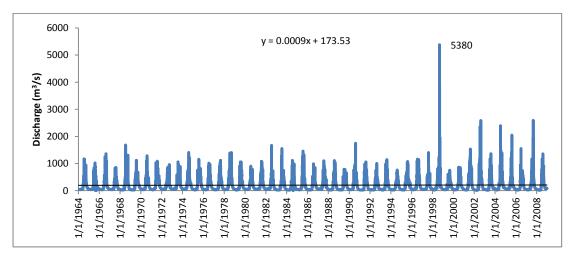


Figure 4.5.5 Daily average discharge of Dudhkoshi river basin

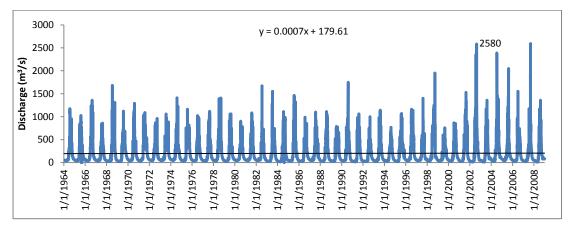


Figure 4.5.6 Corrected daily average discharge of Dudhkoshi river basin

## 4.6 Flow-duration curve of three basins

A flow-duration curve is a cumulative curve that shows the percent of time that flow in a stream is likely to be equal or exceed during a given period (Searcy 2002). It combines in one curve the flow characteristics of a stream throughout the range of discharge, without regard to the sequence of occurrence. In addition, it shows the percentage of time river flow can be expected to exceed a design flow of some specified values and to show the discharge of the stream that occurs or is exceeded some percent of time usually (70 percent of the time). Flow-duration analysis can be used for many purposes in the field of water resources engineering and have been used to solve problems in water management, flood control, hydropower and scientific comparison of stream flow (Vogel and Fennessey 1995, Searcy 2002).

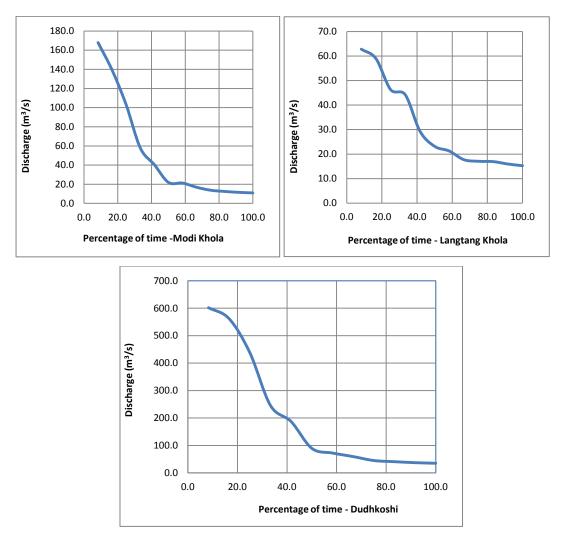


Figure 4.6.1 Modi Khola, Langtang Khola, Dudhkoshi flow duration curve

The flow-duration curve of three basins is provided in Figures 4.6.1, 4.6.2 and 4.6.3. The information from the three stations can be seen in Figure 4.6.3. The figure shows that the Dudhkoshi basin gauging station has the highest magnitude of discharge. The discharge of higher than 100 m<sup>3</sup>/sec occurs more than 50 percent of the time and the lowest flow is higher than 35.1 m<sup>3</sup>/sec. Modi Khola basin has higher than 21.9 m<sup>3</sup>/sec discharge more than 50 percent of the time while the lowest flow is higher than 50 percent of the time while the lowest flow is higher than 10.9 m<sup>3</sup>/sec. Similarly, the discharge higher than 23.2 m<sup>3</sup>/sec occurs more than 50 percent of the time in Langtang Khola Basin while the lowest flow is higher than 16.0 m<sup>3</sup>/sec.

# **CHAPTER 5 SUMMARY AND CONCLUSION**

#### 5.1 Summary

Summary of temperature, precipitation and discharge scenarios obtained from the application of SDSM and HVB-*light 3.0* models are discuss in the following sub sections.

### 5.1.1 Temperature scenario

Projected seasonal baseline NCEP temperature trend for calibration scenarios over the period of 1971-2000 are depicted in Table 5.1-1. During the calibration period, all three regions show highest base line temperature trends (Tmax, Tmin and Tmean) except Khumbu (Tmin) and Langtang (Tmean) in summer (JJAS). The lowest trends are found to occur in different season summer (JJAS) and autumn (ON), except in Khumbu (Tmean). Similarly, highest annual temperature trend of 0.0104 <sup>0</sup>C/year, 0.0089 <sup>0</sup>C/year and 0.0088 <sup>0</sup>C/year in Langtang region and the lowest annual trend of -0.0099 <sup>0</sup>C/year and -0.0022 <sup>0</sup>C/year in Khumbu (Tmax and Tmin) and -0.0049 <sup>0</sup>C/year Annapurna (Tmean) region are evident.

	Base line temperature trend (NCEP: 1971-2000)											
	Maximu	m temperat	ure ( <sup>0</sup> C)	Minimum temperature( <sup>0</sup> C)			Mean temperature ( <sup>0</sup> C)					
Season	Annapurna	Langtang	Khumbu	Annapurna	Langtang	Khumbu	Annapurna	Langtang	Khumbu			
DJF	0.0140	0.1170	0.0147	0.0049	0.0171	-0.0022	0.0097	0.0078	0.0207			
MAM	-0.0060	0.0140	-0.0198	-0.0043	0.0121	-0.0059	0.0028	0.0090	-0.0158			
JJAS	-0.0080	0.0047	-0.0207	0.0035	0.0068	0.0050	0.0057	0.0106	-0.0076			
ON	0.0080	0.0011	-0.0099	-0.0057	0.0007	-0.0113	-0.0019	0.0004	0.0001			
Annual	0.0027	0.0089	-0.0099	0.0006	0.0104	-0.0022	-0.0049	0.0088	-0.0014			

 Table 5.1-1 Base line temperature trend for calibration period

CGCM3 projected seasonal baseline temperature trend for A2 scenarios over the period of 1971-2000 are depicted in Table 5.1-2, in which it is apparent that the highest baseline temperature trends of A2 (Tmax, Tmin and Tmean) is found to occur in spring (MAM) except in Khumbu for Tmin. In all three regions, the lowest temperature trends are found in autumn (ON). Similarly, the highest annual temperature trend of 0.0119  $^{0}$ C/year is found in Langtang region.

	Base line temperature trend of A2 scenario (CGCM3: 1971-2000)											
	Maximu	m temperat	ure ( <sup>0</sup> C)	Minimu	m temperat	ure( <sup>0</sup> C)	Mean temperature ( <sup>0</sup> C)					
Season	Annapurna	Langtang	Khumbu					Langtang	Khumbu			
DJF	0.0013	-0.0050	0.0084	0.0098	0.0185	0.0060	0.0107	0.0198	0.0093			
MAM	0.0305	0.0282	0.0233	0.0334	0.0549	0.0037	0.0336	0.0588	0.0260			
JJAS	0.0052	0.0024	0.0073	0.0100	0.0165	0.0318	0.0085	0.0109	0.0110			
ON	-0.0014 -0.0178 -0.0084 -0.0063 -0.0105 -0.0090 -0.0084 -0.0153								-0.0052			
Annual	0.0119	0.0026	0.0089	0.0137	0.0218	0.0115	0.0134	0.0200	0.0110			

 Table 5.1-2 Base line temperature trend for A2 scenario

CGCM3 projected seasonal maximum temperature trend for A2 scenarios over the period of 2001-2030 and 2031-3060 are depicted in Table 5.1-3. All three regions show highest maximum temperature trend in spring (MAM) and autumn during former period and highest maximum temperature trend in winter (DJF) during later period. However the lowest temperature trends are found in different periods. Highest annual maximum temperature trend of 0.0119 <sup>0</sup>C/year is found in Annapurna among three regions.

	Maximum ter	mperature (20	001-2030)	Maximum temperature(2031-2060)							
Season	Annapurna	Langtang	Khumbu	Annapurna	Langtang	Khumbu					
DJF	0.0137	-0.0089	-0.0006	0.0224	0.0322	0.0186					
MAM	0.0276	-0.0011	0.0309	0.0136	-0.1008	0.0105					
JJAS	0.0052	0.0035	-0.0049	0.0107	0.0110	0.0016					
ON	-0.0014	0.0082	-0.0003	-0.0005	0.0216	0.0018					
Annual	0.0119	0.0014	0.0061	0.0126	0.0130	0.0087					

Table 5.1-3 Maximum temperature trend for A2 scenario

CGCM3 projected seasonal minimum temperature trend for A2 scenarios over the period of 2001-2030 and 2031-3060 are depicted in Table 5.1-4 All three regions show highest minimum temperature trend in spring (MAM) during former period and in summer (JJAS) during later period except in Khumbu. Lowest trends are found in autumn (ON) during both periods. Similarly, highest annual minimum temperature trend of 0.0292<sup>0</sup> C/year is found in Langtang among three regions during later period.

	Minimum ter	nperature (20	001-2030)	Minimum temperature(2031-2060)		
Season	Annapurna	Langtang	Khumbu	Annapurna	Langtang	Khumbu
DJF	0.0132	0.0163	-0.0019	0.0260	0.0470	-0.0025
MAM	0.0412	0.0378	0.0145	0.0235	0.0185	0.0238
JJAS	0.0093	0.0077	0.0417	0.0106	0.0212	0.0764
ON	-0.0014	0.0202	-0.0055	0.0025	0.0300	-0.0031
Annual	0.0166	0.0189	0.0164	0.0171	0.0292	0.0303

Table 5.1-4 Minimum temperature trend for A2 scenario

CGCM3 projected seasonal mean temperature trend for A2 scenarios are over the period of 2001-2030 and 2031-2060 are depicted in Table 5.1-5. All three region show highest mean temperature trend in spring (MAM) during former period except in Khumbu region at later period. Lowest trends are found in autumn (ON) during former period. Similarly, highest annual mean temperature trend of 0.0209 <sup>0</sup>C/year is found in Langtang among three regions during later period.

	Mean temp	perature (2001	1-2030)	Mean temperature(2031-2060)		
Season	Annapurna	Langtang	Khumbu	Annapurna	Langtang	Khumbu
DJF	0.0110	0.0090	-0.0016	0.0214	0.0339	0.0185
MAM	0.0345	0.0347	0.0331	0.0224	0.0980	0.0156
JJAS	0.0050	0.0082	0.0048	0.0062	0.0141	0.0099
ON	-0.0072	0.0097	-0.0020	0.0017	0.0313	0.0184
Annual	0.0127	0.0134	0.0097	0.0137	0.0209	0.0141

 Table 5.1-5 Mean temperature trend for A2 scenario

CGCM3 projected seasonal maximum temperature trend of A1B scenarios are depicted in Table 5.1-6. All three regions show highest maximum temperature increasing trend in spring (MAM) except in Langtang (2001-2030). The lowest maximum temperature trend are found in autumn (ON) all three regions (2031-2060). Similarly, highest annual maximum temperature trend of 0.0203 <sup>0</sup>C/year is found in Annapurna region among in three regions (2031-2060).

	Maximum ter	mperature (20	001-2030)	Maximum temperature(2031-2060)		
Season	Annapurna	Langtang	Khumbu	Annapurna	Langtang	Khumbu
DJF	0.0183	0.0147	0.0216	0.0222	0.0071	0.0131
MAM	0.0285	0.0043	0.0294	0.0413	0.0037	0.0350
JJAS	0.0080	0.0160	0.0038	0.0159	0.0160	-0.0019
ON	0.0120	0.0085	-0.0102	-0.0059	-0.0012	-0.0032
Annual	0.0122	0.0144	0.0123	0.0203	0.0075	0.0116

 Table 5.1-6 Maximum temperature trend for A1B Scenario
 Control

CGCM3 projected Seasonal minimum temperature trend of A1B scenarios are depicted in Table 5.1-7 All three regions show highest minimum temperature trend in spring (MAM) except in Khumbu region (2001-2030). The lowest minimum temperature trends are found in autumn (ON) except in Langtang region. The minimum temperature trend are increasing during spring (MAM) in Annapurna and Langtang except in Khumbu (2031-2060). However, the occurrence of lowest minimum temperature trends are found in different seasons (2031-2060). Similarly, highest annual minimum temperature trend of 0.0300  $^{0}$ C/year is found increasing in Langtang compared to Khumbu and Annapurna regions during both periods.

	Minimum te	emperature (	2001-2030)	Minimum temperature(2031-2060)		
Season	Annapurna	Langtang	Khumbu	Annapurna	Langtang	Khumbu
DJF	0.0170	0.0366	-0.0039	0.0214	0.0249	-0.0013
MAM	0.0410	0.0414	0.0162	0.0517	0.0522	0.0043
JJAS	0.0102	0.0172	0.0241	0.0036	0.0139	0.0303
ON	-0.0650	0.0268	-0.0170	-0.0084	0.0278	0.0062
Annual	0.0151	0.0294	0.0085	0.0188	0.0300	0.0119

Table 5.1-7 Minimum temperature trend for A1B scenario

CGCM3 projected seasonal mean temperature trend of A1B scenarios are depicted in depicted in Table 5.1-8. All three regions show highest mean temperature trends in spring (MAM) in both period 2001-2030 and 2031-2060. The lowest mean temperature trends are found in autumn (ON) except in Langtang region. Highest annual mean temperature trend of 0.0287 0C/year (2001-2030) at Langtang is found to occur among three regions.

	Mean temperature (2001-2030)			Mean temperature(2031-2060)		
Season	Annapurna	Langtang	Khumbu	Annapurna	Langtang	Khumbu
DJF	0.0155	0.0290	0.0217	0.0195	0.0065	0.0182
MAM	0.0368	0.0387	0.0309	0.0499	0.0558	0.0320
JJAS	0.0072	0.0220	0.0092	0.0066	0.0096	-0.0012
ON	-0.0253	0.0214	-0.0092	-0.0178	0.0304	-0.0023
Annual	0.0133	0.0287	0.0149	0.0186	0.0256	0.0126

 Table 5.1-8 Mean temperature trend for A1B scenario

# 5.1.2 Precipitation scenario

Seasonal precipitation trend baseline NCEP and A2 scenarios are presented in Table 5.1-9 (NCEP and CGCM3:1971-2000). During these calibration periods, all three regions show increasing precipitation trends randomly. Precipitation trend are found decreasing in summer (JJAS) except in Khumbu region from NCEP (1971-2000) and the precipitation trend are decreasing randomly from A2 (1971-2000). Likewise, the maximum observed precipitation trend of 0.3614 mm/year is found in Khumbu region in spring (MAM) and annual increasing precipitation trend of 0.7705 mm/year is simulated at Langtang region from A2 SERS scenarios. (CGCM3: 1971-2000) while the annual decreasing precipitation trend is found to be -3.0416 mm/year in Langtang region from NCEP.

	Precipitation	trend of baseline	(NCEP: 1971-2000)	Precipitation trend of A2 (CGCM3: 1971-2000)			
Season	Annapurna	Langtang	Khumbu	Annapurna	Langtang	Khumbu	
DJF	-0.0298	-0.0800	0.0025	-0.1122	-0.0130	-0.0029	
MAM	0.2226	-0.2383	-0.1052	-0.1327	0.0251	0.3614	
JJAS	-0.5761	-0.5153	-0.1537	0.1987	-0.2217	0.0911	
ON	-0.1013	-0.0293	-0.3970	-0.0428	0.0415	-0.1733	
Annual	-1.9919	-3.0416	-1.8330	-0.0485	0.7705	1.0932	

 Table 5.1-9 Baseline precipitation trend for NCEP and A2 scenario

Seasonal precipitation trend of A2 scenarios are depicted in Table 5.1-10 (CGCM3: 2001-2060). All three regions show precipitation increasing trends during spring (MAM) (2001-2030) except in Annapurna (2031-2060). The precipitation trends are found decreasing randomly (2001-2030) and same conditions have been found in summer (JJAS) except in Khumbu region (2031-2060). Similarly, annual precipitation shows increasing trend of 0.9166 mm/year (2001-2030) in Langtang and the annual

precipitation has a decreasing trend of -6.4797 mm/year (2031-2060) in Annapurna among three regions.

		1	5	(		/		
	Precipitation	Precipitation trend of A2 (CGCM3: 2001-2030)			Precipitation trend A2 (CGCM3: 2031-2060)			
Season	Annapurna	Langtang	Khumbu	Annapurna	Langtang	Khumbu		
DJF	-0.0540	0.0150	-0.0093	-0.09340	-0.01570	0.00800		
MAM	0.0940	0.1700	0.3420	-0.01319	0.1646	0.1305		
JJAS	-0.8968	0.0326	-0.1422	-1.7808	-0.2734	-0.07770		
ON	-0.2228	0.0813	-0.1531	0.6889	-0.02230	-0.0918		
Annual	-3.9057	0.9166	0.1272	-6.4797	-0.68970	-0.07910		

 Table 5.1-10 Precipitation trend for A2 scenario (CGCM3:2001-2060)

Seasonal precipitation trend of A1B scenarios are depicted in Table 5.1-10 (CGCM3: 2001-2060). In Annapurna region the precipitation trends are found decreasing for all season and lowest is found to occur in autumn (ON) compared to all three region (2001-2030), whereas highest precipitation trends are found to occur in different season. Likewise, highest precipitation trend of 2.7913 mm /year is found to occur during (ON) compare to Langtang and Khumbu (2031-2060). Lowest precipitation trend of -0.2755 mm/year is found in Khumbu region in summer (JJAS). Similarly, annual precipitation trends are found increasing at the rate of 2.9232 mm/year and 1.4753 mm/year respectively in Annapurna region (2001-2030 and 2031-2060). The annual precipitation trend has been found decreasing at the rate of - 0.8604 mm/year in Khumbu region (2001-2060).

	Precipitation	trend of A1B (C	GCM3: 2001-2030)	Precipitation trend of A1B (CGCM3: 2031-2060)			
Season	Annapurna	Langtang	Khumbu	Annapurna	Langtang	Khumbu	
DJF	-0.0919	0.0174	0.0158	-0.1544	-0.00400	0.00070	
MAM	-0.2728	0.0728	0.4109	0.55800	0.2220	0.2196	
JJAS	-0.1327	0.0949	0.2420	0.02250	-0.1462	-0.2755	
ON	-0.489	0.0072	-0.1277	2.7913	0.05850	-0.20770	
Annual	2.9232	0.7621	1.9991	1.4753	0.20840	-0.8604	

 Table 5.1-11 Precipitation trends for A1B scenario (CGCM3:2001-2060)

## 5.1.3 Discharge scenario

Seasonal maximum and minimum discharge trend baseline NCEP scenarios over the period of 1971-2000 are depicted in Table 5.1-12. All three regions show highest base line discharge trends randomly. The lowest trends are also found to occur

randomly. Likewise, maximum discharge trend are found decreasing in autumn (ON) except in Annapurna (1971-2000) during summer (JJAS) and minimum discharge trends are found decreasing in autumn (ON) except in Langtang region (1971-2000). The trend of annual maximum discharge is found decreasing at the rate of -0.8013  $m^3/s/year$  (1971-2000) in Khumbu region while minimum discharge trend is increasing at the rate of 0.0661  $m^3/s/year$  occurs in Langtang region.

1 4010	<b>Fuble 5.1-12</b> Maximum and minimum discharge trend for base the									
	Maximum (1971-2000)			Minimum (1971-2000)						
Season	Annapurna	Langtang	Khumbu	Annapurna	Langtang	Khumbu				
DJF	-0.0375	-0.0096	0.0782	-0.0218	-0.0045	-0.0666				
MAM	-0.0214	-0.0355	-0.8442	-0.0333	-0.0147	-0.8504				
JJAS	-0.0710	0.0649	-1.1713	-0.0523	0.0143	-0.6595				
ON	-0.0653	-0.1059	-1.1830	-0.0646	0.1009	-1.4549				
Annual	-0.0466	-0.0100	-0.8013	-0.0394	0.0661	-0.6072				

Table 5.1-12 Maximum and minimum discharge trend for base line

CGCM3 projected seasonal maximum and minimum discharge trend of A2 scenarios over the period of 1971-2000 are depicted in Table 5.1-13 (1971-2000). Annapurna and Langtang regions show increasing maximum discharge in summer (JJAS) except in Khumbu region (1971-2000) and minimum discharge are found to occur in different season. Similarly, the seasonal minimum discharges trends are found to be increasing during summer (JJAS) in Langtang and Khumbu region except in Annapurna. The lowest discharge trends are found to occur during autumn (ON) in all three regions. The annual minimum discharge is in increasing trend at the rate of 1.4109 m<sup>3</sup>/s/year in Khumbu region whereas the minimum discharge decreasing trend is found to occur at the rate of -0.4953 m<sup>3</sup>/s/year in the same region (1971-2000).

	Maxim	um (1971-2	(000)	Minimum (1971-2000)						
Season	Annapurna	Langtang	Khumbu	Annapurna	Langtang	Khumbu				
DJF	0.0479	0.0313	0.0899	-0.0030	0.0412	-0.0167				
MAM	0.0184	0.0193	-0.8442	0.0479	0.0428	0.1824				
JJAS	0.3467	0.0495	-0.4428	0.0347	0.1882	0.6129				
ON	-0.0193	0.0042	-0.1830	-0.0193	-0.0204	-0.9169				
Annual	0.0127	0.0265	-0.4953	0.1266	0.0766	1.4109				

Table 5.1-13 Maximum and minimum discharge trend for A2 scenario

NCEP and CGCM3 seasonal mean discharge trend baseline and A2 scenarios over the period of 1971-2000 are depicted in Table 5.1-14. In all three region, mean discharge baseline trends are found increasing in summer (JJAS) (NCEP: 1971-2000) except in Khumbu. The mean discharge A2 trends are also found increased in summer (JJAS) except in Annapurna (CGCM3: 1971-2000). The mean discharge trend are found decreasing in autumn (ON) in all three reason (2001-2030). The mean discharge trend are decreasing in autumn (ON) except in Annapurna region (CGCM3: 1971-2000). Annual mean discharge trend is found decreasing in Khumbu region at the rate of -0.5523 m<sup>3</sup>/s/year (NCEP: 1971-2000) whereas it is found increasing at the rate of 0.3057m<sup>3</sup>/s/year (CGCM3: 1971-2000) same region.

	Mean (NCEP:1971-2000)			Mean (CGCM3: 1971-2000)		
Season	Annapurna	Langtang	Khumbu	Annapurna	Langtang	Khumbu
DJF	-0.0052	0.0109	0.0724	0.0077	0.0362	0.0366
MAM	0.0607	-0.0081	-0.8473	0.0102	0.0310	-0.3309
JJAS	0.5205	0.0572	-0.5512	-0.1359	0.1189	1.7280
ON	-0.0317	-0.0509	-1.3190	-0.0133	-0.0081	-1.0990
Annual	0.1819	0.0083	-0.5523	-0.0452	0.0516	0.3057

Table 5.1-14 Mean discharge trend for base line and A2 scenario

CGCM3 projected seasonal maximum discharge trend A1B scenarios over the period of 2001-2060 are depicted in Table 5.1-15. The maximum discharge in both Annapurna and Khumbu region show are found increasing in summer (JJAS) except in Langtang region (2001-2030). Likewise, maximum discharge trends are found to occur in different seasons (2031-2060). The lowest maximum discharge trend is found to occur during summer (JJAS) in Langtang region (2001-2030). and the lowest is found during autumn (ON) in Khumbu region (2031-2060). Similarly, annual maximum discharge has an increasing trend in Khumbu at the rate of 0.7282  $m^3/s/year$  (2001-2030) and 0.1208  $m^3/s/year$  (2031-2060) respectively compare to other region.

	Maxim	um (2001-2	030)	Maximum (2031-2060)		
Season	Annapurna	Langtang	Khumbu	Annapurna	Langtang	Khumbu
DJF	0.0054	0.0479	0.2841	0.0135	0.0365	-0.0291
MAM	0.0788	0.0611	0.6692	0.0943	-0.0195	0.3399
JJAS	0.1315	-0.1010	1.7764	0.2535	0.0101	0.0984
ON	0.0693	0.1198	0.4291	0.0566	0.1408	-0.5431
Annual	0.0833	0.0277	0.7282	0.1208	0.0315	0.0193

 Table 5.1-15 Maximum discharge trend for A1B scenario

CGCM3 projected seasonal minimum discharge trend A1B scenarios over the period of 2001-2060 are depicted in Table 5.1-16. The minimum discharge trends in Annapurna and Khumbu are found increasing in summer whereas in case of Langtang it is found increasing during autumn (ON) and decreasing in summer (JJAS) (2001-2030). In Langtang and Khumbu, the minimum discharge trend is found increasing during spring (MAM) whereas for Annapurna it is found during spring (JJAS) similarly the minimum discharge trend are found to occur in Annapurna and Khumbu whereas for Langtang during summer (JJAS) (2031-2060). The highest annual minimum discharge trend is found in Khumbu region at the rate 0.6947 m<sup>3</sup>/s/year (2001-2030) whereas, it is 0.0925 m<sup>3</sup>/s/year in Annapurna region (2031-2060) and the lowest value of -0.1522 m<sup>3</sup>/s/year is found to occur in Khumbu region.

	Minimum (2001-2030)			Minimum (2031-2060)		
Season	Annapurna	Langtang	Khumbu	Annapurna	Langtang	Khumbu
DJF	0.0282	0.0279	0.0291	-0.0033	0.0038	0.0128
MAM	0.0235	0.0175	1.1798	0.0531	0.8885	0.9675
JJAS	0.1895	-0.0285	1.2070	0.2500	-0.1545	-0.7023
ON	-0.0051	0.0565	0.2222	-0.0196	-0.0408	-0.9862
Annual	0.0714	0.0234	0.6947	0.0925	-0.0552	-0.1522

 Table 5.1-16 Minimum discharge trend for A1B scenario

CGCM3 projected seasonal mean discharge trend A1B scenarios over the period of 2001-2060 are depicted in Table 5.1-17. The mean discharge trends are found increased in summer whereas in case of Langtang it is found increasing during autumn (ON) and decreasing in summer (JJAS) (2001-2030). In Langtang and Khumbu, the mean discharge trend is found increasing during spring (MAM) whereas

for Annapurna it is found during spring (JJAS) similarly the minimum discharge trend are found to occur in Annapurna and Khumbu whereas for Langtang during summer (JJAS) (2031-2060). The highest mean discharge trends in Khumbu are found as  $0.3738 \text{ m}^3$ /s/year (2001-2030) and  $0.2713 \text{ m}^3$ /s/year (2031-2060) respectively. The lowest value of -0.0159 m<sup>3</sup>/s/year is found only in Langtang region (2031-2060).

<b>Tuble 3.1</b> If mean discharge trend joining seenanto						
	Mean (2001-2030)		Mean (2031-2060)			
Season	Annapurna	Langtang	Khumbu	Annapurna	Langtang	Khumbu
DJF	0.0095	0.0422	0.1275	0.0125	0.0159	0.0209
MAM	0.0866	0.0208	0.5046	0.0383	0.4530	1.0737
JJAS	0.1925	-0.0455	0.9374	0.2198	-0.0915	0.2524
ON	0.0630	0.1303	-0.0570	-0.0124	0.0079	-0.3820
Annual	0.1021	0.0296	0.3738	0.0820	-0.0159	0.2713

Table 5.1-17 Mean discharge trend for A1B scenario

CGCM3 projected seasonal maximum discharge trend A1B scenarios over the period of 2001-2060 are depicted in Table 5.1-18. The maximum discharge trends in Langtang and Khumbu are found increasing in winter (DJF) whereas in case of Annapurna it is found increasing during in summer (JJAS) and decreasing in summer (JJAS) (2001-2030). In Langtang, Khumbu, and Annapurna the maximum discharge trend is found increasing different seasons autumn (ON), spring (MAM), summer (JJAS) (2031-2060) respectively. The highest annual maximum discharge trend is found to occur in Khumbu region at the rate 0.0.1368 m<sup>3</sup>/s/year (2001-2030) whereas, it is 0.0875 m<sup>3</sup>/s/year in Annapurna region (2031-2060).

<b>Tuble 5.1-10</b> Maximum discharge trend for M2 scenario						
	Maximum (2001-2030)			Maximum (2031-2060)		
Season	Annapurna	Langtang	Khumbu	Annapurna	Langtang	Khumbu
DJF	-0.0114	0.0376	0.2474	0.0035	0.0740	0.0551
MAM	0.0882	0.0325	1.0384	0.0442	-0.0179	0.5161
JJAS	0.2236	0.0259	-0.0196	0.2601	-0.0095	-0.2538
ON	-0.0325	0.0203	-0.5158	0.0180	0.0819	-0.0880
Annual	0.0960	0.0417	0.1368	0.0875	0.0233	0.0493

Table 5.1-18 Maximum discharge trend for A2 scenario

CGCM3projected seasonal minimum discharge trend A2 scenarios over the period of 2001-2060 are depicted in Table 6.1-19. The minimum discharge trends are found increasing in summer (JJAS) for all three regions (2001-2030). In Khumbu and Annapurna the minimum discharge trends are found increasing during (JJAS), whereas it is found in winter (DJF) in Langtang region (2031-2060) respectively. The highest annual minimum discharge trend is found to occur in Langtang region at the rate -0.0587 m<sup>3</sup>/s/year (2031-2060). The annual minimum discharges trends are found to occur in Khumbu (2001-2030) and Annapurna (2031-2060) at the rate of 0.2135 m<sup>3</sup>/s/year and 0.0925 m<sup>3</sup>/s/year respectively.

	Minimum (2001-2030)			Minimum (2031-2060)		
Season	Annapurna	Langtang	Khumbu	Annapurna	Langtang	Khumbu
DJF	-0.0240	-0.0059	0.0714	-0.0031	0.0025	-0.0021
MAM	0.0288	0.0037	0.1043	0.0215	0.0023	0.0622
JJAS	0.2627	0.0689	0.6502	0.0279	-0.1705	1.3434
ON	-0.0469	0.0198	-0.1962	-0.0187	-0.0201	0.0879
Annual	0.0858	0.0422	0.2125	0.0925	-0.0587	0.0478

 Table 5.1-19 Minimum discharge trend for A2 scenarios

CGCM3 projected seasonal mean discharge trend A2 scenarios over the period of 2001-2060 are depicted in Table 6.1-20. The mean discharge trends for three regions are found increasing in different seasons during summer (JJAS) in Annapurna, winter (DJF) in Langtang and spring (MAM) in Khumbu regions. Whereas in case of Annapurna and Khumbu it is found decreasing autumn (ON) and summer (JJAS) (2001-2030) respectively. The mean discharge trend in Annapurna and Khumbu region are found decreasing during autumn (ON) and summer (JJAS) (2001-2031). In Khumbu and Annapurna the mean discharge trends are is found increasing during summer (JJAS), where as in case of Langtang, it is during spring (MAM) (2031-2060). The mean discharge trend in Annapurna and Khumbu region are found decreasing during in summer (JJAS), whereas in case of Langtang it is found decreasing during winter (DJF) (2031-2060). The highest annual mean discharge trends are found to occur both in Khumbu region at the rate 0.0931 m<sup>3</sup>/s/year (2001-2030) and 0.1302 m<sup>3</sup>/s/year (2031-2060) respectively.

	Mean (2001-2030)		Mean (2031-2060)			
Season	Annapurna	Langtang	Khumbu	Annapurna	Langtang	Khumbu
DJF	-0.0040	0.0558	0.1513	-0.0136	-0.0017	0.0347
MAM	0.0662	0.0073	0.7773	0.0252	0.0030	0.0833
JJAS	0.2419	0.0082	-0.1367	0.1453	-0.0508	0.9968
ON	-0.0073	0.0511	-0.3019	-0.0328	-0.0001	-0.0542
Annual	0.0918	0.0325	0.0931	0.0892	-0.0083	0.1302

Table 5.1-20 Mean discharge trend for A2 scenario

The overall summary and results of analysis of the seasonal temperature obtained from different scenario of different climate projection show that there is significant increase in temperature during spring (MAM) season whereas the discharge trend is increasing in summer (JJAS) in all regions, this could be due to melting of snow and glacier together with rainfall those regions. Likewise, the seasonal analysis of the precipitation data shows precipitation trends are found to be increased significantly during spring season in most of the cases but the flow regime (discharge) is more pronounced in subsequent season, that is in summer (JJAS), this is due to temperature precipitation responses on discharge.

#### 5.1.4 Impact of climate change on flow regime

The daily projected maximum and minimum temperatures and precipitation data are used for discharge projection (**Appendix (I), Table 1 to Table 9**). Decadal projected seasonal values of these parameters are described for temperature (section 6.6.2), precipitation (section 6.6.3) and discharge (section 6.6.4).

#### 5.1.5 Scenario analysis

CGCM3 simulated A2 and A1B decadal SERS scenarios (annual and seasonal) of maximum, minimum and mean temperature at Annapurna, Langtang and Khumbu are presented as follows:

**Appendix (I) Table 1**, A1B decadal scenarios of maximum, minimum and mean temperatures from 2001 to 2060.

**Appendix** (I), **Table 2**, A2 decadal scenarios of maximum, minimum and mean temperatures from 2001 to 2060.

**Appendix (I) Table 3,** Decadal values of maximum, minimum and mean temperatures from 2001 to 2060 in calibration and validation period from NCEP data.

**Appendix (I) Table 4,** A2 decadal scenarios of maximum, minimum and mean temperatures from 1961 to 2000.

Appendix (I) Table 5, Observed decadal precipitation (mm) of the three regions.

**Appendix (I) Table 6,** Comparisons of decadal precipitation (mm) of Modi Khola, Langtang Khola and Dudhkoshi river basins, A2 scenario after the calibration and validation period 1961 to 2000.

**Appendix (I) Table 7,** Decadal values of precipitation (mm) in calibration and validation period from 1961 to 2000.

**Appendix (I) Table 8,** Decadal observed discharge during calibration and validation period from Modi Khola (1991 to 2010), Langtang Khola (1991 to 2010), and Dudhkoshi river basins (1971 to 2010).

**Appendix (I) Table 9,** A1B and A2 decadal scenario of discharge  $(m^3/s)$  from maximum, minimum and mean temperatures (<sup>0</sup>C) and precipitation (2001-2060).

#### Result obtained from above appendix are summarized as follows;

In Modi Khola river basin (Annapurna region), the A1B decadal average annual maximum temperature is found to have highest of 9.7  $^{0}$ C during 2051-2060 and lowest of 9.0  $^{0}$ C during 2001-2010(Appendix I: Table 1). Decadal average annual total precipitation is found to have maximum value of 2198.3 mm during 2051-2060 and minimum value of 2181 mm during 2001- 2010 (Appendix I: Table 7). Similarly, decadal annual average discharge is found to have maximum of 47.1 m<sup>3</sup>/s during 2051-2060 and minimum value of 42.0 m<sup>3</sup>/s during 2001 -2010 (Appendix I: Table 9).

In Langtang Khola river basin (Langtang region), the A1B decadal annual maximum temperature is found to have highest value of 7.1  $^{0}$ C during 2051-2060 and lowest of 6.8  $^{0}$ C during 2001-2010 (Appendix I: Table 1). Decadal average annual total precipitation is found to have maximum value of 729.1 mm during 2051-2060 and minimum of 710.9 mm during 2001-2010 (Appendix I: Table 7). Similarly, maximum value calculated for decadal annual average discharge is found to be 36.9 m<sup>3</sup>/s during 2051-2060 and minimum value of 35.7 m<sup>3</sup>/s during 2001-2010 (Appendix I: Table 9). There is a similarity found in terms of annual average maximum temperature, annual total precipitation and annual average discharge Adhikari et. al., (2014).

In Dudhkoshi river basin (Khumbu region) the A1B decadal annual maximum temperature is found to have highest value of 2.6  $^{0}$ C during 2051-2060 and lowest of 2.1  $^{0}$ C during 2001-2010 (Appendix I: Table 1). Decadal average annual total precipitation is found to have maximum of 548.1mm during 2051-2060 and minimum of 522.9 mm during 2001-2010 (Appendix I: Table 7). Similarly, decadal annual average discharge is found to have maximum of 257.1 m<sup>3</sup>/s during 2051-2060 and minimum of 238.8 m<sup>3</sup>/s is during 2001-2010 (Appendix I: Table 9).

In Modi Khola river basin (Annapurna region) the A2 decadal annual maximum temperature is found to be highest of 9.7  $^{0}$ C during 2051-2060 and lowest of 9.1 $^{0}$ C during 2001-2010 (Appendix I: Table 2). Decadal average annual total precipitation found to have maximum value of 2295 mm during 2001-2010 and minimum of 239.1 mm during 2051-2060 (Appendix I: Table 7). Similarly, maximum value of decadal annual average discharge is found to be 47.4 m<sup>3</sup>/s during 2051-2060 and lowest minimum value of 43.0 m<sup>3</sup>/s is found during 2001-2010 (Appendix I: Table 9).

In Langtang Khola river basin (Langtang region) the A2 decadal annual maximum temperature is found to be highest of 7.3  $^{0}$ C during 2051-2060 and lowest of 6.8  $^{0}$ C during 2001-2010 (Appendix I: Table 2). Decadal average annual total precipitation found to have maximum value of 676.6 mm during 2051-2060 and minimum value of 691.1mm during 2001-2010 (Appendix I: Table 7). Similarly, maximum value of decadal annual average discharge is found to be 36.7 m<sup>3</sup>/s during 2051-2060 and lowest minimum value of 35.6 m<sup>3</sup>/s during 2001-2010 (Appendix I: Table 9).

In Dudhkoshi river basin (Khumbu region) the A2 decadal annual average maximum temperature is found to be highest of 2.6  $^{0}$ C during 2051-2060 and lowest of 2.2  $^{0}$ C during 2001-2010 (Appendix I: Table 2). Maximum value of decadal average annual total precipitation is found to be 567.2 mm during 2051-2060 and minimum value of 538.8 mm during 2001-2010 (Appendix I: Table 7). Similarly, maximum value of annual average discharge found to be 242.4 m<sup>3</sup>/s during 2051-2060 and lowest minimum value of 230.3 m<sup>3</sup>/s during 2001-2010 (Appendix I: Table 9).

Above results indicated that there in an overall increase of decadal average annual temperature, precipitation and discharge in all three basins. These increases in decadal values during later decades could be due to enhancement of global warming.

### 5.1.6 Water Balance of the study basin

For comparison of climatic water balance in three regions Table 5.2-21 is presented. According to this table, there is lowest water deficiency of 40 mm at Annapurna region. The highest water deficiency of 382 mm is evident at Khumbu. Langtang has intermittent water deficient of 351 mm. Therefore, it suggests that the water deficiency is increasing from western to eastern Nepal Himalaya. Similarly the highest water surplus of 1491 mm is at Annapurna, 177 mm at Langtang and the lowest 49 mm at Khumbu which is similar to the precipitation distribution, i.e. increasing from eastern to western Himalaya due to the altitudinal and monsoonal effects latitudinal different from east to west.

Climatology of water Balance	Annapurna	Langtang	Khumbu
Water Deficiency (mm)	40.0	351.0	382.0
Water Surplus (mm)	1491.0	177.0	49.0

 Table 5.1-21 Comparisons of climatic water balance in three stations

Devkota (2003) found the highest rainfall pocket of more than 320 cm annually over central mountainous region, particularly along the southern flanks of Annapurna range, whereas the driest part is found over the north of the same range with less than

40 cm annually. The strong rainfall gradient across this range shows the importance of topography on spatial variation of annual rainfall distribution in Nepal. The second highest rainfall zone of more than 240 cm per year is located over the northeast mountainous region. Terai belt has rainfall distribution ranging from 160 to 200 cm annually, whereas the western Terai shows less rainfall in comparison to the rest of the Terai. While Devkota (2003) noted that highest rainfall zone is located at the middle mountainous region, Seko (1987) and Shirawa et al. (1992) observed that the amount of precipitation in an altitude of 5090 amsl is almost 1.5 times higher than at the Langtang station located at 3920 amsl during the monsoon periods of 1986 and 1990. This study shows that in the high mountainous region the precipitation decreases with increase in altitude. The water surplus also shows similar chatterers as that of precipitation.

# 5.2 Conclusion

Performance of SDSM downscaling based on NCEP and GCMs predictors at three basin are evaluated using statistical properties of daily climate data. It is found that the application of SDSM for statistical downscaling is suitable for developing daily climate scenarios. To demonstrate the procedure of developing scenarios, SDSM is applied based on daily outputs of common climate variables from GCMs simulation, which has been widely used in the development of daily climate scenarios, and the results can be used in many areas of climate change impact studies. Based on the analysis of results, CGCM3 model has been found as a useful model for the future simulation of temperature and precipitation scenario.

## Temperature

Most of the observation stations in three basins indicate positive increasing annual temperature trends which are statically significant. These stations indicate a gradual increase in annual maximum, minimum and mean temperature in all cases, except for minimum temperature in Annapurna and Lumle stations (Table 5.3-1). During the base line period, annual temperatures (maximum, minimum and mean) are randomly increasing. Similarly, the annual temperature trends of A2, A1B scenario of all three regions are in increasing trends (2001-2030 and 2031-2060). The projected seasonal temperatures trends (maximum, minimum and mean) in three regions are much

warmer in autumn than in spring and summer. Similarly, annual average maximum temperature is warmer in both Annapurna and Langtang regions. On the other hand, annual average minimum temperature is cooler in Khumbu region only.

## Rainfall

The distribution of precipitation is controlled by the orientation of mountain systems. Due to this effect, middle mountain and windward side receive relatively higher precipitation than high mountain, valley and leeward side. Most of the observed stations in three regions indicate increasing annual precipitation trends. These stations indicate a gradual increase in annual precipitation except in Chaurikhark and Dingboche (Table 5.2-1). Observed annual precipitations are increasing in Annapurna and Langtang regions, whereas no such trend is found in Khumbu region (Appendix I, Table 5). The base line (NCEP) A2 scenario annual precipitation is randomly increasing (1971-2000, 2001-2030 and 2031-2060). Similarly, the annual precipitation of A1B scenario of all three regions are in increasing (2001-2030 and 2031-2060).

## Discharge

Observed annual discharge shows negative trend except in Dudhkoshi river basin at Khumbu region. There is a high possibility that the rating curve is less representative for Modi Khola river basin at Annapurna region and Langtang Khola river basin at Langtang region (Table 5.5-1). Observed discharge is found to be similar with the base line NCEP simulated discharge. The base line (1971-2000) NCEP simulated annual discharge (maximum, minimum and mean) for A2 scenarios are decreasing, however that for projected period (2001-2060) from all three regions are increasing, except in Dudhkoshi river basin. Similarly, annual discharge of A1B scenario of these basins are increasing (2001-2030) except in Modi Khola river basin. However, CGCM3 (SRES A1B and A2) simulated seasonal and annual discharge at these basins are increasing, except at Langtang region, where only discharge from A2 scenario is decreasing. Further, the flow regime (discharge) trend is more pronounced after the subsequent summer season in all three regions for both A1B and A2 scenario during 2001-2030 and 2031-2060 period.

Result shows that average annual temperature, precipitation and discharge of the study area of three basins are getting higher in the future decades due to enhancement of global warming.

### **PET and Water balance**

PET is decreasing with increasing elevation similar to the vertical temperature variation. The highest water surplus is found in the Annapurna region, but less amount of water surplus is obtained in Langtang and Khumbu region. In Annapurna region, temperature and precipitation are larger as compared to the other two regions (Langtang and Khumbu region). In Annapurna areas, both temperature and precipitation are high and hence snow accumulation as well as melting is also high as compared to other two stations. Water surplus occurred in three seasons (spring, summer and Autumn) at Annapurna region, but in summer very small quantity of water surplus is found in Langtang and Khumbu region. Water deficiency is increasing from western to eastern regions whereas water surplus is increasing from eastern to western regions. Freezing precipitation and climatic water balance show that Annapurna region has the highest water surplus. This may be due to the fact that this area is located at the highest rainfall pocket of Nepal. The pattern of decreasing rate of precipitation is not similar in three catchments due to the different temperature profile and the freezing precipitation. The snow melting rate is higher in the Annapurna area. The melting rate of glaciers is higher in western region as compared to the middle and eastern regions of Nepal Himalaya.

# 5.3 Recommendation for future work

The research aimed to study the impact of climate change on precipitation trend and river discharge of the study areas (Modi Khola, Langtang Khola and Dudhkoshi river basins). By analyzing the precipitation data and then applying hydrological model, the change in river discharge was computed. The change in global air temperature was found to be the major factor affecting the changes in the precipitation trend as well as river discharge. In this contest the following recommendations are made:

• In Nepal, conclusions regarding the climate change in the higher altitude region were based on limited observation with short time series data and thus

it is suggested to improve observational networks particularly at high altitude regions.

- Because of the diverse topographical, physical and environmental characteristics of the basins in Nepal, a number of empirical studies related to the climate change impact are required in order to segregate the climatic and non-climatic impacts. Therefore, more representative studies for the identification of potential impacts of climate change on water resources are needed.
- In this study, the capability of the automatic calibration algorithm and the uncertainty analysis was weakened due to relatively short duration of data. The study would have been more reliable if the data was of longer duration. So it is recommended to give continuation to the current data stations so that no such problem will be faced for future researchers.
- In this study, lack of reliable land-use and groundwater data were responsible for not computing water balance properly. It is therefore recommended to the concerned authority to develop an accessible, comprehensive database to overcome these issues.
- Since the most of the research in the study area are conducted by hydropower and infrastructure developers, basic issues like climate change are neglected and hence study in climate change issue needs to be strengthened.
- In order to implement adaptation and mitigation plans in future, as the areas are at high risk due to impact of the precipitation change and flood regime, concentrated study on climate change effect on glaciers should be enhanced.

## REFERENCES

- Adhikari, R. K. (2008). Organic Agriculture Promotion Program Progress Report, Society for Environment Conservation and Agricultural Research and Development, Nepal.
- Adhikari, T. R. and Devkota, L. P., (2012). Climatic water balance of Annapurna, Langtang and Khumbu region of Nepal Himalaya, Journal of hydrology and meteorology page: 47-56.
- Adhikari, T. R., Devkot L. P. and Shrestha, A. B., (2014). Climate change scenarios and its impact on water resources of Langtang Khola Basin, Nepal, Jun 2014. Publish in IAHS Read Book, Evolving Water Resources Systems: Understanding, Predicting and Managing Water–Society Interactions Proceedings of ICWRS2014, Bologna, Italy (IAHS Publ. 364), page 9.
- Ageta, Y. and Higuchi, K., (1984). Estimation of mass balance components of summer-accumulation type glacier in the Nepal Himalaya. Geogr. Ann. 66A(3): page 245-255.
- Alford, D.,(1992). Hydrological Aspect of the Himalayan Region, ICIMOD, Kathmandu.
- Allen, R. G., Pereira, L., Raes, D., Smith, M., (1998). Crop evapotranspiration: Guidelines for computing crop water requirements. FAO Irrigation and Drainage Paper 56, FAO, Rome page 17.
- Angele, A., Jean-Oliver, J., Selim, K., Tarek, T., Chadi, B., Claude, B., and Wajdi, N., (2005). Snow in Lebanon: a preliminary study for snow cover over mount Lebanon and a simple snowmelt model, Hydrological Science-Journal 50 (3), page 555-570.
- Anthwal, A., Joshi, V., Sharma, A., and Anthwal, S., (2006). Retreat of Himalayan glaciers- Indicator of climate change. Nature and Sciences 4(4): page 53-59.
- Arnell, N. W., Brown, R. P. C. and Reynard, N. S., (1990). Impact of climatic variability and change on river flow regimes in the UK. Report no. 107, Institute of Hydrology, Wallingford, UK.

- Arnell, N. W., Hudson, D. A., Jones, R. G., (2003). Climate change scenarios from a regional climate model: Estimating change in runoff in southern Africa. Journal of Geophysical Research 108 (D16), 4519.
- Arnell, N. W., Reynard, N. S., (1996). The effects of climate change due to global warming on river flows in Great Britain. Journal of Hydrology 183 (3–4), page 397-424.
- Arnold, N. S., I.C. Willis, M. J. Sherp., K. S. Richards and W. J. Lawson (1996). A distributed surface energy balance model for a small valley glacier. Development and testing for Haut Glacier d' Arolla, Valais, Switzerland, J glacial, 42(140) pp. 77-89.
- Baidya, S., K., Regmi, R., K., Shrestha, M., L., (2007). Climate Profile and Observed Climate Change and Climate Variability in Nepal. Department of Hydrology and Meteorology, Kathmandu, Nepal, July 2007.
- Bajracharaya, S. R., Mool, P. K. and Shrestha, B. R., (2007). Impact of Climate Change on Himalayan Glacier and Glacier Lakes, ICIMOD.
- Bajracharya S. R., Mool, P. K. and Shrestha, B. R., (2008). Global Climate Change and Melting of Himalayan Glaciers, Melting Glaciers and Rising sea levels: Impacts and implications, page 28-46.
- Barnett, T. P., Adam, J. C., and Lettenmaier, D. P., (2005). Potential impacts of a warming climate on water availability in snow-dominated regions. Nature, 04141, Vol. 438 (17) page 303-309.
- Beltaos, S. and Prowse. T. D., (2001). Climate impacts on extreme jam events in Canadian rivers. Hvdrol. Sci. J. 46(1), page 157-183.
- Beniston, M., Diaz, H. F., and Bradley, R. S., (1997). Climatic change at high elevation sites: An overview. Climatic Change, 36, page 233-251.
- Bergstorm, S., (1992). The HBV Model Its Structure and Applications. SMHI Reports Hydrology, No. 4, Norkioping, Sweden, page.32.
- Bergstrom S., and Graham L. P., (1998). The Baltic basin A focus for interdisciplinary research. Nordic Hydrological Conference August 11-12, Helsinki.
- Bergstrom, S., (1972). The application of a simple rainfall-runoff model to a catchment with incomplete data coverage. Sveriges Meteorologiska och

Hydrologiska Institut. Notiser och preliminara rapporter. Serie Iiydrologi nr. 26.

- Bergstrom, S., (1976). Development and application of a conceptual runoff model for Scandinavian catchments, SMHI, Report No. RHO 7, Norrkoping, page 134.
- Bergstrom, S., (1990). Parametervarden for HBV-modellen i Sverige, Erfarenheter frin modelkalibreringar under perioden 1975-1989 (Parametervalues for the HBV model in Sweden, in Swedish), SMHI Hydrologi, No.28, Norrkoping, page 35.
- Bergstrom, S., (1992). The HBV model its structure and applications, SMHI Hydrology, RH No.4, Norrkoping, page 35.
- Bergstrom, S., Carlsson, B., Gardelin, M., Lindstrom, G., Pettersson, A., Rummukainen, M., (2001). Climate change impacts on runoff in Sweden – assessments by global climate models, dynamical downscaling and hydrological modeling, Climate Research 16, page 101-112.
- Beven, K. and Binley, A., (1992). The future of distributed models: model calibration and uncertainty prediction. Hydrological Processes, vol 6, page 279-298.
- Boakye P. G., (1993). Filling gap in hydrological runoff data series in west-Africa, RUHR-UNIVERSITAT BOCHUM.
- Bouraoui, F., Vachaud, G., Li, L. Z. X, Le Treut, H. and Chen, T., (1999). Evaluation of the impact of climate changes on water storage and groundwater recharge at the watershed scale. Clim. Dyn. 15, page 153-161.
- Braithwaite, R.J. and Zhang Y., (2000). Sensitivity of mass balance of five Swiss glacier ablation from air temperature Changes assessed by tuning a degree day model, j. Glacial 46(152): page 7-14.
- Braun, L.N., Grabs, W., and Rana, B., (1993). Application of a conceptual precipitation runoff model in Langtang Khola Basin, Nepal Himalaya. Snow and Glacier Hydrology, 218, page 221-237.
- CBS, (2011). A statistical year book of Nepal, Central Bureau of Statistics, Kathmandu.

- Chalise, S. R., (1994). Mountain environments and climate change in the Hindu Kush- Himalayas. In: Mountain Environments in Changing Climate [Beniston, M (ed.)], London, page 382-404.
- Charlton, R., Fealy, R., Moore, S., Sweeney, J., Murphy, C., (2006). Assessing the impact of climate change on water supply and flood hazard in Ireland using statistical downscaling and hydrological modeling techniques. Climatic Change 74, page 475-491.
- Chaulagain, N. P., (2003). Change in precipitation parameters and its impacts on micro hydropower development: A case study at Jiri. In: Conference papers of international conference on Renewable Energy Technology for Rural Development 12-14 October 2003, Kathmandu, Nepal, page 186-189.
- Christensen, N. S., Wood, A. W., Voisin, N., Lettenmaier, D. P., Palmer, R. N., (2004). The effects of climate change on the hydrology and water resources of the Colorado River basin, Climatic Change 62, page 337–363.
- CNRCC, (2007). China's National Report on Climate Change 2007 (in Chinese).
- Combes, S., Prentice, M. L., Hansen, L., and Rosentrater, L., (2004). Going, going, gone! Climate change and global glacier decline. WWF brochure on glacier decline; WWF Climate Change Programme, Germany.
- CROPWAT 8, (2009). Food and Agriculture Organization (of the United Nations). http://www.fao.org/nr/water/infores\_databases\_cropwat.html
- CSE, (2002). Melting into Oblivion, In Down To Earth, 15 May 2002.
- Dai, A., (2003). Precipitation characteristics of eighteen coupled models, J. Clim. Submitted.
- Devkota, L. P., (2003). Climate variability over Nepal: observations, forecasting, model evaluation and impact on agriculture and water resources, (unpublished Doctoral thesis).Central Department of Hydrology and Meteorology, Institute of Science and Technology, Tribhuvan University, Kathmandu, Nepal.
- Dietz, E. J. and Kileen, A., (1981). A Nonparametric Multivariate Test for Monotone Trend with Pharmaceutical Applications, Journal of the American Statistical Association 76, page 169-174.

- Dwivedi, S. K., Acharya, M. D., and Joshi, S. P., (1999), Tam Pokhari GLOF of 3rd September 1998, preliminary report, WECS Bulletin. 10(1): page 11-13.
- Dyurgerov, M. D. and Meier, M. F., (2005). Glaciers and Changing Earth System, A 2004 Snapshot, page 117. Boulder (Colorado): Institute of Arctic and Alpine Research, University of Colorado.
- Eriksson, M., Xu, J., Shrestha A. B., Vaidya, R. A., Nepal, S., Sandstrom, K., (2009). The changing Himalayas: Impact of climate change on water resources and livelihoods in the greater Himalaya. Kathmandu: ICIMOD.
- FAO, (2009). Asian-Pacific Forestry Sector outlook study II, Working paper No. APFSOSII/WP/2009/05, country-reports/4245, country-reports/4245.
- Frederick, K. D. and Gleick, P. H., (1999). Water and Global Climate Change: Potential Impacts on U.S Water Resources, Prepared for the Pew Center on Global Climate Change, page 48.
- Fujita, K., Lonnie, G., Thompson, A., Yutaka, Y., Tetsuzo, K., Yoshiyuki, S. A., and Takeuchi, N., (2006). Thirty-year history of glacier melting in the Nepal Himalayas, Journal of Geophysical Research, 111(D3), page.3-8.
- Fujita, K., Kadota, T., Rana, B., Kayastha, R.B., and Ageta, Y., (2001a). Shrinkage of Glacier AX010 in Shorong region, Nepal Himalayas in the 1990s, In the Bulletin of Glaciological Research 18, Japanese society of snow and ice, page 51-54.
- Fujita, K., Nakawo, M., Fujii, Y. and Paudyal, P., (1997). Changes in glaciers in Hidden Valley, Mukut Himal, Nepal Himalayas from 1974-1994, In: Journal of Glaciology, Vol. 43, No. 145, page 583-588.
- Fukushima, Y. Watgnabe, O. and Higuchi, K., (1991). Estimation of Stream Flow change by global warming in a glacier-covered high mountain area of Nepal Himalaya, In: Snow, Hydrology and forest in high alpine areas (ed. By H. Bergmann et al.) Processed, Vienna Symposium August (1991), page 181-188. IAHS Pub. No. 205.
- Fukushima, Y., (1987). Runoff characteristics in three glacier covered watersheds of Langtang Valley, Nepal Himalayas. Bull. Glacier Res., Vol. 5, page 11-18.

- Gao, S., Wang, J., Xiong, L., Yin, A., Li, D., (2002). A macro-scale and semidistributed monthly water balance model to predict climate change impacts in China. Journal of Hydrology, 268, page 1-15.
- Garr, C. E. and Fitsharris, B. B., (1994). Sensitivity of mountain runoff and hydro-electricity to changing climate, In: Mountain environments in changing climates [Beniston, M.(ed.)], London and New York, page 366-381.
- Gemmer, M., Becker, S., Jiang, T., (2004). Observed monthly precipitation trends in China 1951-2002, Theoretical and Applied Climatology 77 (1-2), page 39-45.
- Gilbert, R. O., (1987). Statistical methods for environmental pollution monitoring. Van Nostrand Reinhold, New York.
- Giorgi, F. and Bi, X., (2005). Regional changes in surface climate in Terrannual variability for the 21<sup>st</sup> century from ensembles of global model simulations. Geophys. Res. Lett. 32, L13701, doi: 10.1029/2005GL023002.
- Giorgi, F. and Whetton, P.H. and Jones, R.G., (2001). Emerging patterns of simulated regional climatic changes for the 21<sup>st</sup> century due to anthropogenic forcing, Geophysics. Res. Lett. 28 3317-3321.
- Gordon, C., Cooper, C., Senior, C. A., Banks, H., Gregory, J. M., Johns, T. C., Mitchell, J. F. B., Wood, R. A., (2000). The simulation of SST, sea ice extents and ocean heat transport in a version of the Hadley Centre coupled model without flux adjustments. Climate Dynamics 16, page 147-168.
- Gottschalk, L., (1985). Hydrological regionalization of Sweden. Hydrol. Sci. J. 30(1), page 65-83.
- Gurung, T. M., (1997). Vulnerability and Adaptation Assessment of Water Resources to Climate Change in Koshi Basin of Nepal. In: Proceedings of the Workshop on Climate Change in Nepal, USCSP, Kathmandu, page 76.
- Haines, A. T., Finlayson, B. L. and McMahon, T. A., (1988) A global classification of river regimes. Appl. Geogr. 8. page 255-272.
- Hall, M. H. P., and Fagre, D. B., (2003). Modelled climate-induced glacier change in Glacier National Park, 1850-2100. Bioscience 53(2): page 131-140.
- Hamed, K. H., (2008). Trend detection in hydrologic data: The Mann-Kendall trend test under the scaling hypothesis. Journal of Hydrology 349 (3-4), page 350-363.

- Hann, C. T., Johneson, H. P., Brakensiek, D. L., (1982). Hydrologic Modeling of Small watershed, ASAE, page 533.
- Helsel, D. R., Hirsch, R. M., (1992). Statistical Methods in Water Resources. Elsevier, New York.
- Helsel, D. R., Hirsch, R. M., (2002). Statistical methods in water resources. Tech. rep., U. S. Geological Survey.
- Hirsch, R. M., Slack, J. R. and Smith, R. A., (1982). Techniques of Trend Analysis for Monthly Water Quality Data, Water Resources Research 18(1), 107-121.
- Hohmeyer, O., (1997). Social costs of climate change: strong sustainability and social costs. In Social costs and sustainability: valuation and implementation in the energy and transport sector, Springer, Berlin, pp 61-83.
- IHMS, (2006). Integrated Hydrological Modelling System Manual. Version 5.1.
- Immerzeel, W. W., van Beek, L. P. H., Konz, M., Shrestha, A. B. and Bierkens M. F. P., (2011). "Hydrological response to climate change in a glacierized catchment in the Himalayas" Climatic Change DOI 10.1007/s10584-011-0143-4.
- Ines, A., and Hansen, J., (2006). Bias correction of daily GCM rainfall for crop simulation studies. Agricultural Forest Meteorology, 138, page 44-53.
- IPCC, (1996b). Climate Change (1995), Impacts, adaptations and mitigation of climate change: scientific technical analyses. Contribution of Working Group II to the Second Assessment Report of the Intergovernmental Panel on Climate Change [Watson, R.T., M.C. Zinyowera, R.H. Moss and D.J. Dokken (eds.)], Cambridge University Press, page 880.
- IPCC, (1998). The regional impacts of climate change: An assessment of vulnerability. Special report of IPCC working group II [Watson, R. T.; M. C. Zinyowera, R. H. Moss R. H. and D. J. Dokken (eds.)], Cambridge University Press, Cambridge, page 516.
- IPCC, (2001). IPCC Third Assessment Report- Climate Change (2001), Working Group II: Impacts, Adaptation and Vulnerability. Summary for Policy Makers. Geneva, WMO and UNEP.
- IPCC, (2001a). Climate Change (2001), Synthesis Report. Contribution of Working Gorup I, II and III to Third Assessment Report of the

Intergovernmental Panel on Climate Change. [Watson, R.T. and Core Writing Team (eds.)] Cambridge University Press, page. 46-398.

- IPCC, (2001b). Climate Change (2001), Impacts, Adaptation and Vulnerability. Contribution of Working Group II to Third Assessment Report of the Intergovernmental panel on Climate Change. [MacCarthy, M.C., Canziani, O. F., Leary, N. A., Dokken, D. J. and White, K. S. (eds.)]. Cambridge University Press, page. 212-1033.
- IPCC, (2007). Climate Change (2007), Synthesis Report. Contribution of Working Group I, II and III to the Fourth Assessment Report of the Intergovernmental Panel on Climate Change. [Core Writing Team, Pachauri, R. K. and Reisinger, A. (eds.)]. IPCC, Geneva, Switzerland, page 5-109.
- IPCC, (2007). Summary of the policy makers, Climate Change (2007). The Physical Science Basis. Contribution of Working Group I to the Fourth Assessment Report of the Intergovernmental Panel on Climate Change.
- IPCC, (2007a). Climate change (2007), Impacts, adaptation and vulnerability. Cambridge: Cambridge University Press.
- IPCC, (2008). Technical Paper of Intergovernmental Panel on Climate change. Climate Change and Water [Bates, B. C., Kundzewicz, Z. W. Wu, S. and Palutikof J. P., (eds.)]. IPCC Secretraint, Geneva, page 210.
- IPCC, (2008). Technical Paper on Climate Change and Water, Synthesis Report, A report of the Intergovernmental Panel on Climate Change.
- Jansson, P., Hock, R., and Schneider, T., (2003). The concept of glacier storage – A review. Journal of Hydrology 282(1-4): page 116-129.
- Jha, P. K.; (1992). Environment and Man in Nepal. Craftsman Press, Bangkok.
- Johennesson, T., Sigursson, O., Laumann, T., and Kennet, M., (1995).
   Degree-day glacier mass-balance modeling with application to glaciers in Iceland, Norway and Greenland. J. Glaciol Vol 41 (138), page 345-358.
- Jordan, E., L. Ungerechts, B. caceres, a Penafiel and B. Francou, (2005). Estimation by photogrametry of the glacier recession on the Cotopaxi Volcano (Ecuador) between 1956 and 1997. Hydrological Science-Journal, Vol 50 (6) page 949-961.
- Kaczmarek, Z., arnell, N. and Starkel, L., (1996). Climate, Hydrology and Water Resources. In: Water resources Management in the face of

climatic/hydrological uncertainties. International Tnstitute for Applied Systems Analysis, Laxenburg, page 3-29, 48.

- Kadota, T., Fujita, K., Seko, K., Kayastha, R.B., and Ageta, Y., (1997). Monitoring and prediction of shrinkage of a small glacier in the Nepal Himalaya. International Glaciological Society; Annals of Glaciology (24): page 90-94.
- Kalnay, E., (1996). The NCEP/NCAR 40-Year Reanalysis Project. Bulletin of the American Meteorological Society, Vol.77, page 437-471.
- Kattelmann, R., (1987). Uncertainty in Assessing Himalayan Water Resources. In Mountain Research and Development, 7(3): page 279-286.
- Katz, R. W., Parlange, M. B. and Naveau P., (2002). Statistics of Extreme in Hydrology. Advances in Water Resources, 25, page 1287-1304.
- Kayastha, R. B., Ohata, T. and Agata, Y., (1999). Application of a glacier mass balance model to Himalayan Glacier, Journal of Glaciology 45, page 559-567.
- Kayastha, R. B., Ageta, Y. and Fujita, K., (2005). Use of Positive Degree day Methods for calculating Snow and Ice melting and Discharge in Glacierized Basin in the Langtang Valley, central Nepal. Climate and Hydrology in Mountain Areas, page 7-14.
- Kayastha, R. B., Takeuchi, Y., Nakawo, M. Y., and Agata, Y., (2000). Practical prediction of ice melting beneath various thickness of debris cover on Khumbu Glacier, Nepal, Using a Positive degree-day factor. IAHS, page 264.
- Kendall, M. G., (1975). Rank Correlation Methods, Charles Griffin, London.
- Kistler, R.,(2001). The NCEP/NCAR 50-Year Reanalysis. Bulletin of the American Meteorological Society, Vol.82(2), page 247-267.
- Konz, M. and Merz, J., (2010). An application of the HBV model to the Tamor basin in Eastern Nepal. Journal of Hydrology, (December), page 49-58.
- Krasovskaia, I., Gottschalk, L. and Kundzewicz, Z. W., (1999). Dimensionality of Scandinavian river flow regimes. Hydro. Sci. J. 44(5), page 705-723.
- Krasovskaia, I. and Gottschalk, L., (1992). Stability of river flow regimes. Nordic Hydro I. 23, page 137-154.

- Krasovskaia, I. and Gottschalk, L., (1995). Analysis of regional drought characteristics with empirical orthogonal functions, In: New Uncertainty Concepts in Hydrology and Water Resources (ed. by Z. W. Kundzewicz). Cambridge Univ. Press, Cambridge, UK.
- Kripalani, R. H., Inamdar, S. and Sontakke, N. A., (1996). Rainfall variability over Bangladesh and Nepal: Comparison and connections with features over India. In: International Journal of Climatology, Vol. 16, page 689-703.
- Lal, M., (2002). Possible Impacts of Global Climate Change on Water Availability in India,Report to Global Environment and Energy in the 21st Century. New Delhi: Indian Institute of Technology.
- Laumanna, T. and Reeh, L., (1993). Sensitivity to climate change of mass balance of glaciers in southern Norway, J.Glacial. 39(133), page 656-665.
- Lee, C., Bergin-Seers, S., Graeme G., O'Mahony, B., and Mc Murray, A., (2008). Seasonality in Tourism industry, Impacts and Strategies First published in Australia in by CRC for Sustainable Tourism Pty Ltd.
- Liu, S., Ding, Y., Li, J., Shangguan, D., Zhang, Y., (2006). Glaciers in response to recent climate warming in western china. Quaternary sciences, 26(5): page 762-771.
- Lu, C., Yuan, H. Barry E., Schwartz, and Benjamin, S. G., (2007). Short-Range Numerical Weather Prediction Using Time-Lagged Ensembles.Wea. Forecasting, 22, 580–595.
- Mahmood, R. and Mukand, B. S., (2012). Evaluation of SDSM developed by annual and monthly sub-models for downscaling temperature and precipitation in the Jhelum basin, Pakistan and India.
- Male, D. H. and Gray, D. M., (1981). Snow covers ablation and runoff. In Handbook of Snow. Pergamon Press, Toronto, Canada.
- Manley, R. E., (1993). HYSIM Reference Manual. R. E. Manley Consultancy, Cambridge.
- Mann H. B., (1945). Nonparametric Tests against Trend, Econometrica 13, page 245-259.
- Marahatta, S., Dongol, B. S., Gurung, G. B., (2009). Temporal and Spatial Variability of climate change over Nepal (1976-2005). Practical Action Nepal Office, 2009.

- Martimec, J., Rango, A. and Roberts, R., (2007). Snowmelt Runoff Model (SRM) User's Manual (Updated Edition Window Version 1.11) (ed. By M. Baumgartner). Department of Geography, University of Bern, Switzerland.
- Mather, J. R., (1969). The average annual water balance of the world, in Symposium on Water Balance in North America, Series No.7, Proceedings: Banff, Alberta, Canada, American Water Resources Association, page 29-40.
- Mather, J. R., (1978). The climatic water balance in environmental analysis: Lexington, Mass., D.C. Heath and Company, page 239.
- McCabe, G. J., and Wolock, D. M., (1999). Future snowpack conditions in the western United States derived from general circulation model climate simulations: Journal of the American Water Resources Association, v. 35, page 1,473–1,484.
- McKay, M. D., Conover, W. J., Beckman, R. J., (1979). A comparison of three methods for selection values of input variables in the analysis of output from a computer code. Technometrics 2, page 239–245.
- Menzel, L., Burger, G., (2002). Climate change scenarios and runoff response in the Mulde catchment (Southern Elbe, Germany). Journal of Hydrology 267 (1–2), page 53–64.
- Merz, R. and Boloschl, G., (2003). A process typology of regional floods.
   Water Resources Research, VOL. 39, NO. 12, page 1340.
- Merz, R. and Boloschl, G., (2004). Regionalisation of catchment model parameters. Journal of Hydrology 287, page 95-123.
- Middelkoop, H., Daamen, K., Gellens, D., Grabs, W., Kwadijk, J. C. J., Lang, H., Parmet, B. W. A.H., Schadler, B., Schulla, J., Wilke, K., (2001). Impact of climate change on hydrological regimes and water resources management in the Rhine basin Climatic Change 49 (1–2), page 105–128.
- Mirza, M. Q. and A. Dixit, (1997). Climate change and water management in the GBM basins. In: Water Nepal, Vol. 5 No. 1, Nepal Water Conservation Foundation, Kathmandu, page 71-100.
- Mool, P. K., Bajracharya, S. R., and Joshi, S. P., (2001a). Inventory of Glaciers, Glacial Lakes and Glacial Lake Outburst Floods Monitoring and Early Warning Systems in the Hindu Kush-Himalayan Region, Nepal. ICIMOD, Kathmandu, page 363.

- Mool, P. K., Bajracharya, S. R., and Joshi, S. P., (2001b). Glacial Lakes and Glacial Lake Outburst Floods Events in the Hindu Kush-Himalayan Region, In: Global Change and Himalayan Mountains [Shrestha, K.L., (eds.)], Institute for development and Innovation, Lalitpur, Nepal, page 75-83.
- MOPE, (2001). State of the Environment Nepal (Agriculture and Forest), Pub. By His Majesty's Government, Ministry of Population and Environment, Kathmandu, Nepal, 1-39.
- MOPE, (2004). Nepal Initial National communication to the Conference of Parties of the United Nations Framework Convention on Climate Change: Ministry of Population and Environment of Nepal, Kathmandu page 153.
- Motoyama, H., Ohata, T. and Yamada, T., (1987). Winter runoff in the glacierized drainage basin in Langtang Valley, Nepal Himalayas. Bull. Glacier Res., 5, page 29-33.
- Murphy, C., Charlton, R., Sweeney, J., Fealy, R., (2006a). Catering for uncertainty in a conceptual rainfall runoff model: model preparation for climate change impact assessment and the application of GLUE using Latin Hypercube Sampling. In: Proceedings of the National Hydrology Seminar, Tullamore, 2006.
- Murphy, C., Fealy, R., Charlton, R., Sweeney, J., (2006b). The reliability of an 'off-the-shelf' conceptual rainfall runoff model for use in climate impact assessment: uncertainty quantification using Latin hypercube sampling. Area 38.1, page 65–78.
- Nakawo, M. and Takahashi, S., (1982). A Simplified model for estimating glacier abalation under a debris layer. Glen, j. W. (ed) Hydrological Aspect of Alpine and high Mountain area, IAHS 138, page 137-145.
- Nayava, J. L.,(1974): Heavy monsoon rainfall in nepal, Weather, Roy. Met. Soci., U. K., Vol. 29, Page no 443-450.
- Nazrul, N. M., (2009). Rainfall and Temperature Scenario for Bangladesh. The Open Atmospheric Science Journal, 3, page 93-103, SAARC Meteorological Research Centre, E-4/C Agargaon, Dhaka-1207, Bangladesh.
- Nesler, J. M, Long K. S., (1997). Development of hydrological indices to aid cumulative impact analysis of riverrine wetlands. Regulated Rivers 13; page 317-334.

- Nijssen, B., Odonnell, G. M., Hamlet, A. F., and Lettenmaier, D. P., (2001). Hydrologic sensitivity of global rivers to climate change. Climatic Change, 50, page 143-175.
- Ohamura, A., (2001). Physical basis for the temperature-based melt index method. J.Appl. Meteorology. 40, pp 753-761.
- Parajka, J., Merz, R., and Bloschl, G., (2004). Regionale wasserbilanzkomponenten fur Osterreich auf Tagesbasis (Regional water balance components in Austria on a daily basis). Osterr. Wasser- und Abfallwirtschaft. Accepted.
- Puri, V. M. K. and Swaroop, S., (1995). Relationship of glacierized area and summer mean daily discharge of glacier basin in Jhelum, Satluj and Alaknanda catchments in Northernestern Himalaya. Geol. Surv. India Space. Publ., 21, page 315-319.
- Quick, M. C., Pipes, A., (1977). UBS watershed model. Hydrological Sciences Bulletin 22, page 161-253.
- Raghunath, H. M., (2006). Hydrology, Principles, Analysis and Design. New Age International (P) Limited, New Delhi, India.
- Rana, B., Fukushima, Y., Ageta, Y. and Nakawo, M., (1996). Runoff modeling of a river basin with a debris-covered glacier in Langtang Valley, Nepal Himalaya. Bukk Glacier Res, 14, page 1-6.
- Rango, A. and Martinec, J., (1997). Water storage in mountain basin from satellite snow cover mentoring. In: Remote Sensing and Geographic information Systems for Design and Operation of Water Resources Systems (ed. By M. F. Baumgartner, G.A. Schultz and A. I. Johnson), Proc. 5th Scientific assembly of IAHS, Rabat, Morocco, IAHS Publication no. 242, page 83-91.
- Rangwala, I., Sinsky, E. and Miller, J. R., (2013). Amplified warming projections for high altitude regions of the northern hemisphere mid-latitudes from CMIP5 models.
- Ren, J., Jing, Z., Pu, J., and Qin, X., (2006). Glacier variations and climate change in the central Himalaya over the past few decades. Annals of Glaciology (43): page 218-222.

- Ren, J., Qin, D., Kang, S., Hou, S., Pu, J., and Jing, Z., (2004). Glacier variations and climate warming and drying in the central Himalayas. Chinese Science Bulletin 49(1), DOI: 10.1360/03wd0148: page 65-69.
- Renoj. J. T., Gergan, J. T. and Dobhl, D. P., (2007). Role of glacier and snow cover on headwater river hydrology in monsoon regime-Micro-scale study of Din Gad catchment. Garhwal Himalaya, India, Current Science, Vol. 92 No. 3 page 376-382.
- Robert, L. W. and Christian, W. D., (2007). Statistical downscaling model SDSM Version 4.2 user manual.
- Ruiz-Barradas, A. and Nigam, S., (2003). IPCC's 20<sup>th</sup> century climate simulations: Varied representation of North American hydro climate variability. J. Clim. (Submitted).
- Salzmann, N., Frei C., Vidale P., Hoelzle M., (2007). The application of Regional Climate Model output for the simulation of high-mountain permafrost scenarios, ScienceDirect, Global and Planetary Change 56 (2007) 188–202.
- Searcy, J. K., (2002). Flow duration curves Manual of hydrology, Part 2. Low flow techniques. USGS, Water Supply Paper 1542-A.
- Seibert, J. and McDonnell, J. J., (2010). Land-cover impacts on stream flow: A change-detection modeling approach that incorporates parameter uncertainty, Hydrological Sciences Journal, 55(3), page 316 - 332.
- Seibert, J., (1997). Estimation of Parameter Uncertainty in the HBV Model. Earth, 28(1982), page 247–262.
- Seibert, J., (1999). Regionalization of parameters for a conceptual rainfallrunoff model. Agricultural and Forest Meteorology 98-99: page 279-293.
- Seibert, J., (2003). Reliability of model predictions outside calibration conditions, Nordic Hydrology, 34: 477-492.
- Seibert, J., (2005), HBV light version 2, User's Manual, Uppsala University, Institute of Earth Sciences, Department of Hydrology, Uppsala, Sweden.
- Seibert, J., (2005). HBV light version 2, User's manual, Stockholm University. (<a href="http://people.su.se/\_jseib/HBV/HBV\_manual\_2005.pdf">http://people.su.se/\_jseib/HBV/HBV\_manual\_2005.pdf</a>).
- Seko, K., (1987). Seasonal variation of altitudinal dependence of precipitation in Langtang Valley, Nepal Himalaya. Bulletin Glacier Res 5, page 41-47.

- Sen, P. K., (1968). Estimates of the regression coefficient based on Kendall's tau. Journal of the American Statistical Association, 63:page 1379–1389.
- Shankar, K. and P. B. Shrestha, (1985) Climate. In: Nepal- Nature's Paradise: Insight into diverse facets of topography, flora and ecology [Majupuria, T.C. (ed.)], White Lotus Co. Ltd, Bangkok, page 39-44.
- Sharma, K. P., Vorosmarty, C. J. and Moore III, (2001b). Sensitivity of the Himalayan Hydrology to Land-use and Climate Changes. Climate Change 47, Kluwer Academic Publisher, Dordrecht, the Netherland, page 136.
- Shirawa, T., Ueno, K and Yamada, T., (1992). Distribution of mass input on glaciers in the Langtang valley, Nepal Himalayas. Bulletin of Glacier Research 10, page 21-30.
- Shrestha, M., (2008). Runoff Modeling of Glacierized Watershed: A Case Study of Imja Watershed, M.Sc. Thesis, IOE, Tribhuvan University, Nepal.
- Shrestha, A. B., (2001). Tsho Rolpa Glacier Lake: Is it linked to Climate Change? In: Global Change in Himalayan Mountains. Proceedings of a scoping workshop, Kathmandu Nepal, 2-5 October 2001 [Shrestha, K.L. (ed.)], page 85-95.
- Shrestha, A. B., Wake, C. P., Dibb, J. E and Mayewski, P. A., (2000). Precipitation Fluctuations in the Nepal Himalaya and its vicinity and Relationship with some Large Scale Climatological Parameters. In: International Journal of Climatology, Vol. 20, Royal Meteorological Society, page 317-325.
- Shrestha, A. B., Wake, C.P., Dibb, J. E., and Mayewski, P. A., (1999). Maximum Temperature Trends in the Himalaya and its Vicinity: an Analysis Based on Temperature Records from Nepal for 50 the Period 1971-94. In: Journal of Climate Vol. 12, American Meteorological Society.
- Silveira, L., (1997). Multivariate analysis in hydrology: the factor correspondence analysis method applied to annual rainfall data. Hydrological Sciences-Journal-des Sciences Hydrologiques 42(2), page 215–224.
- Singh, K., Kumar, (2001). Coastal Infrastructure Design, construction and Maintenance" Environmental Management Authority Trinidad, West Indies Chapter 8.

- Singh, P. and Jain, S.K., (2002). Snow and glacier melt in the Satluj River at Bhakra Dam in the western Himalayan region. Hydrology Science Journal, 47. page 93-106.
- Singh, P., (1998). Effect of global warming on the stream flow of a highaltitude Spiti River. In: Ecohydrology of high mountain areas (Proceedings of the International Conference of high mountain areas, Kathmandu, Nepal, 24-28 March 1996), ICIMOD, Kathmandu, page 103-114.
- Singh, P., and Bengtsson, L., (2004). Hydrological sensitivity of a large Himalayan basin to climate change. Hydrology. Process. 18, page 2363-2385.
- Singh, P., and Kumar, N,. (1997b). Effects of Orography on precipitation in the western Himalayan region, Journal of Hydrology, 199, page 183-206.
- Swaroop, S., shukla, S.P., Oberoi, L.K., Siddiqui. M.A. and Bejarniya, B.R., (2001). Short term runoff and ablation characteristics of Triloknath glacier. Lahul and Spiti district. Geological Survey, India, spec.pub., 53, page 91-96.
- Teutschbin, C. and Seibert, J., (2012). Bias correction of regional climate model simulations for hydrological climate- change impact study: Review and evaluation of different methods, Journal of hydrology 456-457, ELSEVIER, page 12-29.
- Thompson, E. M., (2006). Abrupt climate change and our future. Paper presented by Ice Core Paleoclimate Research Group (20 October, 2006), Department of Geography and Byrd Polar Research Centre, The Ohio State University.
- Thompson, M., Gyawali, D., (2007). Introduction: Uncertainty revisited. In Thompson, M., Warburton, M., Hatley, T (eds) Uncertainty on a Himalayan Scale. Kathmandu: Himal Books.
- Thornthwaite water balance model, (2010). Develop by USGS wwwbrr.cr.usgs.gov/projects/SW\_MoWS/Thornthwaite.html
- Thornthwaite, C. W., (1948). An approach toward a rational classification of climate: Geographical Review, v. 38, page 55–94.
- UNDP, (2004). Reducing disaster risk: a challenge for development. New York: UNDP Bureau for Crisis Prevention and Recovery, 2004.

- UNDP, (2006). Summary Human Development Report, Beyond scarcity: power, poverty and the global water cycle. Summary Human Development Report, Palgrave Macmillam, Newyork, USA.
- UNEP, (2001). Nepal: State of the Environment 2001. United Nations Environment Programme and International Centre for Integrated Mountain Development, Kathmandu, Nepal, page 211.
- UNEP, (2010). High Mountain Glacier and Climate Change-Challenges to Human livelihood and Adaptation [Kaltenborn, B.P., Nellemann, C., Vistnes, I.I. (eds.)]. United Nations Environment Programme, Grid- Arendal.
- Viviroli, D., Durr, H. H., Messerli, B., Meybeck, M., and Weingartner, R. (2007). Mountains of the world, water towers for humanity: Typology, mapping, and global significance. Water Resources Research, 43, W07447. doi:10.1029/2006WR005653.
- Vogel, R. M., Fennessey, N. M., (1995). Flow duration curves II: A review of applications in water resources planning. Journal of the American Water Resources Association 31(6), 1029–1039.
- Wang, H., (2006). Inter-annual and Seasonal Variation of the Huang He (Yellow River) Water Discharge over the Past 50 Years: Connection to Impacts from ENSO Events and Dams. In Global and Planetary Change, vol.50, page 212-225.
- Westmacott, J. R. and Burn, D. H., (1997). Climate change on the hydrological regime within the Churchill-Nelson River Basin J.Hydrol 202, page 263-279.
- Wilby, R. L., (1998). Statistical downscaling of general circulation model output : A comparison of methods. Water Resources, 34(11), page.2995–3008.
- Wilby, R. L., (2004). Guidelines for Use of Climate Scenarios Developed from Statistical Downscaling Methods. Analysis, (August), page.1–27.
- Wilby, R. L., and Dawson, C., (2007). User Manual SDSM 4.2 A decision support tool for the assessment of regional climate change impacts.
- WMO, (1988). Analyzing long time series of hydrological data with respect to climate variability, Project description, WCAP -3. Tech. rep., World Meteorological Organization.

- Wolock, D. M., and McCabe, G. J., (1990). Effects of potential climatic change on annual runoff in the conterminous United States: Journal of the American Water Resources Association, v. 35, page 341-350.
- WWF, (2005). WWF Nepal annual report 2004/2005. World wide fund for nature conservation, Nepal.
- Yao, T. D., Guo, X. J., Lonnie, T., Duan, K. Q., Wang, N. L., Pu, J. C., Xu, B. Q., Yang, x. X., and Sun, W.z., (2006). 'd180 Record and Temperature Change over the Past 100 years in Ice Cores on the Tibetian Plateau. In Science in China: Series D Earth Science, 49(1) : page 1-9.

## APPENDIX

		Annapurna							Lang	tang					Khur	nbu		
Tmax ( <sup>0</sup> C) A1B Sco	enario																	
Season/Decadel	2000s	2010s	2020s	2030s	2040s	2050s	2000s	2010s	2020s	2030s	2040s	2050s	2000s	2010s	2020s	2030s	2040s	20509
DJF	3.7	3.9	4.1	4.0	4.4	4.5	1.1	0.9	1.4	1.6	1.5	1.6	-3.8	-3.6	-3.4	-3.4	-3.1	-3.1
MAM	10.0	10.4	10.5	10.7	11.2	11.5	7.1	7.2	7.1	7.2	6.9	7.2	3.6	3.9	4.2	4.3	4.7	5.0
JJAS	12.6	12.7	12.7	12.8	12.9	13.1	10.5	10.5	10.8	10.8	11.0	11.0	5.6	5.7	5.7	5.7	5.6	5.6
ON	8.2	8.2	8.0	8.1	8.0	8.0	7.7	7.5	7.8	8.0	7.9	8.3	1.5	1.3	1.2	1.3	1.1	1.2
Annual	9.0	9.2	9.2	9.3	9.5	9.7	6.8	6.8	7.1	7.1	7.1	7.3	2.1	2.2	2.3	2.3	2.5	2.6
TMin ( <sup>0</sup> C) A1B Sce	nario																	
Season/Decadel	2000s	2010s	2020s	2030s	2040s	2050s	2000s	2010s	2020s	2030s	2040s	2050s	2000s	2010s	2020s	2030s	2040s	2050s
DJF	-4.2	-4.1	-3.9	-3.8	-3.6	-3.4	-6.9	-6.7	-6.2	-6.0	-5.8	-5.4	-13.9	-13.9	-13.9	-13.9	-13.9	-14.0
MAM	1.6	2.0	2.3	2.6	3.1	3.6	-1.5	-0.9	-0.7	-0.4	0.0	0.6	-11.7	-11.4	-11.4	-11.4	-11.3	-11.2
JJAS	6.8	6.9	7.0	7.0	7.1	7.1	6.4	6.6	6.8	6.9	6.9	7.2	-2.8	-3.1	-2.3	-2.1	-1.4	-1.3
ON	1.6	1.4	1.3	1.4	1.1	1.3	1.1	1.2	1.6	1.9	1.9	2.5	-12.4	-12.6	-12.8	-12.6	-12.7	-12.5
Annual	1.9	2.0	2.1	2.3	2.4	2.6	0.2	0.5	0.8	1.0	1.2	1.6	-9.4	-9.4	-9.2	-9.1	-8.9	-8.8
TMean ( <sup>0</sup> C) A1B S	cenario																	
Season/Decadel	2000s	2010s	2020s	2030s	2040s	2050s	2000s	2010s	2020s	2030s	2040s	2050s	2000s	2010s	2020s	2030s	2040s	2050s
DJF	-2.0	-1.9	-1.7	-1.7	-1.4	-1.3	-3.2	-3.1	-2.5	-2.2	-2.3	-2.1	-7.9	-7.7	-7.5	-7.4	-7.1	-7.1
MAM	4.0	4.4	4.7	5.0	5.5	6.0	3.0	3.6	3.7	4.1	4.3	5.1	-0.6	-0.3	-0.1	0.1	0.4	0.7
JJAS	7.8	7.9	8.0	8.0	8.1	8.2	9.4	9.5	9.9	9.9	9.9	10.2	3.0	3.1	3.2	3.2	3.1	3.2
ON	6.1	5.8	5.6	5.7	5.2	5.5	4.1	4.2	4.5	5.0	5.0	5.6	-2.7	-2.9	-3.0	-2.9	-3.1	-2.9
Annual	3.6	3.8	3.9	4.0	4.1	4.4	3.8	4.0	4.4	4.6	4.6	5.1	-1.6	-1.4	-1.3	-1.2	-1.1	-1.0

Appendix (I) Table 1, A1B decadal scenarios of maximum (Tmax), minimum (Tmin) and mean (Tmean) temperatures from 2001 to 2060.

*Appendix (I), Table 2,* A2 decadal scenarios of maximum (Tmax), minimum (Tmin) and mean (Tmean) temperatures from 2001 to 2060.

	Temperature A2 Scenario Annapurna																	
			Anna	purna					Lang	tang					Khu	mbu		
Tmax A2 Scenario	C																	
Season/Decadel	2000s	2010s	2020s	2030s	2040s	2050s	2000s	2010s	2020s	2030s	2040s	2050s	2000s	2010s	2020s	2030s	2040s	2050s
DJF	3.5	3.8	3.9	4.2	4.4	4.5	1.0	1.2	0.9	1.4	1.6	2.0	-3.8	-3.6	-3.7	-3.3	-3.1	-3.1
MAM	10.3	10.5	10.9	11.0	11.1	11.2	7.2	7.4	7.2	7.1	7.1	6.9	3.8	4.0	4.4	4.5	4.6	4.7
JJAS	12.7	12.7	12.7	12.9	13.0	13.1	10.5	10.6	10.6	10.8	11.0	11.1	5.7	5.6	5.6	5.8	5.8	5.8
ON	8.4	8.1	8.3	8.3	8.2	8.2	7.6	7.7	7.9	7.9	8.3	8.3	1.4	1.2	1.4	1.3	1.3	1.3
Annual	nual 9.1 9.1 9.3 9.5 9.6 9.					9.7	6.8	6.9	6.9	7.1	7.2	7.3	2.2	2.1	2.3	2.4	2.5	2.6
TMin A2 Scenario	)																	
Season/Decadel	2000s	2010s	2020s	2030s	2040s	2050s	2000s	2010s	2020s	2030s	2040s	2050s	2000s	2010s	2020s	2030s	2040s	2050s
DJF	-4.4	-4.1	-4.1	-3.8	-3.5	-3.4	-7.1	-6.6	-6.7	-5.9	-5.6	-5.2	-13.9	-13.9	-13.9	-13.9	-14.0	-13.9
MAM	1.8	2.2	2.6	2.9	3.1	3.3	-1.1	-0.7	-0.3	-0.2	0.2	0.0	-11.6	-11.5	-11.3	-11.4	-11.2	-10.9
JJAS	6.8	6.8	7.0	7.0	7.2	7.2	6.6	6.6	6.7	6.8	7.0	7.2	-3.4	-3.0	-2.7	-2.8	-2.2	-1.2
ON	1.6	1.2	1.6	1.5	1.5	1.4	1.2	1.1	1.8	2.0	2.6	2.6	-12.5	-12.8	-12.6	-12.7	-12.6	-12.8
Annual	1.9	2.0	2.2	2.3	2.5	2.6	0.4	0.5	0.8	1.1	1.4	1.6	-9.6	-9.5	-9.3	-9.4	-9.1	-8.8
TMean A2 Scenai	rio																	
Season/Decadel	2000s	2010s	2020s	2030s	2040s	2050s	2000s	2010s	2020s	2030s	2040s	2050s	2000s	2010s	2020s	2030s	2040s	2050s
DJF	-2.2	-2.0	-1.9	-1.6	-1.4	-1.3	-3.2	-2.9	-3.2	-2.3	-2.0	-1.6	-8.0	-7.8	-7.9	-7.5	-7.3	-7.3
MAM	4.3	4.6	5.0	5.2	5.4	5.6	3.5	3.9	4.2	4.3	4.7	4.5	-1.0	-0.7	-0.3	-0.2	-0.1	0.1
JJAS	7.9	7.9	8.0	8.1	8.2	8.2	9.5	9.7	9.7	9.9	10.2	10.1	3.2	3.1	3.3	3.4	3.5	3.5
ON	6.3	5.6	6.1	6.0	5.9	5.9	4.2	4.4	4.6	4.9	5.5	5.9	-4.5	-5.0	-4.4	-4.7	-4.5	-4.4
Annual	3.7	3.8	4.0	4.1	4.2	4.3	4.0	4.2	4.3	4.6	5.0	5.0	-1.5	-1.5	-1.3	-1.2	-1.0	-1.0

*Appendix (I) Table 3,* Decadal values of maximum (Tmax), minimum (Tmin) and mean (Tmean) temperatures from 2001 to 2060 in calibration and validation period from NCEP data.

Temperature calibration and validation												
Temperature cali												
		Anna	purna			Lang	tang			Khu	mbu	
Tmax												
Season/Decadel	1970s	1980s	1990s	2000s	1970s	1980s	1990s	2000s	1970s	1980s	1990s	2000s
DJF	3.4	3.2	3.4	3.4	1.9	2.1	2.5	2.3	-4.1	-4.1	-3.7	-3.8
МАМ	11.1	10.9	10.6	11.0	6.4	6.6	6.7	6.9	3.2	3.3	3.1	2.9
JJAS	12.1	12.3	12.5	12.5	10.3	10.4	10.5	10.5	5.8	5.8	5.9	5.3
ON	8.3	8.3	8.4	8.3	6.7	6.5	6.1	6.5	1.3	1.3	1.4	1.1
Annual	9.1	9.0	9.1	9.1	6.6	6.8	6.8	6.9	1.9	2.0	2.0	1.7
TMin												
Season/Decadel	1970s	1980s	1990s	2000s	1970s	1980s	1990s	2000s	1970s	1980s	1990s	2000s
DJF	-4.5	-4.7	-4.5	-4.5	-7.5	-7.2	-6.6	-6.9	-13.8	-13.8	-13.9	-13.8
MAM	2.4	2.0	1.8	2.0	-1.7	-1.4	-1.5	-1.2	-11.8	-11.8	-11.7	-11.9
JJAS	6.3	6.2	6.4	6.2	6.1	6.2	6.3	6.3	-3.3	-2.9	-2.4	-2.9
ON	1.1	0.9	0.7	0.8	-0.9	-1.1	-1.5	-1.2	-12.8	-12.6	-12.8	-12.8
Annual	1.8	1.6	1.6	1.6	-0.4	-0.2	-0.2	-0.1	-9.6	-9.5	-9.3	-9.5
Tmean												
Season/Decadel	1970s	1980s	1990s	2000s	1970s	1980s	1990s	2000s	1970s	1980s	1990s	2000s
DJF	-2.3	-2.5	-2.3	-2.4	-2.6	-2.1	-1.7	-2.0	-8.4	-8.4	-7.9	-8.0
MAM	4.9	4.7	4.4	4.7	2.4	2.8	2.8	3.0	-1.4	-1.2	-1.3	-1.4
JJAS	7.5	7.5	7.6	7.5	8.4	8.7	8.8	8.8	2.7	2.7	2.9	2.5
ON	5.8	5.6	5.5	5.5	3.0	3.2	2.9	3.1	-5.7	-5.2	-5.0	-5.4
Annual	3.6	3.5	3.5	3.6	3.3	3.6	3.7	3.7	-2.0	-1.9	-1.7	-2.0

*Appendix (I) Table 4,* A2 decadal scenarios of maximum (Tmax), minimum (Tmin) and mean (Tmean) temperatures from 1961 to 2000.

Tempe	rature A	2 Scena	rio									
		Anna	purna			Lang	tang			Khu	mbu	
Tm	ax A2 Sc	enario										
Season/Decadel	1970s	1980s	1990s	2000s	1970s	1980s	1990s	2000s	1970s	1980s	1990s	2000s
DJF	3.2	3.3	3.4	3.6	0.6	0.9	0.6	0.6	-4.2	-4.1	-4.0	-3.9
MAM	9.6	9.8	10.3	10.3	6.8	7.0	7.6	7.6	3.1	3.4	3.7	3.9
JJAS	12.2	12.2	12.3	12.4	10.2	10.4	10.4	10.5	5.2	5.1	5.2	5.2
ON	7.9	7.9	7.7	7.9	7.0	7.0	6.7	6.7	1.0	1.0	0.7	0.8
Annual	8.6	8.7	8.8	8.9	6.4	6.6	6.6	6.7	1.6	1.7	1.8	1.9
TMin A2 Scenario												
Season/Decadel	1970s	1980s	1990s	2000s	1970s	1980s	1990s	2000s	1970s	1980s	1990s	2000s
DJF	-4.7	-4.7	-4.6	-4.4	-8.0	-7.6	-7.5	-7.3	-13.8	-13.8	-13.9	-13.8
МАМ	1.0	1.3	2.0	2.0	-2.1	-1.6	-0.6	-0.4	-11.8	-11.8	-11.7	-11.9
JJAS	6.3	6.3	6.4	6.5	6.1	6.2	6.4	6.5	-3.3	-2.9	-2.4	-2.9
ON	1.0	0.9	0.5	0.8	-0.1	0.0	-0.3	-0.1	-12.8	-12.6	-12.8	-12.8
Annual	1.3	1.4	1.6	1.7	-0.5	-0.2	0.1	0.2	-9.6	-9.5	-9.3	-9.5
TMean A2 Scenario												
Season/Decadel	1970s	1980s	1990s	2000s	1970s	1980s	1990s	2000s	1970s	1980s	1990s	2000s
DJF	-2.5	-2.4	-2.3	-2.2	-4.2	-3.8	-3.7	-3.6	-8.3	-8.3	-8.3	-8.1
МАМ	3.5	3.8	4.4	4.4	2.6	3.1	4.3	4.3	-1.6	-1.3	-1.0	-0.8
JJAS	7.5	7.5	7.6	7.6	9.0	9.1	9.2	9.4	2.6	2.5	2.6	2.7
ON	5.2	5.1	4.6	5.0	3.1	3.3	2.9	3.0	-2.8	-2.8	-3.1	-2.9
Annual	3.2	3.2	3.4	3.5	3.1	3.4	3.7	3.8	-2.1	-2.0	-2.0	-1.8

Precipitation (mn	n) observ	ed peric	d								
		Anr	napurna		Langta	ang			Khumbu		
Season/Decadel	1980s	1990s	2000s	2010s	2000s	2010s	1970s	1980s	1990s	2000s	2010s
DJF	16.9	23.6	23.1	19.0	10.4	7.7	3.3	2.9	3.4	3.2	3.1
MAM	100.4	97.2	106.0	113.1	29.5	35.2	17.0	20.0	19.0	19.3	22.8
JJAS	672.8	718.5	754.6	733.9	105.6	139.4	92.9	85.3	86.7	90.8	89.2
ON	90.4	62.8	70.5	86.6	9.6	13.7	10.7	12.2	10.2	8.4	9.2
Annual	3222.8	3361.9	3546.3	3506.4	561.3	713.9	453.1	434.4	434.3	447.7	453.1

Appendix (I) Table 5, Observed decadal precipitation (mm) of the three regions.

Appendix (I) Table 6, Comparisons of decadal precipitation (mm) of Modi Khola, Langtang Khola and Dudhkoshi river basins, A2 scenario after the calibration and validation period 1961 to 2000.

Precipitation (mm) A2, calibraton and validatin perio												
		Anr	napurna			Langta	ing			Khum	ıbu	
Season/Decadel	1970s	1980s	1990s	2000s	1970s	1980s	1990s	2000s	1970s	1980s	1990s	2000s
DJF	20.0	16.7	12.9	16.8	12.1	11.9	10.3	11.8	1.5	0.8	0.8	0.9
MAM	87.7	77.3	82.6	82.8	31.2	35.5	33.6	29.7	18.1	18.9	20.5	16.5
JJAS	504.1	521.4	547.6	506.8	131.2	125.2	122.7	116.4	97.3	100.9	104.0	90.9
ON	98.1	70.0	55.5	71.7	12.9	11.3	9.8	10.5	12.3	13.7	12.7	6.4
Annual	2532.3	2507.9	2588.2	2468.3	678.3	665.7	642.0	610.8	471.9	489.9	505.1	428.6
Precipitation (mn	n)A2 , cal	ibraton a	and valid	atin period								
		Anr	napurna			Langta	ng			Khum	ıbu	
Season/Decadel	1970s	1980s	1990s	2000s	1970s	1980s	1990s	2000s	1970s	1980s	1990s	2000s
DJF	19.3	18.9	18.6	16.8	10.5	9.7	10.5	9.3	0.8	0.9	0.7	0.7
MAM	102.6	107.4	100.6	105.2	31.3	32.4	34.1	32.4	22.5	23.4	30.8	30.4
JJAS	415.2	413.2	404.1	418.7	137.9	142.0	144.1	136.7	91.5	91.7	93.6	92.3
ON	112.6	126.2	126.1	119.8	11.3	11.0	11.5	12.0	10.1	9.7	6.2	5.7
Annual				2280.9	698.4	716.1	733.5	696.1	456.0	459.2	481.5	474.2

Appendix (I) Table 7, Decadal values of precipitation (mm) in calibration and validation period from 1961 to 2000.

Precipitation	ecipitation (mm) A1B Scenario Annapurna																	
			Anna	ourna					Lang	tang					Khui	mbu		
Season/Dec adel	2000s	2010s	2020s	2030s	2040s	2050s	2000s	2010s	2020s	2030s	2040s	2050s	2000s	2010s	2020s	2030s	2040s	2050s
DJF	13.0	12.8	12.0	10.1	10.1	8.3	10.2	11.4	10.7	9.9	9.6	10.1	0.5	0.7	0.9	0.7	0.7	0.6
MAM	102.3	106.1	94.8	97.7	96.4	88.2	29.3	27.9	31.2	31.5	33.0	35.8	24.3	29.8	33.0	34.5	36.4	38.9
JJAS	407.5						143.2	141.7	144.4	143.1	138.8	141.7	105.2	104.9	109.8	109.3	105.1	103.7
ON	102.7	102.7 123.5 131.8 114.0 109.2 13					10.4	13.3	11.0	10.6	11.3	12.3	13.8	11.6	10.9	11.5	7.8	7.4
Annual	2181.0	2261.2	2204.3	2207.9	2164.1	2198.3	710.9	711.5	725.4	717.8	705.9	729.1	522.9	534.2	562.7	565.7	547.2	548.1
Precipitation	ı (mm) A2	Scenari	0															
			Anna	ourna				-	Lang	tang	-		Khumbu					
Season/Dec adel	2000s	2010s	2020s	2030s	2040s	2050s	2000s	2010s	2020s	2030s	2040s	2050s	2000s	2010s	2020s	2030s	2040s	2050s
DJF	13.6	13.8	12.6	9.7	8.7	8.5	7.3	7.6	7.7	7.2	5.8	7.5	0.8	0.9	0.7	0.5	0.7	0.7
MAM	105.2	100.9	106.1	98.7	92.8	97.9	26.5	30.8	30.7	28.2	35.0	32.1	27.4	31.6	34.6	35.9	38.0	38.4
JJAS	419.8	425.9	405.6	442.3	418.1	405.5	143.0	142.2	143.2	140.8	142.6	134.8	107.1	103.2	104.2	110.9	111.7	108.7
ON	130.3	130.9	120.9	124.1	131.1	140.6	9.4	9.7	10.8	9.7	9.6	9.4	12.9	10.4	10.7	10.0	9.8	7.4
Annual	2295.1	2310.3	2219.7	2342.5	2239.1	2222.1	691.1	703.2	709.6	688.8	712.3	676.6	538.8	531.1	544.1	572.9	582.5	567.2

Appendix (I) Table 8, Decadal observed discharge during calibration and validation period from Modi Khola (1991 to 2010), Langtang Khola (1991 to 2010), and Dudhkoshi river basins (1971 to 2010).

Observed discharge (m <sup>3</sup> /s	5)								
	Annapurna (1	991-2010)	Langtar	ng (1991-2010)		Khumb	ou (1961-2	2010)	
Season/Decadal	1990s	2000s	1990s	2000s	1960s	1970s	1980s	2000s	2000s
DJF	11.1	15.8	17.5	16.5	48.6	51.4	44.6	43.1	47.9
МАМ	13.7	17.3	19.6	17.8	46.7	55.2	49.4	48.1	46.4
JJAS	129.3	101.6	58.4	49.3	439.7	462.7	453.7	432.0	525.9
ON	66.0	57.8	54.9	47.7	295.7	319.7	251.3	267.2	247.5
Annual	54.9	47.1	33.4	28.9	195.1	207.6	195.4	189.2	219.8

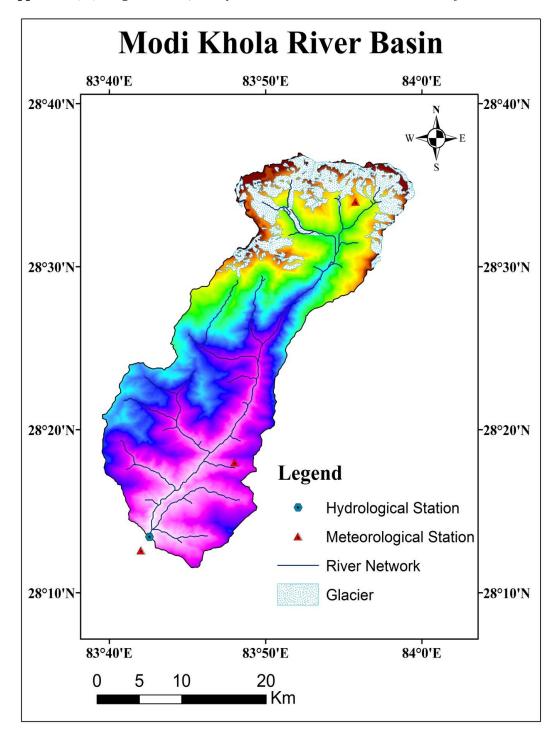
Distric	arge A1	B Scena	rio from	n Max Te	mp													
			Anna	purna					Lang	gtang					Khu	mbu		1
Season/Decadel	2000s	2010s	2020s	2030s	2040s	2050s	2000s	2010s	2020s	2030s	2040s	2050s	2000s	2010s	2020s	2030s	2040s	2050
DJF	8.5	9.2	9.6	9.3	9.4	9.6	15.9	17.7	18.3	18.9	19.2	19.7	79.0	83.1	83.4	83.6	83.1	82.
MAM	15.6	17.5	17.1	18.2	19.2	19.9	20.5	21.5	21.7	21.7	20.4	21.2	100.0	110.9	113.1	115.7	119.9	122
JJAS	90.4	92.6	93.1	95.1	99.6	100.9	59.2	57.7	57.1	56.7	57.1	56.7	487.4	490.3	522.3	523.3	529.6	529
ON	34.6	34.7	36.1	35.4	34.7	36.6	40.1	39.8	42.0	43.8	44.0	46.6	186.4	180.7	178.8	185.5	171.6	174
Annual	42.0	43.4	43.7	44.5	46.1	47.1	35.7	35.7	36.0	36.4	36.2	36.9	238.8	242.0	253.0	255.2	255.9	257
Disch	arge A1	B Scena	rio Fron	n Min Te	mp													
			Anna	purna					Lang	tang					Khu	mbu		
Season/Decadel	2000s	2010s	2020s	2030s	2040s	2050s	2000s	2010s	2020s	2030s	2040s	2050s	2000s	2010s	2020s	2030s	2040s	205
DJF	4.0	4.3	4.5	4.5	4.2	4.4	7.2	8.2	8.6	8.6	8.6	8.7	45.2	48.8	49.6	49.9	50.6	50.
MAM	1.9	2.4	2.3	2.8	3.2	3.8	3.4	3.9	4.1	4.2	4.2	4.3	105.9	120.6	129.9	135.2	144.7	153
JJAS	50.3	52.6	54.1	55.6	59.8	61.2	24.9	25.0	24.1	22.5	22.5	19.2	464.3	467.2	487.5	484.6	473.9	470
ON	20.8	20.7	20.7	20.8	20.0	20.6	15.7	16.9	16.8	17.2	16.8	16.3	183.8	178.7	179.4	184.4	168.0	165
Annual	21.8	22.7	23.2	23.8	25.1	25.9	13.7	14.2	14.0	13.6	13.5	12.4	223.8	227.9	237.3	238.6	234.7	235
Discha	rge A1B	Scenar	io From	Mean T	emp													
			Anna	purna					Lang	tang					Khu	mbu		
Season/Decadel	2000s	2010s	2020s	2030s	2040s	2050s	2000s	2010s	2020s	2030s	2040s	2050s	2000s	2010s	2020s	2030s	2040s	205
DJF	6.2	6.8	7.0	6.9	6.8	7.0	11.6	12.9	13.5	13.7	13.9	14.2	62.1	65.9	66.5	66.7	66.9	66.
MAM	8.7	10.0	9.7	10.5	11.2	11.9	12.0	12.7	12.9	12.9	12.3	12.8	103.0	115.8	121.5	125.4	132.3	138
JJAS	70.4	72.6	73.6	75.3	79.7	81.0	42.0	41.3	40.6	39.6	39.8	38.0	475.9	478.7	504.9	504.0	501.7	500
ON	27.7	27.7	28.4	28.1	27.3	28.6	27.9	28.4	29.4	30.5	30.4	31.5	185.1	179.7	179.1	184.9	169.8	169
Annual	31.9	33.0	33.4	34.1	35.6	36.5	24.7	24.9	25.0	25.0	24.9	24.6	231.3	235.0	245.2	246.9	245.3	246
Disch	narge A2	2 from m	iax Tem	p Scena	rio													
Disch	narge A2	from m		p Scena purna	rio				Lang	tang					Khu	mbu		
Disch Season/Decadel	-		Anna			2050s	2000s	2010s	Lang 2020s		2040s	2050s	2000s	2010s	Khui 2020s		2040s	205
Season/Decadel	2000s	2010s	Anna 2020s	purna 2030s	2040s				2020s	2030s					2020s	2030s		
Season/Decadel DJF	2000s 8.7	2010s 9.4	Anna 2020s 9.4	purna 2030s 9.9	2040s 10.0	10.0	15.9	18.0	2020s 18.3	2030s 19.1	19.6	20.5	44.9	48.8	2020s 48.9	2030s 51.5	51.1	51.
Season/Decadel DJF MAM	2000s 8.7 16.8	2010s 9.4 17.6	Anna 2020s 9.4 18.5	purna 2030s 9.9 19.1	2040s 10.0 19.5	10.0 19.9	15.9 21.0	18.0 22.6	2020s 18.3 21.4	2030s 19.1 21.8	19.6 22.3	20.5 21.2	44.9 114.7	48.8 126.5	2020s 48.9 136.4	2030s 51.5 140.9	51.1 149.6	51. 150
Season/Decadel DJF MAM JJAS	2000s 8.7 16.8 91.4	2010s 9.4 17.6 92.6	Anna 2020s 9.4 18.5 95.6	purna 2030s 9.9 19.1 96.0	2040s 10.0 19.5 99.0	10.0 19.9 101.3	15.9 21.0 58.5	18.0 22.6 58.4	2020s 18.3 21.4 58.9	2030s 19.1 21.8 58.3	19.6 22.3 58.2	20.5 21.2 57.9	44.9 114.7 476.4	48.8 126.5 469.3	2020s 48.9 136.4 473.6	2030s 51.5 140.9 497.2	51.1 149.6 497.3	51. 150 489
Season/Decadel DJF MAM JJAS ON	2000s 8.7 16.8 91.4 36.5	2010s 9.4 17.6 92.6 35.6	Anna 2020s 9.4 18.5 95.6 36.0	purna 2030s 9.9 19.1 96.0 36.9	2040s 10.0 19.5 99.0 37.7	10.0 19.9 101.3 37.0	15.9 21.0 58.5 39.7	18.0 22.6 58.4 40.5	2020s 18.3 21.4 58.9 40.7	2030s 19.1 21.8 58.3 40.7	19.6 22.3 58.2 42.8	20.5 21.2 57.9 42.0	44.9 114.7 476.4 186.0	48.8 126.5 469.3 174.4	2020s 48.9 136.4 473.6 177.5	2030s 51.5 140.9 497.2 175.2	51.1 149.6 497.3 181.9	51. 150 489 172
Season/Decadel DJF MAM JJAS ON Annual	2000s 8.7 16.8 91.4 36.5 43.0	2010s 9.4 17.6 92.6 35.6 43.6	Anna 2020s 9.4 18.5 95.6 36.0 44.9	purna 2030s 9.9 19.1 96.0 36.9 45.4	2040s 10.0 19.5 99.0 37.7 46.7	10.0 19.9 101.3	15.9 21.0 58.5	18.0 22.6 58.4	2020s 18.3 21.4 58.9	2030s 19.1 21.8 58.3	19.6 22.3 58.2	20.5 21.2 57.9	44.9 114.7 476.4	48.8 126.5 469.3	2020s 48.9 136.4 473.6	2030s 51.5 140.9 497.2	51.1 149.6 497.3	2050 51. 150 489 172 242
Season/Decadel DJF MAM JJAS ON Annual	2000s 8.7 16.8 91.4 36.5 43.0	2010s 9.4 17.6 92.6 35.6 43.6	Anna 2020s 9.4 18.5 95.6 36.0 44.9	purna 2030s 9.9 19.1 96.0 36.9 45.4 5 Scena	2040s 10.0 19.5 99.0 37.7 46.7	10.0 19.9 101.3 37.0	15.9 21.0 58.5 39.7	18.0 22.6 58.4 40.5	2020s 18.3 21.4 58.9 40.7 36.4	2030s 19.1 21.8 58.3 40.7 36.4	19.6 22.3 58.2 42.8	20.5 21.2 57.9 42.0	44.9 114.7 476.4 186.0	48.8 126.5 469.3 174.4	2020s 48.9 136.4 473.6 177.5 233.9	2030s 51.5 140.9 497.2 175.2 243.0	51.1 149.6 497.3 181.9	51. 150 489 172
Season/Decadel DJF MAM JJAS ON Annual	2000s 8.7 16.8 91.4 36.5 43.0 harge A2	2010s 9.4 17.6 92.6 35.6 43.6 2 from m	Anna 2020s 9.4 18.5 95.6 36.0 44.9 hin Temp Anna	2030s 9.9 19.1 96.0 36.9 45.4 o Scena purna	2040s 10.0 19.5 99.0 37.7 46.7 rio	10.0 19.9 101.3 37.0 47.4	15.9 21.0 58.5 39.7 35.6	18.0 22.6 58.4 40.5 36.4	2020s 18.3 21.4 58.9 40.7 36.4 Lang	2030s 19.1 21.8 58.3 40.7 36.4	19.6 22.3 58.2 42.8 37.0	20.5 21.2 57.9 42.0 36.7	44.9 114.7 476.4 186.0	48.8 126.5 469.3 174.4 229.3	2020s 48.9 136.4 473.6 177.5 233.9 Khuu	2030s 51.5 140.9 497.2 175.2 243.0 mbu	51.1 149.6 497.3 181.9 246.3	51. 150 489 172 242
Season/Decadel DJF MAM JJAS ON Annual Discl Season/Decadel	2000s 8.7 16.8 91.4 36.5 43.0 narge A2 2000s	2010s 9.4 17.6 92.6 35.6 43.6 2 from m 2010s	Anna 2020s 9.4 18.5 95.6 36.0 44.9 hin Temp Anna 2020s	2030s 9.9 19.1 96.0 36.9 45.4 5 Scena purna 2030s	2040s 10.0 19.5 99.0 37.7 46.7 rio	10.0 19.9 101.3 37.0 47.4 2050s	15.9 21.0 58.5 39.7 35.6 2000s	18.0 22.6 58.4 40.5 36.4 2010s	2020s 18.3 21.4 58.9 40.7 36.4 Lang 2020s	2030s 19.1 21.8 58.3 40.7 36.4 tang 2030s	19.6 22.3 58.2 42.8 37.0 2040s	20.5 21.2 57.9 42.0 36.7 2050s	44.9 114.7 476.4 186.0 230.3 2000s	48.8 126.5 469.3 174.4 229.3 2010s	2020s 48.9 136.4 473.6 177.5 233.9 Khui 2020s	2030s 51.5 140.9 497.2 175.2 243.0 wbu 2030s	51.1 149.6 497.3 181.9 246.3 2040s	51. 150 489 172 242
Season/Decadel DJF MAM JJAS ON Annual Discl Season/Decadel DJF	2000s 8.7 16.8 91.4 36.5 43.0 harge A2 2000s 4.3	2010s 9.4 17.6 92.6 35.6 43.6 2 from m 2010s 4.3	Anna 2020s 9.4 18.5 95.6 36.0 44.9 in Temp Anna 2020s 4.5	purna 2030s 9.9 19.1 96.0 36.9 45.4 5 Scena purna 2030s 4.5	2040s 10.0 19.5 99.0 37.7 46.7 rio 2040s 4.7	10.0 19.9 101.3 37.0 47.4 2050s 4.5	15.9 21.0 58.5 39.7 35.6 2000s 7.6	18.0 22.6 58.4 40.5 36.4 2010s 8.2	2020s 18.3 21.4 58.9 40.7 36.4 Lang 2020s 8.6	2030s 19.1 21.8 58.3 40.7 36.4 trang 2030s 8.6	19.6 22.3 58.2 42.8 37.0 2040s 8.6	20.5 21.2 57.9 42.0 36.7 2050s 8.7	44.9 114.7 476.4 186.0 230.3 2000s 18.0	48.8 126.5 469.3 174.4 229.3 2010s 19.0	2020s 48.9 136.4 473.6 177.5 233.9 Khui 2020s 19.1	2030s 51.5 140.9 497.2 175.2 243.0 mbu 2030s 19.4	51.1 149.6 497.3 181.9 246.3 2040s 19.6	51. 150 489 172 242 205 19.
Season/Decadel DJF MAM JJAS ON Annual Discl Season/Decadel DJF MAM	2000s 8.7 16.8 91.4 36.5 43.0 harge A2 2000s 4.3 2.3	2010s 9.4 17.6 92.6 35.6 43.6 2 from m 2010s 4.3 2.5	Anna 2020s 9.4 18.5 95.6 36.0 44.9 in Temp Anna 2020s 4.5 2.9	purna 2030s 9.9 19.1 96.0 36.9 45.4 5 Scena purna 2030s 4.5 3.0	2040s 10.0 19.5 99.0 37.7 46.7 rio 2040s 4.7 3.4	10.0 19.9 101.3 37.0 47.4 2050s 4.5 3.4	15.9 21.0 58.5 39.7 35.6 2000s 7.6 3.8	18.0 22.6 58.4 40.5 36.4 2010s 8.2 4.0	2020s 18.3 21.4 58.9 40.7 36.4 Lang 2020s 8.6 4.2	2030s 19.1 21.8 58.3 40.7 36.4 2030s 8.6 4.2	19.6 22.3 58.2 42.8 37.0 2040s 8.6 4.3	20.5 21.2 57.9 42.0 36.7 2050s 8.7 4.3	44.9 114.7 476.4 186.0 230.3 2000s 18.0 7.3	48.8 126.5 469.3 174.4 229.3 2010s 19.0 8.2	2020s 48.9 136.4 473.6 177.5 233.9 Khu 2020s 19.1 9.7	2030s 51.5 140.9 497.2 243.0 243.0 2030s 19.4 9.0	51.1 149.6 497.3 181.9 246.3 2040s 19.6 10.1	51. 150 489 172 242 205 19. 10.
Season/Decadel DJF MAM JJAS ON Annual Disct Season/Decadel DJF MAM JJAS	2000s 8.7 16.8 91.4 36.5 43.0 harge A2 2000s 4.3 2.3 50.8	2010s 9.4 17.6 92.6 35.6 43.6 2 from m 2010s 4.3 2.5 53.0	Anna 2020s 9.4 18.5 95.6 36.0 44.9 in Temp Anna 2020s 4.5 2.9 55.7	2030s 9.9 19.1 96.0 36.9 45.4 5 Scena purna 2030s 4.5 3.0 56.2	2040s 10.0 19.5 99.0 37.7 46.7 rio 2040s 4.7 3.4 59.4	10.0 19.9 101.3 37.0 47.4 2050s 4.5 3.4 62.4	15.9 21.0 58.5 39.7 35.6 2000s 7.6 3.8 25.2	18.0 22.6 58.4 40.5 36.4 2010s 8.2 4.0 26.0	2020s 18.3 21.4 58.9 40.7 36.4 2020s 8.6 4.2 26.4	2030s 19.1 21.8 58.3 40.7 36.4 2030s 8.6 4.2 24.9	19.6 22.3 58.2 42.8 37.0 2040s 8.6 4.3 22.8	20.5 21.2 57.9 42.0 36.7 2050s 8.7 4.3 21.4	44.9 114.7 476.4 186.0 230.3 230.3 2000s 18.0 7.3 310.5	48.8 126.5 469.3 174.4 229.3 2010s 19.0 8.2 311.5	2020s 48.9 136.4 473.6 177.5 233.9 Khui 2020s 19.1 9.7 323.0	2030s 51.5 140.9 497.2 175.2 243.0 mbu 2030s 19.4 9.0 346.8	51.1 149.6 497.3 181.9 246.3 246.3 2040s 19.6 10.1 358.5	51. 150 489 172 242 205 19. 10. 371
Season/Decadel DJF MAM JJAS ON Annual Disct Season/Decadel DJF MAM JJAS ON	2000s 8.7 16.8 91.4 36.5 43.0 arage A2 2000s 4.3 2.3 50.8 21.9	2010s 9,4 17.6 92.6 35.6 43.6 2 from m 2010s 4.3 2.5 53.0 20.1	Anna 2020s 9,4 18.5 95.6 36.0 44.9 ini Temp Anna 2020s 4.5 2.9 55.7 21.1	purna 2030s 9.9 19.1 96.0 36.9 45.4 2030s 4.5 3.0 56.2 21.2	2040s 10.0 19.5 99.0 37.7 46.7 rio 2040s 4.7 3.4 59.4 21.9	10.0 19.9 101.3 37.0 47.4 2050s 4.5 3.4 62.4 20.7	15.9 21.0 58.5 39.7 35.6 2000s 7.6 3.8 25.2 16.9	18.0 22.6 58.4 40.5 36.4 2010s 8.2 4.0 26.0 16.2	2020s 18.3 21.4 58.9 40.7 36.4 2020s 8.6 4.2 2020s 8.6 4.2 26.4 17.4	2030s 19.1 21.8 58.3 40.7 36.4 2030s 8.6 4.2 24.9 16.8	19.6 22.3 58.2 42.8 37.0 2040s 8.6 4.3 22.8 16.6	20.5 21.2 57.9 42.0 36.7 2050s 8.7 4.3 21.4 16.2	44.9 114.7 476.4 186.0 230.3 230.3 2000s 18.0 7.3 310.5 92.9	48.8 126.5 469.3 174.4 229.3 2010s 19.0 8.2 311.5 85.6	2020s 48.9 136.4 473.6 177.5 233.9 Khu 2020s 19.1 9.7 323.0 89.2	2030s 51.5 140.9 497.2 243.0 243.0 2030s 19.4 9.0 346.8 88.1	51.1 149.6 497.3 181.9 246.3 246.3 2040s 19.6 10.1 358.5 95.4	51. 150 489 172 242 205 19. 371 91.
Season/Decadel DJF MAM JJAS ON Annual Disct Season/Decadel DJF MAM JJAS ON	2000s 8.7 16.8 91.4 36.5 43.0 harge A2 2000s 4.3 2.3 50.8	2010s 9.4 17.6 92.6 35.6 43.6 2 from m 2010s 4.3 2.5 53.0	Anna 2020s 9.4 18.5 95.6 36.0 44.9 in Temp Anna 2020s 4.5 2.9 55.7	2030s 9.9 19.1 96.0 36.9 45.4 5 Scena purna 2030s 4.5 3.0 56.2	2040s 10.0 19.5 99.0 37.7 46.7 rio 2040s 4.7 3.4 59.4	10.0 19.9 101.3 37.0 47.4 2050s 4.5 3.4 62.4	15.9 21.0 58.5 39.7 35.6 2000s 7.6 3.8 25.2	18.0 22.6 58.4 40.5 36.4 2010s 8.2 4.0 26.0	2020s 18.3 21.4 58.9 40.7 36.4 2020s 8.6 4.2 26.4	2030s 19.1 21.8 58.3 40.7 36.4 2030s 8.6 4.2 24.9	19.6 22.3 58.2 42.8 37.0 2040s 8.6 4.3 22.8	20.5 21.2 57.9 42.0 36.7 2050s 8.7 4.3 21.4	44.9 114.7 476.4 186.0 230.3 230.3 2000s 18.0 7.3 310.5	48.8 126.5 469.3 174.4 229.3 2010s 19.0 8.2 311.5	2020s 48.9 136.4 473.6 177.5 233.9 Khui 2020s 19.1 9.7 323.0	2030s 51.5 140.9 497.2 175.2 243.0 mbu 2030s 19.4 9.0 346.8	51.1 149.6 497.3 181.9 246.3 246.3 2040s 19.6 10.1 358.5	51. 150 489 172 242 205
Season/Decadel DJF MAM JJAS ON Annual Discf Season/Decadel DJF MAM JJAS ON Annual	2000s 8.7 16.8 91.4 36.5 43.0 2000s 4.3 2.3 50.8 21.9 22.3	2010s 9.4 17.6 92.6 35.6 43.6 2010s 4.3 2.5 53.0 20.1 22.7	Anna 2020s 9.4 18.5 95.6 36.0 44.9 2020s 4.5 2.9 55.7 21.1 23.9	2030s 9.9 19.1 96.0 36.9 45.4 2030s 4.5 3.0 56.2 21.2 24.1	2040s 10.0 19.5 99.0 37.7 46.7 7 2040s 4.7 3.4 59.4 21.9 25.5	10.0 19.9 101.3 37.0 47.4 2050s 4.5 3.4 62.4 20.7	15.9 21.0 58.5 39.7 35.6 2000s 7.6 3.8 25.2 16.9	18.0 22.6 58.4 40.5 36.4 2010s 8.2 4.0 26.0 16.2	2020s 18.3 21.4 58.9 40.7 36.4 2020s 8.6 4.2 2020s 8.6 4.2 26.4 17.4	2030s 19.1 21.8 58.3 40.7 36.4 2030s 8.6 4.2 24.9 16.8	19.6 22.3 58.2 42.8 37.0 2040s 8.6 4.3 22.8 16.6	20.5 21.2 57.9 42.0 36.7 2050s 8.7 4.3 21.4 16.2	44.9 114.7 476.4 186.0 230.3 230.3 2000s 18.0 7.3 310.5 92.9	48.8 126.5 469.3 174.4 229.3 2010s 19.0 8.2 311.5 85.6	2020s 48.9 136.4 473.6 177.5 233.9 Khu 2020s 19.1 9.7 323.0 89.2	2030s 51.5 140.9 497.2 243.0 243.0 2030s 19.4 9.0 346.8 88.1	51.1 149.6 497.3 181.9 246.3 246.3 2040s 19.6 10.1 358.5 95.4	51. 150 489 172 242 205 19. 371 91.
Season/Decadel DJF MAM JJAS ON Annual Discf Season/Decadel DJF MAM JJAS ON Annual	2000s 8.7 16.8 91.4 36.5 43.0 2000s 4.3 2.3 50.8 21.9 22.3	2010s 9.4 17.6 92.6 35.6 43.6 2010s 4.3 2.5 53.0 20.1 22.7	Anna 2020s 9.4 18.5 95.6 36.0 44.9 2020s 4.5 2.9 55.7 21.1 23.9 23.9	2030s 9.9 19.1 96.0 36.9 45.4 2030s 4.5 3.0 56.2 21.2 24.1 24.1	2040s 10.0 19.5 99.0 37.7 46.7 7 2040s 4.7 3.4 59.4 21.9 25.5	10.0 19.9 101.3 37.0 47.4 2050s 4.5 3.4 62.4 20.7	15.9 21.0 58.5 39.7 35.6 2000s 7.6 3.8 25.2 16.9	18.0 22.6 58.4 40.5 36.4 2010s 8.2 4.0 26.0 16.2	2020s 18.3 21.4 58.9 40.7 36.4 2020s 8.6 4.2 26.4 17.4 14.9	2030s 19.1 21.8 58.3 40.7 36.4 2030s 8.6 4.2 24.9 16.8 14.3	19.6 22.3 58.2 42.8 37.0 2040s 8.6 4.3 22.8 16.6	20.5 21.2 57.9 42.0 36.7 2050s 8.7 4.3 21.4 16.2	44.9 114.7 476.4 186.0 230.3 230.3 2000s 18.0 7.3 310.5 92.9	48.8 126.5 469.3 174.4 229.3 2010s 19.0 8.2 311.5 85.6	2020s 48.9 136.4 473.6 177.5 233.9 2020s 19.1 9.7 323.0 89.2 129.8	2030s 51.5 140.9 497.2 243.0 2230s 19.4 9.0 346.8 88.1 137.3	51.1 149.6 497.3 181.9 246.3 246.3 2040s 19.6 10.1 358.5 95.4	51. 150 489 172 242 205 19. 371 91.
Season/Decadel DJF MAM JJAS ON Annual Discf Season/Decadel DJF MAM JJAS ON Annual	2000s 8.7 16.8 91.4 36.5 43.0 arge A2 2000s 4.3 2.3 50.8 21.9 22.3 arge A2	2010s 9.4 17.6 92.6 35.6 43.6 2010s 4.3 2.5 53.0 20.1 22.7 from m	Anna 2020s 9.4 18.5 95.6 36.0 44.9 in Temp Anna 2020s 4.5 2.9 55.7 21.1 23.9	2030s 9.9 19.1 96.0 36.9 45.4 5 Scena purna 2030s 4.5 3.0 56.2 21.2 24.1 24.1	2040s 10.0 19.5 99.0 37.7 46.7 rio 2040s 4.7 3.4 59.4 21.9 25.5	10.0 19.9 101.3 37.0 47.4 2050s 4.5 3.4 62.4 20.7 26.2	15.9 21.0 58.5 39.7 35.6 2000s 7.6 3.8 25.2 16.9 14.1	18.0 22.6 58.4 40.5 36.4 2010s 8.2 4.0 26.0 16.2 14.4	2020s 18.3 21.4 58.9 40.7 36.4 Lang 2020s 8.6 4.2 26.4 17.4 14.9	2030s 19.1 21.8 58.3 40.7 36.4 2030s 8.6 4.2 24.9 16.8 14.3	19.6 22.3 58.2 42.8 37.0 2040s 8.6 4.3 22.8 16.6 13.6	20.5 21.2 57.9 42.0 36.7 2050s 8.7 4.3 21.4 16.2 13.1	44.9 114.7 476.4 186.0 230.3 230.3 2000s 18.0 7.3 310.5 92.9	48.8 126.5 469.3 174.4 229.3 2010s 19.0 8.2 311.5 85.6 124.9	2020s 48.9 136.4 473.6 177.5 233.9 Khun 2020s 19.1 9.7 323.0 89.2 129.8 Khun	2030s 51.5 140.9 497.2 243.0 2030s 19.4 9.0 346.8 88.1 137.3	51.1 149.6 497.3 181.9 246.3 2040s 19.6 10.1 358.5 95.4 142.9	51. 150 489 172 242 205 19 10. 371 91. 146
Season/Decadel DJF MAM JJAS ON Annual Disch Season/Decadel JJF MAM JJAS ON Annual Disch Season/Decadel	2000s 8.7 16.8 91.4 36.5 43.0 2000s 4.3 2.3 50.8 21.9 22.3 22.3 arge A2 2000s	2010s 9.4 17.6 92.6 35.6 43.6 2010s 4.3 2.5 53.0 20.1 22.7 from m 2010s	Anna 2020s 9.4 18.5 95.6 36.0 44.9 2020s 4.5 2.9 55.7 21.1 23.9 21.1 23.9 2020s 2020s	purna 2030s 9,9 19,1 96,0 36,9 45,4 2030s 45,4 2030s 4,5 3,0 56,2 21,2 24,1 24,1 24,1 2030s	2040s 10.0 19.5 99.0 37.7 46.7 2040s 4.7 3.4 59.4 21.9 25.5 2040s	10.0 19.9 101.3 37.0 47.4 2050s 4.5 3.4 62.4 20.7 26.2 2050s	15.9 21.0 58.5 39.7 35.6 2000s 7.6 3.8 25.2 16.9 14.1 2000s	18.0 22.6 58.4 40.5 36.4 2010s 8.2 4.0 26.0 16.2 14.4 2010s	2020s 18.3 21.4 58.9 40.7 36.4 2020s 8.6 4.2 26.4 17.4 14.9 2020s 2020s	2030s 19.1 21.8 58.3 40.7 36.4 2030s 8.6 4.2 24.9 16.8 14.3 14.3 2030s	19.6 22.3 58.2 42.8 37.0 2040s 8.6 4.3 22.8 16.6 13.6 13.6	20.5 21.2 57.9 42.0 36.7 2050s 8.7 4.3 21.4 16.2 13.1 2050s	44.9 114.7 476.4 186.0 230.3 2000s 18.0 7.3 310.5 92.9 125.6 2000s	48.8 126.5 469.3 174.4 229.3 2010s 19.0 8.2 311.5 85.6 124.9 2010s	2020s 48.9 136.4 473.6 177.5 233.9 2020s 19.1 9.7 323.0 89.2 129.8 129.8 Khuu 2020s	2030s 51.5 140.9 497.2 243.0 2230s 19.4 9.0 346.8 88.1 137.3 137.3 2030s	51.1 149.6 497.3 181.9 246.3 2040s 19.6 10.1 358.5 95.4 142.9 2040s	51. 150 489 172 242 205 19 10. 371 91. 146
Season/Decadel DJF MAM JJAS ON Annual Disch Season/Decadel DJF MAM JJAS ON Annual Disch Season/Decadel DJF	2000s 8.7 16.8 91.4 36.5 43.0 2000s 4.3 2.3 50.8 21.9 22.3 3 arge A2 2000s 6.5	2010s 9.4 17.6 92.6 35.6 43.6 2 from m 2010s 4.3 2.5 53.0 20.1 22.7 from m 2010s 6.9	Anna 2020s 9.4 18.5 95.6 36.0 44.9 2020s 4.5 2.9 55.7 21.1 23.9 21.1 23.9 2020s an Terr Anna 2020s 6.9	purna           2030s           9.9           19.1           96.0           36.9           45.4           2030s           45.4           2030s           4.5           3.0           56.2           21.2           24.1           purna           2030s           7.2	2040s 10.0 19.5 99.0 37.7 46.7 2040s 4.7 3.4 21.9 25.5 ario 2040s 7.4	10.0 19.9 101.3 37.0 47.4 2050s 4.5 3.4 62.4 20.7 26.2 2050s 7.3	15.9 21.0 58.5 39.7 35.6 2000s 7.6 3.8 25.2 16.9 14.1 2000s 11.8	18.0 22.6 58.4 40.5 36.4 2010s 8.2 4.0 26.0 16.2 14.4 2010s 13.1	2020s 18.3 21.4 58.9 40.7 36.4 2020s 8.6 4.2 26.4 17.4 14.9 Lang 2020s 13.4	2030s 19.1 21.8 58.3 40.7 36.4 2030s 8.6 4.2 24.9 16.8 14.3 14.3 2030s 13.8	19.6 22.3 58.2 42.8 37.0 2040s 8.6 4.3 22.8 16.6 13.6 13.6 2040s 14.1	20.5 21.2 57.9 42.0 36.7 2050s 8.7 4.3 21.4 16.2 13.1 2050s 14.6	44.9 114.7 476.4 186.0 230.3 2000s 18.0 7.3 310.5 92.9 125.6 2000s 31.5	48.8 126.5 469.3 174.4 229.3 19.0 8.2 311.5 85.6 124.9 2010s 33.9	2020s 48.9 136.4 473.6 177.5 233.9 2020s 19.1 9.7 323.0 89.2 129.8 89.2 129.8 Khuu 2020s 34.0	2030s 51.5 140.9 497.2 243.0 243.0 2030s 19.4 9.0 346.8 88.1 137.3 137.3 2030s 35.4	51.1 149.6 497.3 181.9 246.3 19.6 10.1 358.5 95.4 142.9 2040s 35.3	51 150 489 172 242 205 19 10 371 91 146 205 35
Season/Decadel DJF MAM JJAS ON Annual Disch Season/Decadel DJF MAM JJAS ON Annual Disch Season/Decadel DJF	2000s 8.7 16.8 91.4 36.5 43.0 2000s 4.3 2.000s 4.3 2.3 50.8 21.9 22.3 22.3 22.3 20.8 21.9 22.3 20.0 50.8 21.9 22.3 20.0 50.8 21.9 22.3 20.0 50.8 21.9 22.3 50.8 21.9 22.3 50.8 21.9 22.3 50.8 21.9 22.3 50.8 21.9 22.3 50.8 21.9 22.3 50.8 21.9 22.3 50.8 21.9 22.3 50.8 21.9 22.3 50.8 21.9 22.3 50.8 21.9 22.3 50.8 21.9 22.3 50.8 21.9 22.3 50.8 22.5 23.5 22.5 23.5 22.5 23.5 23.5 23.5	2010s 9.4 17.6 92.6 35.6 43.6 2 from m 2010s 4.3 2.5 53.0 20.1 22.7 from m 2010s 6.9 10.1	Anna 2020s 9.4 18.5 95.6 36.0 44.9 2020s 4.5 2.9 55.7 21.1 23.9 21.1 23.9 2020s 6.9 10.7	purna           2030s           9.9           19.1           96.0           36.9           45.4           2030s           45.4           2030s           4.5           3.0           56.2           21.2           24.1           purna           2030s           7.2           11.1	2040s 10.0 19.5 99.0 37.7 46.7 2040s 4.7 3.4 59.4 21.9 25.5 2040s 21.9 25.5 2040s 21.9	10.0 19.9 101.3 37.0 47.4 2050s 4.5 3.4 62.4 20.7 26.2 2050s 7.3 11.6	15.9 21.0 58.5 39.7 35.6 2000s 7.6 3.8 25.2 16.9 14.1 2000s 11.8 11.8 12.4	18.0 22.6 58.4 40.5 36.4 2010s 8.2 4.0 26.0 16.2 14.4 2010s 13.1 13.3	2020s 18.3 21.4 58.9 40.7 36.4 2020s 8.6 4.2 26.4 17.4 14.9 Lang 2020s 13.4 12.8	2030s 19.1 21.8 58.3 40.7 36.4 2030s 8.6 4.2 24.9 16.8 14.3 14.3 2030s 13.8 13.0	19.6 22.3 58.2 42.8 37.0 2040s 8.6 4.3 22.8 16.6 13.6 13.6 2040s 14.1 13.3	20.5 21.2 57.9 42.0 36.7 2050s 8.7 4.3 21.4 16.2 13.1 2050s 14.6 12.7	44.9 114.7 476.4 186.0 230.3 2000s 18.0 7.3 310.5 92.9 125.6 125.6 31.5 61.0	48.8 126.5 469.3 174.4 229.3 19.0 8.2 311.5 85.6 124.9 2010s 33.9 67.3	2020s 48.9 136.4 473.6 177.5 233.9 2020s 19.1 9.7 323.0 89.2 129.8 54.0 2020s 34.0 73.0	2030s 51.5 140.9 497.2 243.0 2030s 19.4 9.0 346.8 88.1 137.3 2030s 35.4 75.0	51.1 149.6 497.3 181.9 246.3 19.6 10.1 358.5 95.4 142.9 2040s 35.3 79.9	51 150 489 172 242 205 19 10 371 91 146 205 35 80
Season/Decadel DJF MAM JJAS ON Annual Disch Season/Decadel DJF MAM JJAS ON Annual Disch Season/Decadel DJF	2000s 8.7 16.8 91.4 36.5 43.0 2000s 4.3 2.3 50.8 21.9 22.3 3 arge A2 2000s 6.5	2010s 9.4 17.6 92.6 35.6 43.6 2 from m 2010s 4.3 2.5 53.0 20.1 22.7 from m 2010s 6.9	Anna 2020s 9.4 18.5 95.6 36.0 44.9 2020s 4.5 2.9 55.7 21.1 23.9 21.1 23.9 2020s an Terr Anna 2020s 6.9	purna           2030s           9.9           19.1           96.0           36.9           45.4           2030s           45.4           2030s           4.5           3.0           56.2           21.2           24.1           purna           2030s           7.2	2040s 10.0 19.5 99.0 37.7 46.7 2040s 4.7 3.4 21.9 25.5 ario 2040s 7.4	10.0 19.9 101.3 37.0 47.4 2050s 4.5 3.4 62.4 20.7 26.2 2050s 7.3	15.9 21.0 58.5 39.7 35.6 2000s 7.6 3.8 25.2 16.9 14.1 2000s 11.8	18.0 22.6 58.4 40.5 36.4 2010s 8.2 4.0 26.0 16.2 14.4 2010s 13.1	2020s 18.3 21.4 58.9 40.7 36.4 2020s 8.6 4.2 26.4 17.4 14.9 Lang 2020s 13.4	2030s 19.1 21.8 58.3 40.7 36.4 2030s 8.6 4.2 24.9 16.8 14.3 14.3 2030s 13.8	19.6 22.3 58.2 42.8 37.0 2040s 8.6 4.3 22.8 16.6 13.6 13.6 2040s 14.1	20.5 21.2 57.9 42.0 36.7 2050s 8.7 4.3 21.4 16.2 13.1 2050s 14.6	44.9 114.7 476.4 186.0 230.3 2000s 18.0 7.3 310.5 92.9 125.6 2000s 31.5	48.8 126.5 469.3 174.4 229.3 19.0 8.2 311.5 85.6 124.9 2010s 33.9	2020s 48.9 136.4 473.6 177.5 233.9 2020s 19.1 9.7 323.0 89.2 129.8 89.2 129.8 Khuu 2020s 34.0	2030s 51.5 140.9 497.2 243.0 2230s 19.4 9.0 346.8 88.1 137.3 137.3 2030s 35.4	51.1 149.6 497.3 181.9 246.3 19.6 10.1 358.5 95.4 142.9 2040s 35.3	51 150 489 172 242 205 19 10 371 91 146 205 35

**Appendix (I) Table 9,** A1B and A2 decadal scenario of discharge  $(m^3/s)$  from maximum, minimum and mean temperatures  $({}^{0}C)$  and precipitation (2001-2060).

## Appendix (I) Table 10, Observed instantaneous maximum and minimum discharge

of Dudhkoshi river basin.

	MAXIMUM INSTA	NTANEOUS		MINIMUM IN	STANTANEOUS	
Year	Discharge (m3/s)	Gauge height	Date	Discharge (m3/s)	Gauge height(m)	Date
1964	1840	4.68	22/07/1964	-	-	-
1965	1740	4.55	15/08/1965	38.8	0.31	22/03/1965
1966	1900	4.75	24/08/1966	34.4	0.38	12/4/1966
1967	1260	3.9	16/08/1967	35.5	0.05	13/04/1967
1968	1700	4.5	16/07/1968	25.2	0.12	4/4/1968
1969	1920	4.78	28/07/1969	24.6	0.06	4/5/1969
1970	1530	5	20/07/1970	40	-0.02	18/02/1970
1971	1310	4.7	3/8/1971	29.2	0.36	18/03/1971
1972	1140	4.46	28/07/1972	43.8	0.74	24/04/1972
1973	1380	4.8	8/8/1973	43.2	0.94	6/3/1973
1974	1690	5.2	5/8/1974	46.4	0.98	21/03/1974
1975	1510	4.98	27/07/1975	31	0.55	27/03/1975
1976	2320	5.86	10/7/1976	31.6	0.56	30/03/1976
1977	1670	5.18	27/08/1977	32.2	0.77	6/3/1977
1978	1640	5.14	11/8/1978	34.6	0.81	7/4/1978
1979	1470	4.92	21/08/1979	27	0.68	21/03/1979
1980	1380	4.8	15/07/1980	40.8	0.91	19/03/1980
1981	1530	5	12/8/1981	40	0.9	24/03/1981
1982	1920	5.45	19/07/1982	35.7	1.13	28/12/1982
1983	2630	6.15	15/07/1983	20.4	0.92	24/03/1983
1984	1280	4.65	17/09/1984	18	0.74	9/4/1984
1985	4480	7.5	4/8/1985	33	1	25/03/1985
1986	2010	5.55	22/09/1986	24	0.85	24/03/1986
1987	1430	4.47	25/07/1987	38.1	1.2	11/3/1987
1988	1310	4.7	1/8/1988	24.6	0.98	28/03/1988
1989	1010	4.25	6/7/1989	23.8	0.53	18/03/1989
1990	1870	5.4	12/8/1990	30.2	1.06	3/4/1990
1991	1310	4.7	9/8/1991	19	0.9	24/04/1991
1992	1140	4.46	25/08/1992	26	1	3/4/1992
1993	1470	4.5	12/8/1993	26.1	1.06	23/03/1993
1994	870	4	27/07/1994	26.2	0.57	28/04/1994
1995	1210	4.55	13/08/1995	27.5	0.79	10/3/1995
1996	1530	5	4/9/1996	34.7	0.91	6/3/1996
1997	1870	5.4	12/8/1997	41.6	0.92	11/3/1997
1998	9880	10	3/9/1998	28.6	0.61	13/00/1998
1999	920	5	26/08/1999	108	2.57	17/03/1999
2000	3600	7.1	24/07/2000	26	1.65	19/03/2000
2001	2470	6	18/08/2001	27.2	1.2	22/03/2001
2002	3720	7	21/08/2002	13.4	0.88	18/03/2002
2003	2710	6.22	20/07/2003	19	0.9	12/3/2003
2004	3050	6.5	10/7/2004	28.4	1.22	11/3/2004
2005	2260	5.8	15/08/2005	32.6	1.5	4/3/2005
2006	2040	6.15	30/06/2006	21.5	1.57	10/3/2006



Appendix (II) Figure 1-24, Study Area, Watershed characteristics of three basins.

Figure 1 Modi Khola river basin (Annapurna region)

Appendix (II)

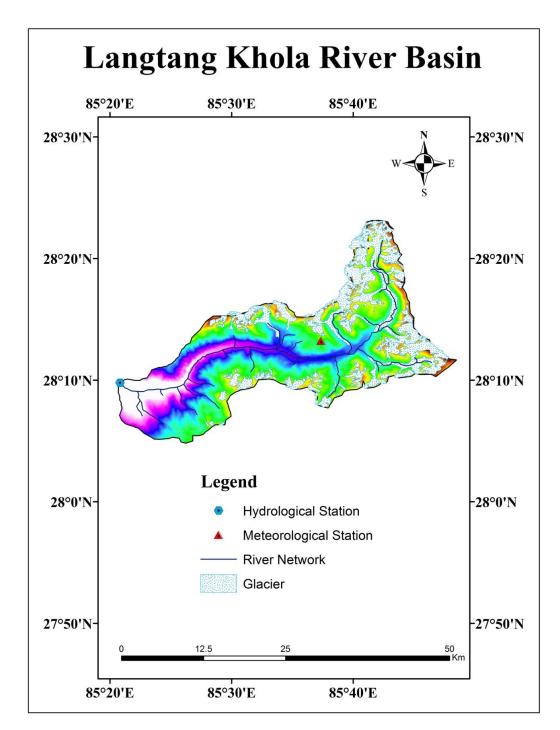


Figure 2 Langtang Khola river basin (Langtang region)

Appendix (II)

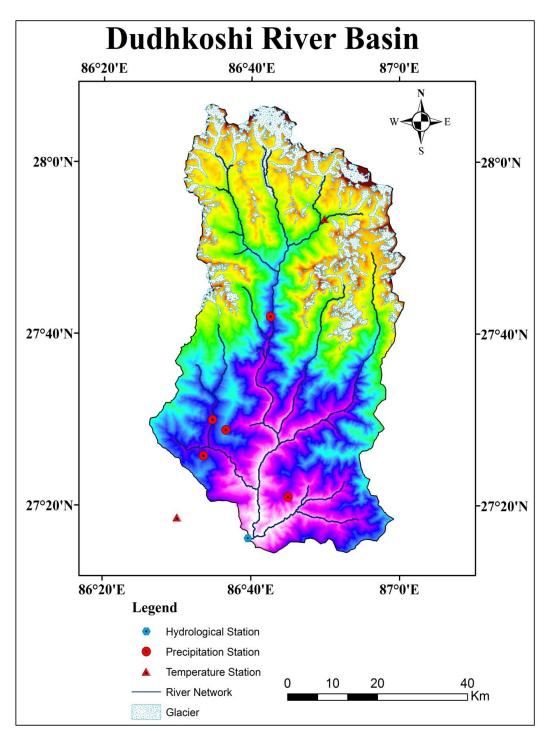


Figure 3 Dudhkoshi river basin (Khumbu region)

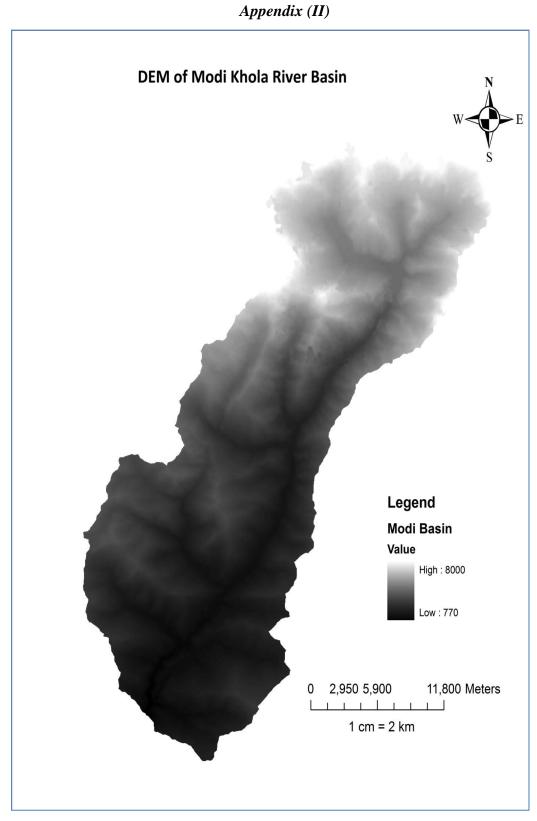


Figure 4 DEM of Modi Khola river basin (Annapurna)

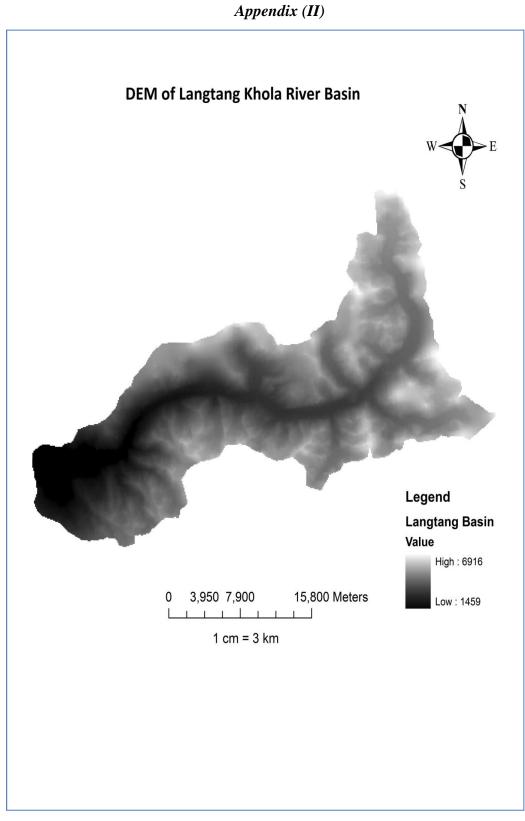


Figure 5 DEM of Langtang Khola river basin (Langtang)

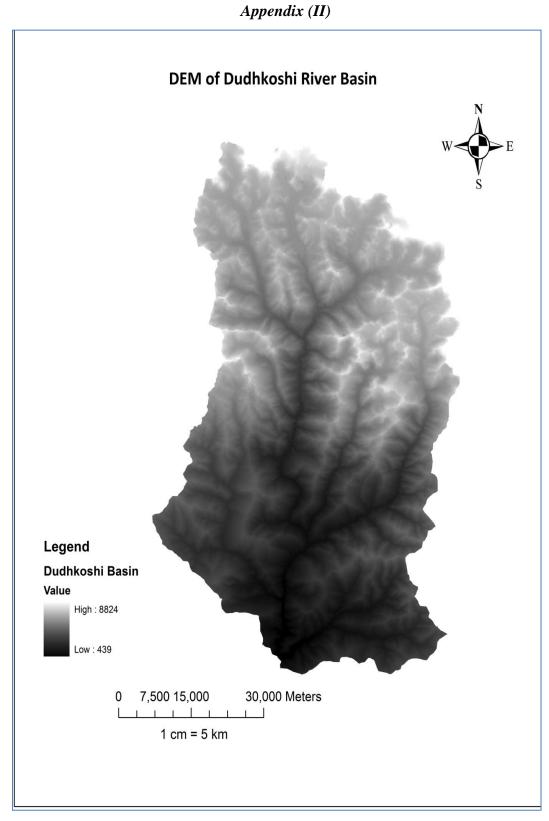
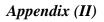


Figure 6 DEM of Dudhkoshi river basin (Khumbu)



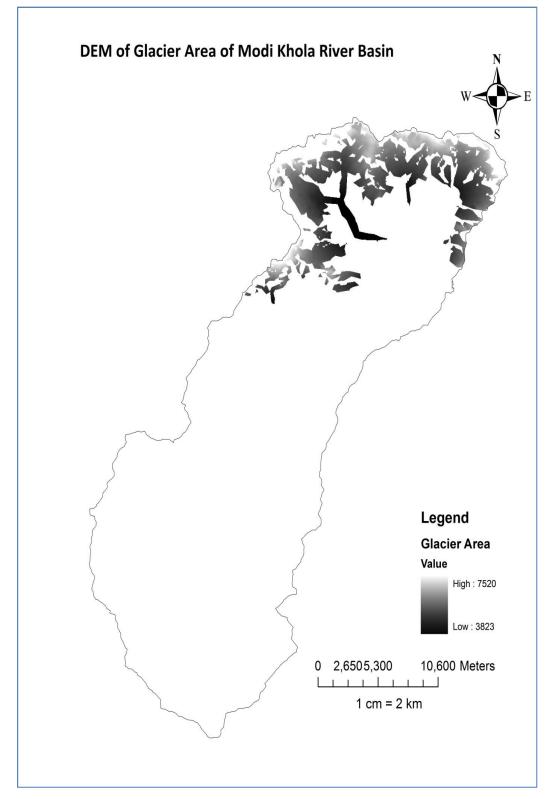
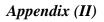


Figure 7 Glacier area of Modi Khola river basin (Annapurna)



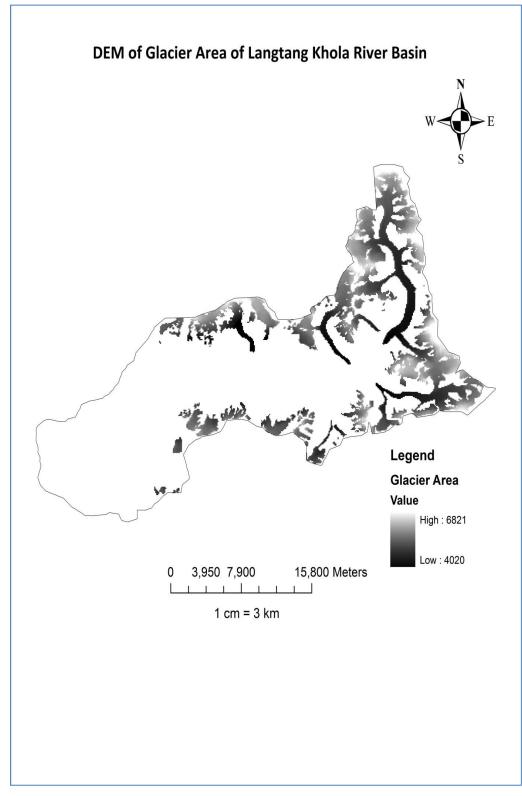
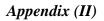


Figure 8 Glacier area of Langtang Khola river basin (Langtang)



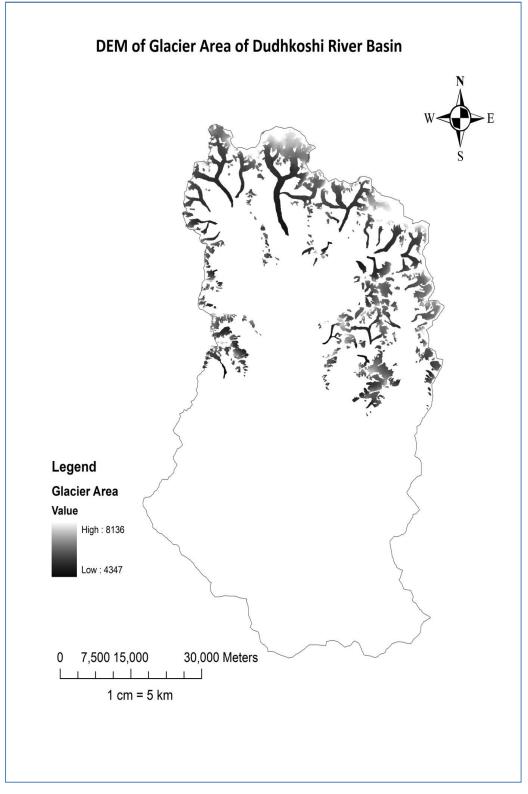
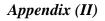


Figure 9 Glacier area of Dudhkoshi river basin (Khumbu)



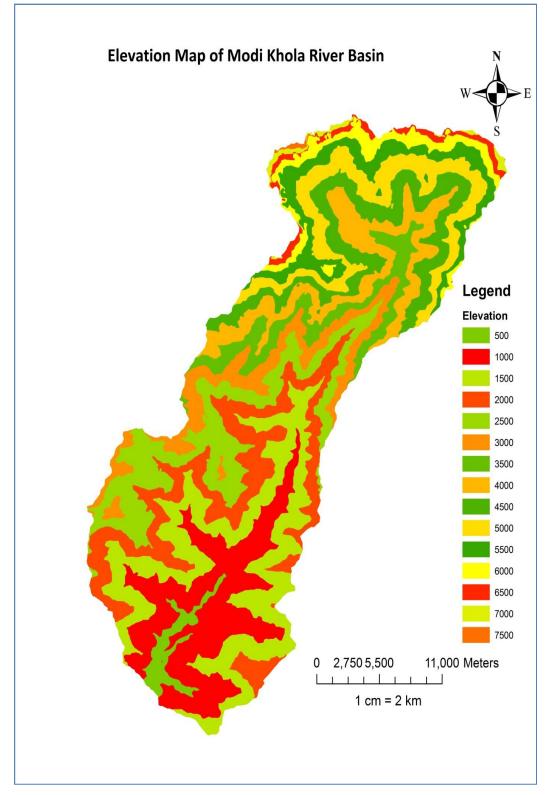
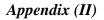


Figure 10 Elevation map of Modi Khola river basin(Annapurna)



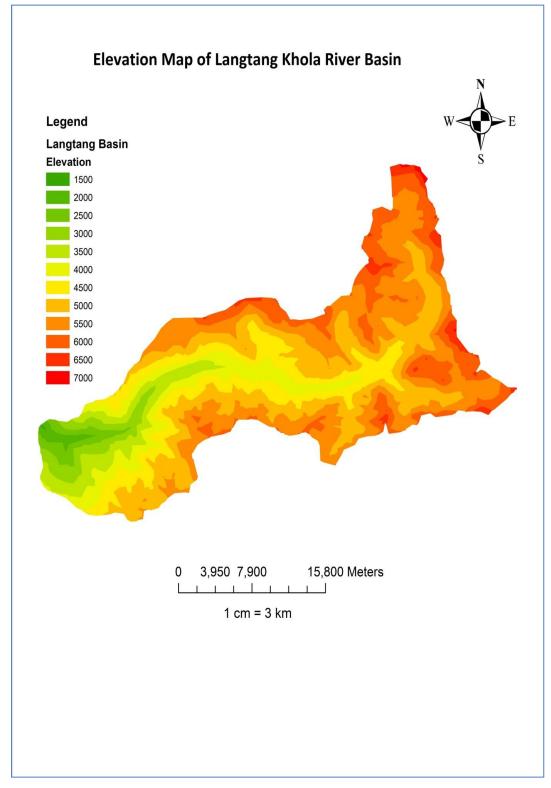
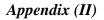


Figure 11 Elevation map of Langtang Khola river basin (Langtang)



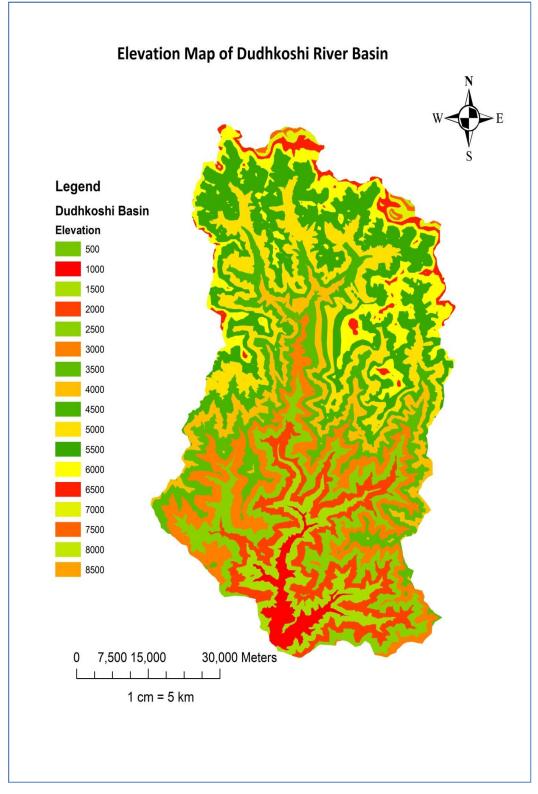
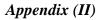


Figure 12 Elevation map of Dudhkoshi river basin (Khumbu)



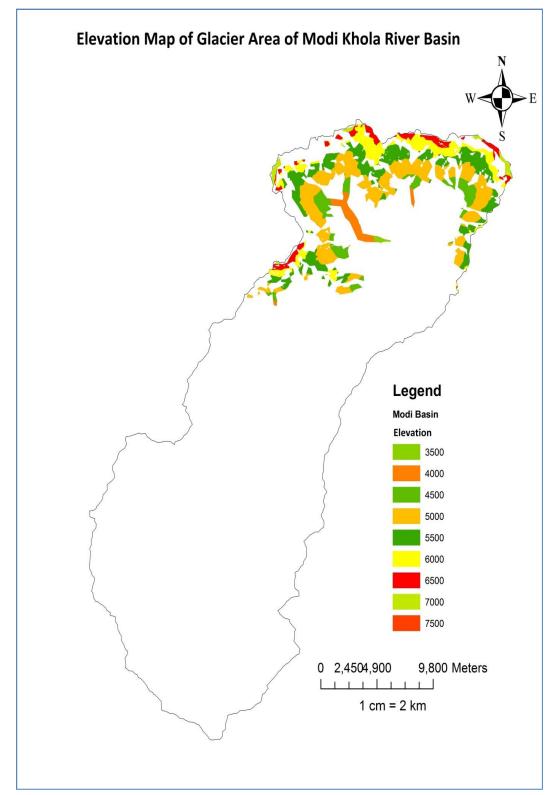
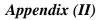
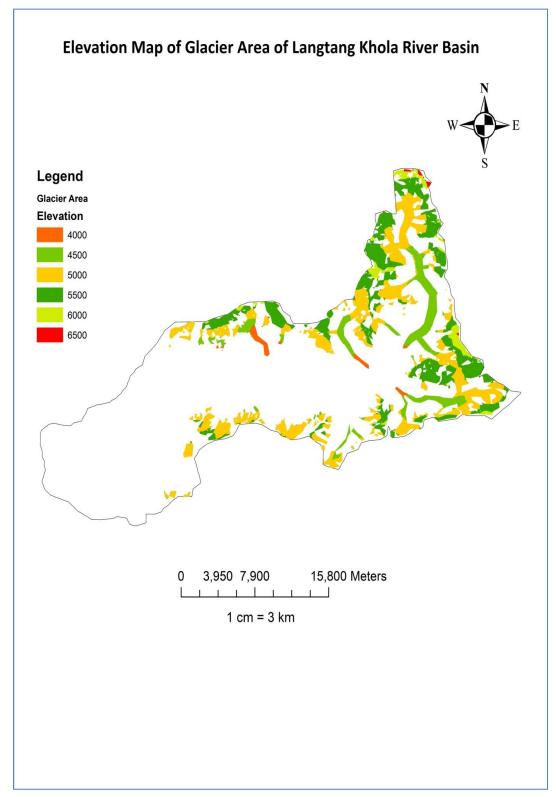
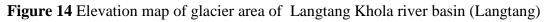
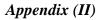


Figure 13 Elevation map of glacier area of Modi Khoal river basin (Annapurna)









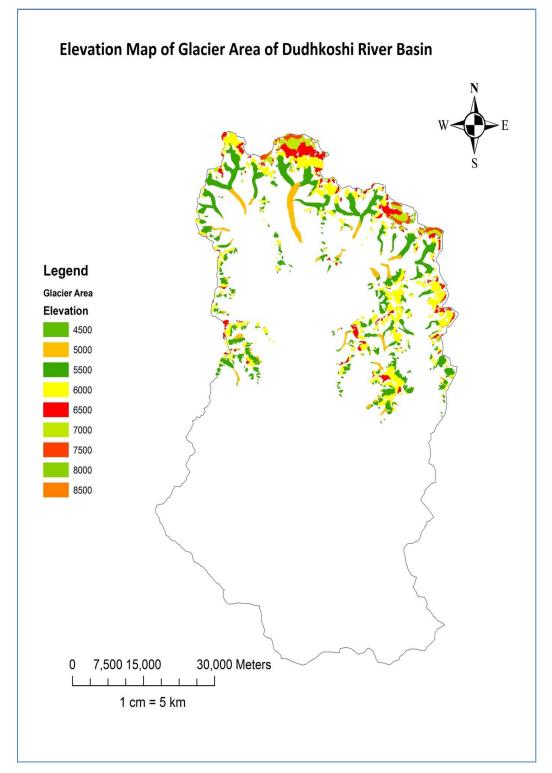
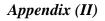


Figure 15 Elevation map of glacier area of Dudhkoshi river basin (Khumbu)



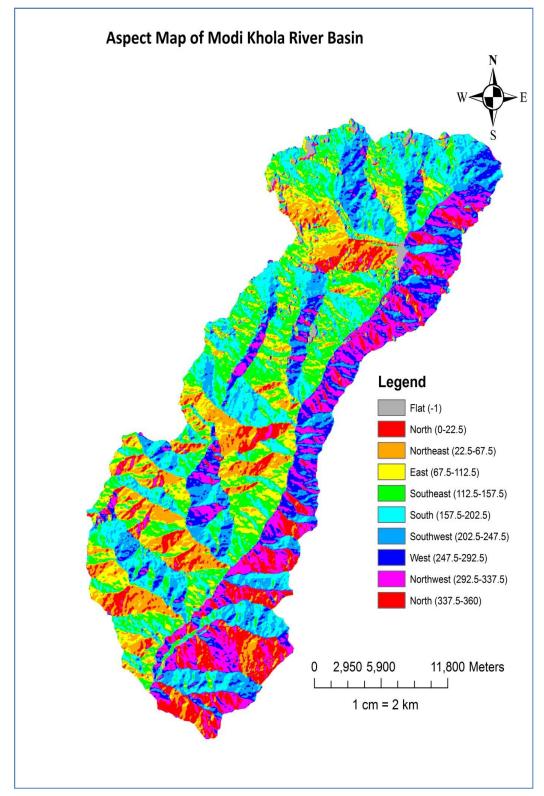
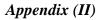


Figure 16 Aspect map area of Modi Khoal river basin (Annapurna)



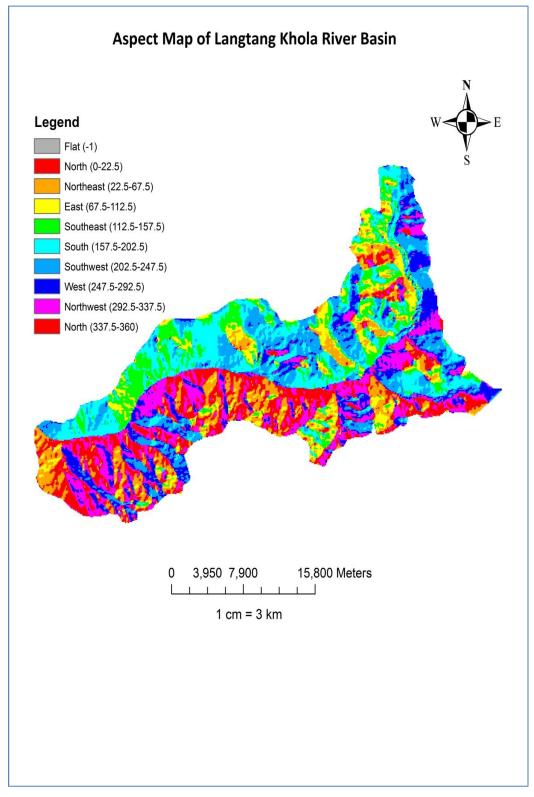
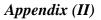


Figure 17 Aspect map of Langtang Khoal river basin (Langtang)



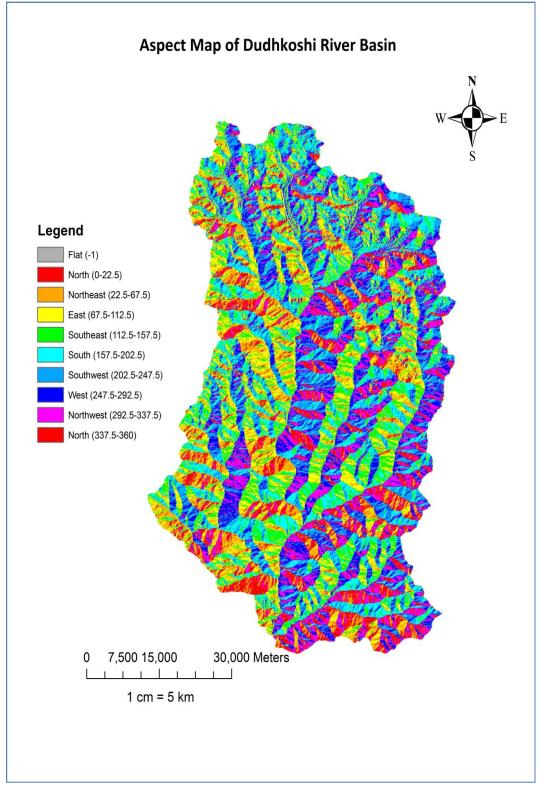
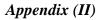


Figure 18 Aspect map of Dudhkoshi river basin (Khumbu)



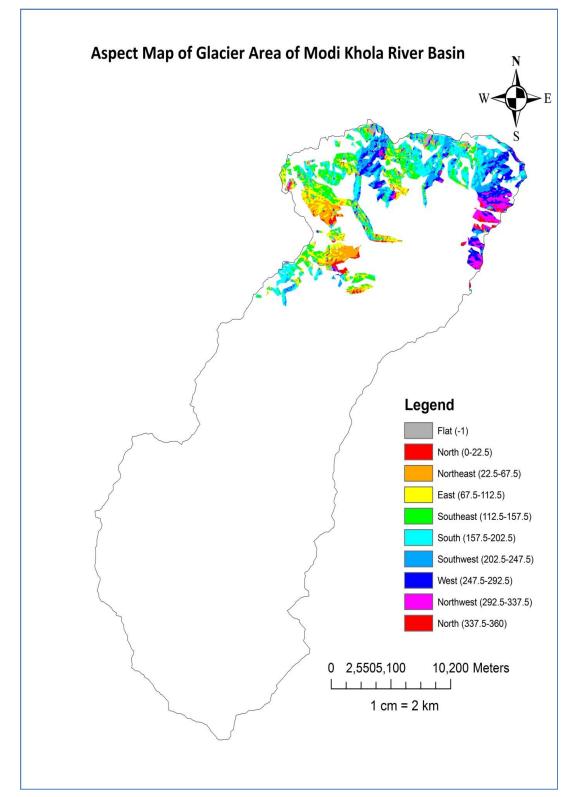
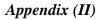


Figure 19 Aspect map of glacier area of Modi Khoal river basin (Annapurna)



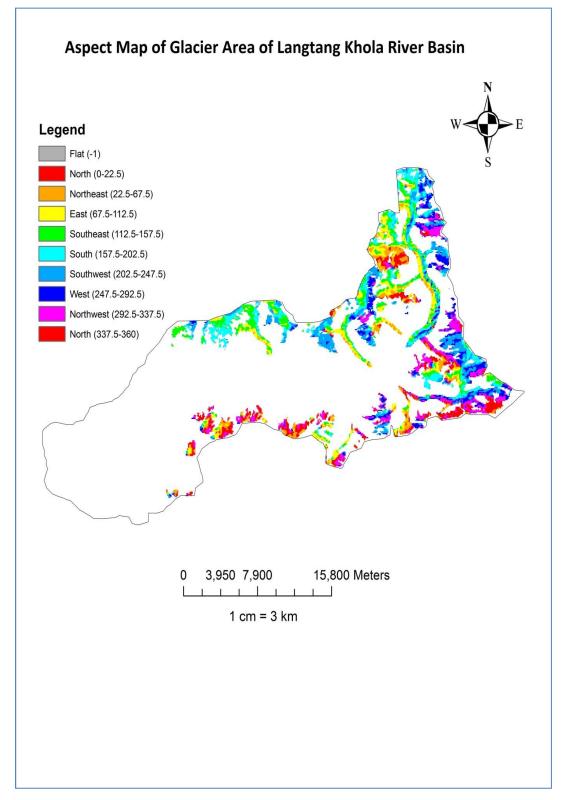
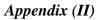


Figure 20 Aspect map of glacier area of Langtang Khoal river basin (Langtang)



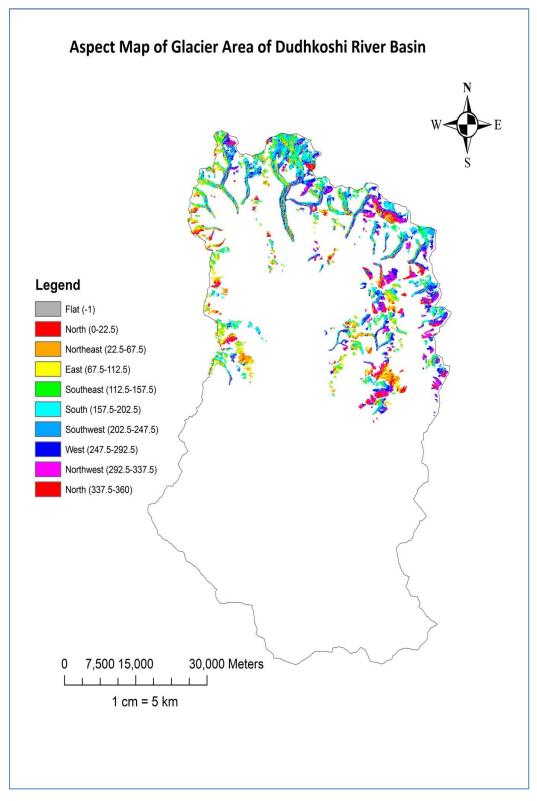
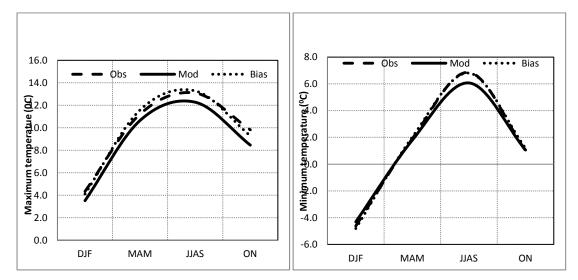


Figure 21 Aspect map of glacier area of Dudhkoshi river basin (Khumbu)



Appendix (III) Figure 1 to Figure 9, calibration, validation and seasonal bias correction of three basins.

Figure 1 Annapurna validated Tmax bias corrected

Figure 2 Annapurna validated Tmin bias corrected

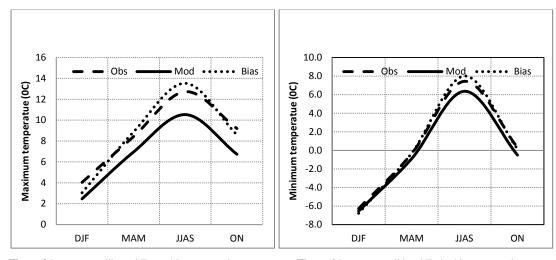


Figure 3 Langtang calibrated Tmax bias corrected

Figure 4 Langtang validated Tmin bias corrected

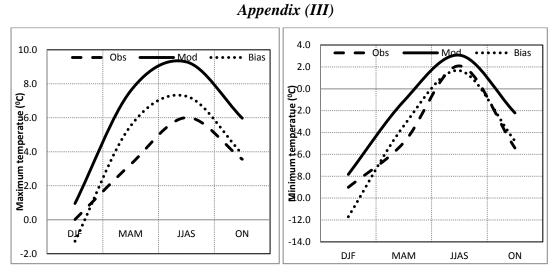


Figure 5 Khumbu Validated Tmax seasonal bias corrected

Figure 6 Khumbu Validated Tmin seasonal bias corrected

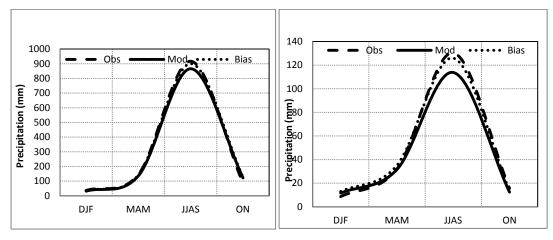


Figure 7 Annapurna PPT validation seasonal bias corrected

Figure 8 Langtang PPT validation seasonal bias corrected

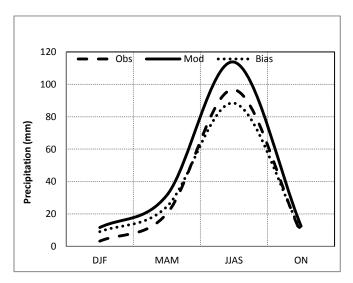
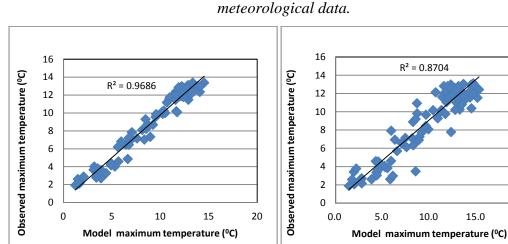


Figure 9 Khumbu PPT validation seasonal bias corrected



Appendix (IV) Figure 3.3.1 to Figure 3.3.18, calibration and validation of



20.0

8 6  $R^2 = 0.9711$ Observed minimum temperature (°C) 4 2 0 -2 -4 -6 -8 10 -10 -5 0 5 10 Model minimum temperature (°C)

Figure 3.3.2 Annapurna Tmax calibration (1988\_1995)

 $R^2 = 0.9882$ 

8

6

4

2

0

-2

-4

-6

-8

-10

Observed minimum tmperature (°C)

Figure 3.3.4 Annapurna Tmin calibration (1988\_1995)

-5

0

Model minimum temperature (°C)

Figure 3.3.5 Annapurna Tmin validation (1996\_2003)

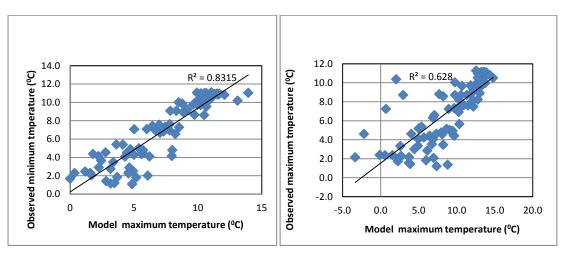


Figure 3.3.6 Langtang Tmax calibration (1988\_1995)

Figure 3.3.7 Langtang Tmax validation (1996\_2003)

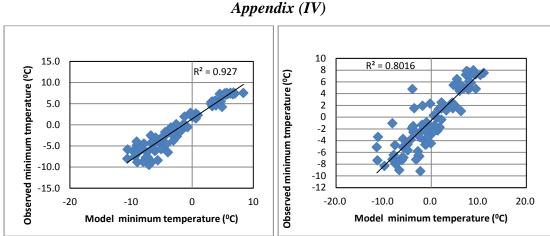


Figure 3.3.8 Langtang Tmin calibration (1988\_1995)



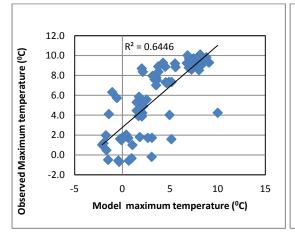


Figure 3.3.10 Khumbu Tmax calibration (1988\_1995)

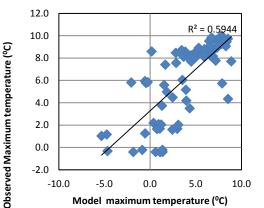


Figure 3.3.11 Khumbu Tmax validation (1996\_2003)

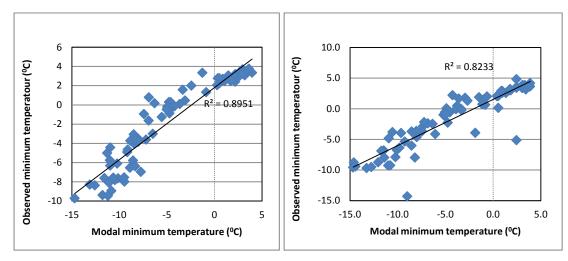


Figure 3.3.12 Khumbu Tmin calibration (1988\_1995)

Figure 3.3.13 Khumbu Tmin validation (1996\_2003)

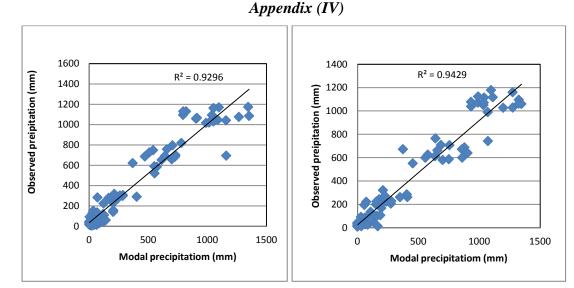
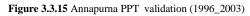
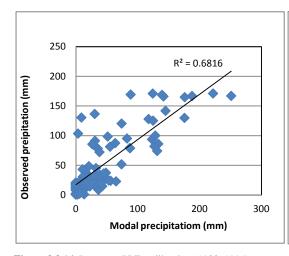


Figure 3.3.14 Annapurna PPT calibration (1988\_1995)





 $R^2 = 0.827$ Oobserved preipitation (mm) Modal precipitatiom (mm)

Figure 3.3.16 Langtang PPT calibration (1988\_1995)

Figure 3.3.17 Langtang PPT validation (1996\_2003)

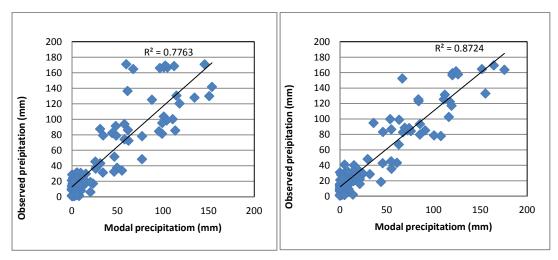


Figure 3.3.18 Khumbu PPT calibration (1988\_1995)

Figure 3.3.19 Khumbu PPT validation (1996\_2003)

Appendix (V) Figure 3.4.8 (a) to Figure 3.4.8, (i) Calibration and validation of Hydrological data

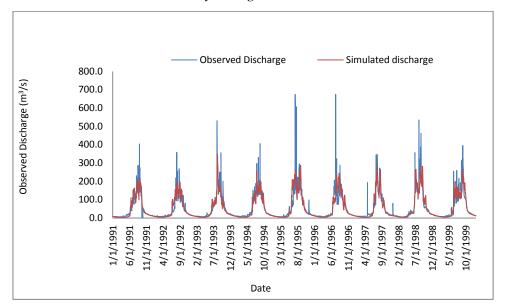


Figure 3.4.8 (a) Modi Khola river basin model calibration (1991-1999)

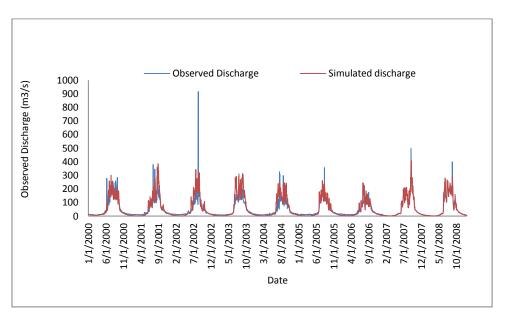


Figure 3.4.8 (b) Modi Khola river basin model validation (2000-2008)

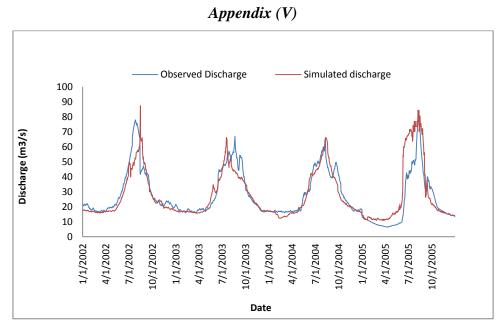


Figure 3.4.8 (c) Langtang Khola river basin model calibration (2002-2004)

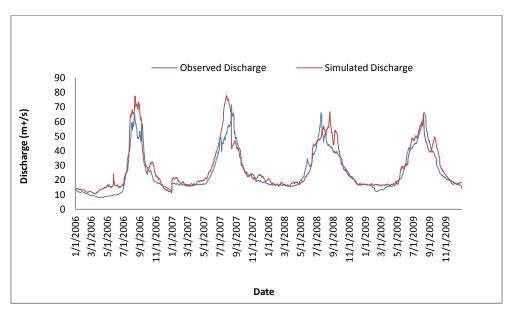


Figure 3.4.8 (d) Langtang Khola river basin model validation (2005-2009).

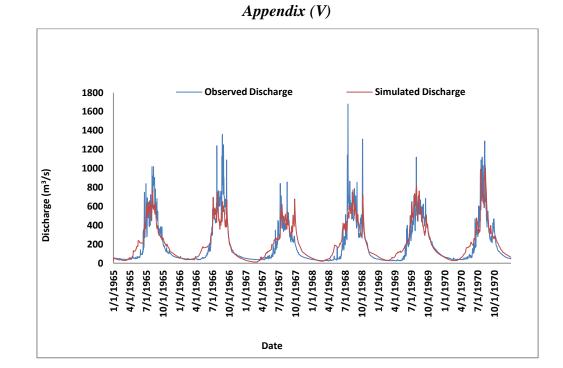


Figure 3.4.8 (e) Dudhkoshi river basin model calibration (1965-1970)

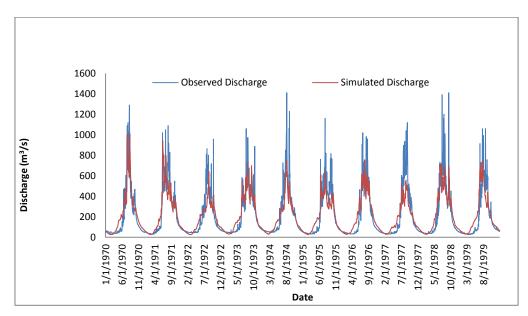


Figure 3.4.8 (f) Dudhkoshi river basin model validation (1970-1979)

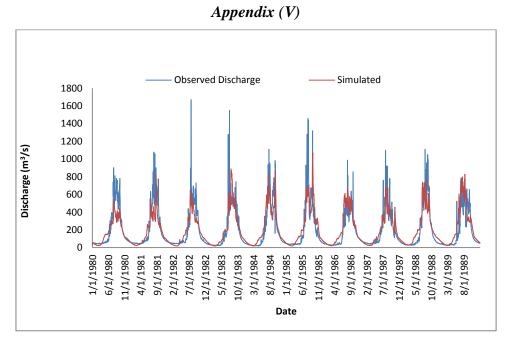


Figure 3.4.8 (h) Dudhkoshi river basin model calibration (1980-1989)

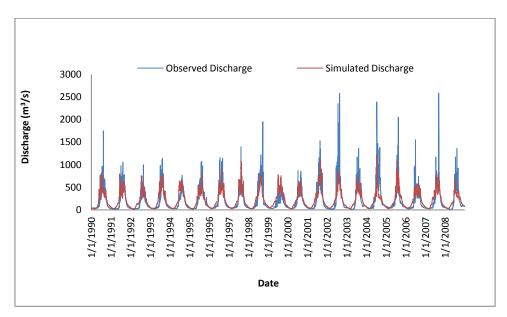
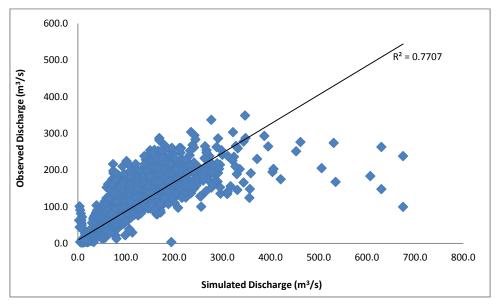


Figure 3.4.8 (i) Dudhkoshi river basin model validation (1991-2008)

Appendix (VI) Figure 3.4.14(a) to Figure 3.4.14 (h), Simulated and observed



discharge of three basins.

Figure 3.4.14 (a) Modi Khola river basin observed and simulated discharge(1991\_1999)

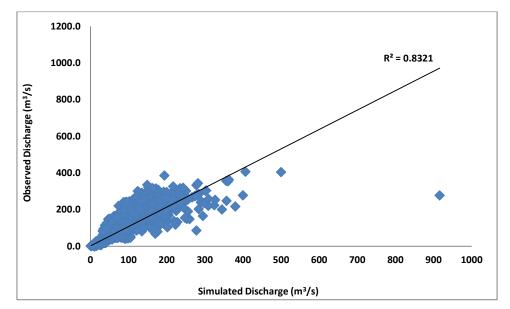


Figure 3.4.14 (b) Modi Khola river basin observed and simulated discharge (2000\_2008)

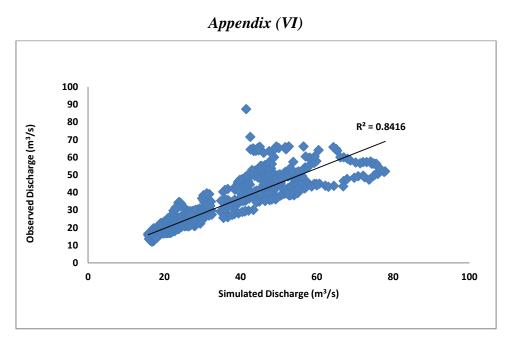


Figure 3.4.14 (c) Langtang Khola river basin observed and simulated discharge(2002\_2005)

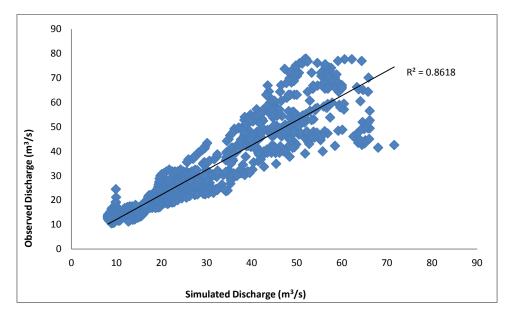


Figure 3.4.14 (d) Langtang Khola river basin observed and simulated discharge (2006-2009).

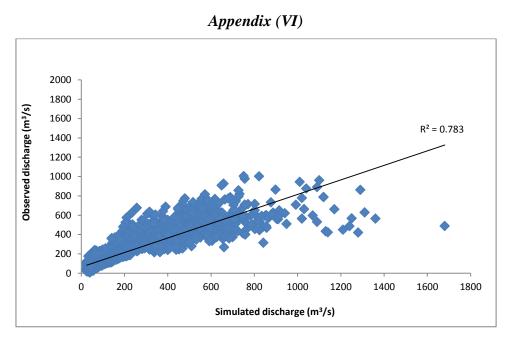


Figure 3.4.14 (e) Dudhkoshi river basin observed and simulated discharge (1965\_1970)

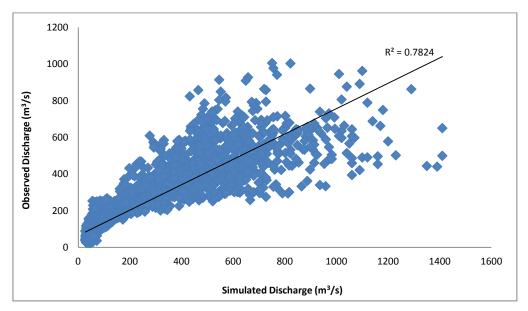


Figure 3.4.14 (f) Dudhkoshi river basin observed and simulated discharge (1970\_1979)

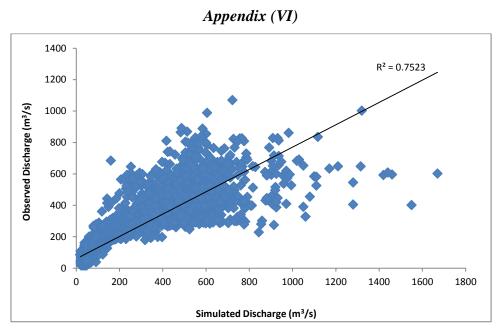


Figure 3.4.14 (g) Dudhkoshi river basin observed and simulated discharge (1980\_1989)

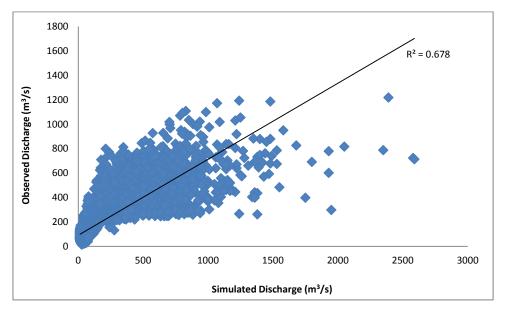


Figure 3.4.14 (h) Dudhkoshi river basin observed and simulated discharge (1990\_2008)

Volume 8, Number 1 August 2012 ISSN 1818-2518

Journal of Hydrology and Meteorology



Society of Hydrologists and Meteorologists - Nepal SOHAM-Nepal

# Climatic Water Balance of Annapurna, Langtang and Khumbu regions of Nepal Himalaya

Tirthe Raj Adhikari and Lochan Prasad Devkota

Central Department of Hydrology and Meteorology, TU, Nepal

#### ABSTRACT

For the protection of the environment, climatic water balance studies play key role. This study attempts to assess the potential water availability at the Annaparna, Langsang and Khumbu regions of Nepai Hidwalaya. Potential evapotramplitation (PET) is calculated by CROPRAT 8 with the help of maximum and minimum temperature, relative humidity, wind speed and sureshine hour. The climatic water balance of water balance is calculated on the basis of Thornthwait procedure. These calculations help to examine annual water surplus (WS) and water deficit (WD) periods. Potential water surplus at three selected station is calculated by above techniques after averaging the data of time period from 1987 to 2008. The mate aim of this study is to compare the obtained result from the climatic water balance for the selected states of the Nepal Himalaya region. This study will provide climatic water balance information of the given area which will be surplif for sustainable management of water resources in local and small area of the Nepal Himalaya

Key words: Potential Evapotranspiration, Annual Bater Surples, Annaptimo, Langtong

### 1. INTRODUCTION

Snow and glacier are natural fresh water reservoir in solid form which is one of the important components of hydrological cycle in Nepalese Himalayas. Glacierized environments are one of the most vulnerable to climate change with regard to future availability of freshwater in the region (Mats et al., 2009). The perennial flow of major rivers in Nepal is maintained by melt water coming from these sources, which are vital for the water resources development of the country. Climatic water balance is one of the important factors while predicting glacier melt runoff (Barnett et al., 2005). Glaciers in Nepal are being hazardous due to the rising temperature trend, deposited carbon particles, decreasing winter precipitations and impact of

Journal of Hydrology and Meteorology, Vol. 8, No. 1

global warming as a whole (Mats et al. ,2009). It may be vanished after few years because the glacier retreating rate was 10 to 60m per year in Dudh Koshi basin (Bajracharya et al., 2008). In other countries as well such cases are being identified. For example, the park's largest glaciers in USA- Montana, is also retreating due to the effect of climate change (Hall and Fagre, 2003). This forecast was predicted by a computer-based climatological model as only computer based models are suitable for such scenario. The park's glaciers could disappear in the next several decades if the forecast appears to be true. The summer mean temperature in 2100 is predicted to reach 19.76°C; however, glacier disappearance may occur even earlier, as many of the glaciers are retreating faster than their predicted rates (Half and Fagre, 2003).

#### SOHAM-Nepal

47

This study attempts to calculate water deficit (WD) and water surplus (WS) by using Thornthwaite procedures and tries to identify the climatic water balance (CWB) in the study area. The result of CWB can be beneficial to understand the glaciers accumulation and ablation and its response with temperature, humidity, sunshine, wind speed and precipitation analysis. Seasonal cycle of precipitation, maximum, minimum and mean temperature analysis are also carried out as a part of analysis.

### 2. STUDY AREA

48.

Department of Hydrology and Meteorology (DHM), Snow and Glacier Hydrological section was established in 1987 with an aim to monitor hydro-meteorological stations in the higher region (Northern belt) of Nepal. Now, DHM is operating eleven hydro-meteorological stations in different location of higher region of Nepal. But in this research three stations are selected as Annapuma (Latitude 28:53', Longitude 83:95') in western part whose elevation is 3470 m a.m.s. I, Langtang (Latitude 28'22', Longitude 85%2') the elevation 3920m a.m.s.l. in Middle part and Khumbu (Latitude 27°89', Longitude 85'83') the elevation 4355m a.m.s.l. in eastern part of the country in Himalaya Region Nepal. The research stations are depicted in Figure 1.

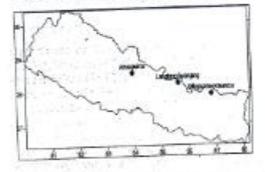


Figure 1: Study Area of Snow and Glacker Hydro-Meteorological Stations

Journal of Hydrology and Meteorology, Vol. 8, No. 1

## 3. METHODOLOGY

Climatic Water Balance is actual Precipitation (P) minus potential Evapotranspiration. Where, P is the hill shaded terrain based precipitation (Rainfall + Snew melting) data.

CWB = P - PET

(1)

proposed been Several methods have in the literature for colculating actual Water evapotranspiration Climatic and Balance. Monteith (1963, 1965) introduced resistance terms into the well-known method of Penman (1948) and derived an equation for evapotranspiration from surfaces with either optimal or limited water supply. This method, often referred to as Penman-Monteith method, has been successfully used to estimate evapotranspiration from different land covers. The method requires data on aerodynamic resistance and surface resistance which are not readily available, so that the standard Peaman-Monteith method for estimating actual evapotranspiration (AE) has been limited in practical used. For this practice CROPWAT 8.0 models is used for calculating the PET using different steps of the model. Several methods exist to determine AE. The FAO Pennan? Monteith method has been recommended as the appropriate combination method to calculate PET and determine AE using the following:

- Maximum temperature
- Minimum temperature
- Humidity
- Sunshine duration
- · Wind speed.

Daily maximum and minimum temperature, humidity, wind speed and precipitation (1987-2008) are collected from DHM, these data were averaged for three stations. The surabine hour (1947 - 1990) was taken from the climate and hydrological Atlas of Nepal (ICIMOD, 1996).

The sunshine hour and other climatological parameters are of not similar period but day length is similar in each and every year, therefore day length is considered in analysis. These data were used feed into the CROPWAT 8 model for calculating the potential evapotranspiration (PET), which uses Penman-Monteith method to estimate PET (ALLEN et.al, 1998). This method has also been applied in Xizhuang watershed (XZW) which lies in the middle mountains Baoshan region of southwest China with elevations ranging from 1695 to 3060 m by Ma Xing et al. (2008).

 $\frac{PET := \frac{4.4035(8v-5) + y \frac{960}{p+200} u_1(w-m)}{4 + p(s+0.31vT)}$ (2) Where

PT DET E

PET = Potential evapotranspiration [mm day<sup>4</sup>].

Rn = Net radiation at the crop surface [MI m<sup>4</sup> day<sup>4</sup>].

G = Soil heat flux density [MJ m3 day-]].

T - Mean daily air temperature at 2 m bright [°C],

u, - Wind speed at 2 m height [m s<sup>-1</sup>],

en - Saturation vapour pressure [kPn],

ca ~ Actual vapour pressure [kPa],

(cs-ca) = Saturation vapour pressure deficit [ kPa],

γ = Psychometric constant [kPa °C<sup>4]</sup>,

A = Slope vapour pressure curve [kPa "C"],

The equation uses standard climatological records of solar radiation (sunshine), air temperature, humidity and wind speed. Apart from the site location, the FAO Penman-Monteith equation requires air temperature, humidity, radiation and wind speed data for daily, weekly, ten-day or monthly calculations. Thronthwaite, and Mather (1955) method has been used to calculate the climitic water balance. This method shows the relationship between rainfall, PET and actual evapotranspiration from which water surplus (WS) and water deficiency (WD) can be calculated at any place or region

Journal of Hydrology and Meteorology, Vol. 8, No. 1

over a given period of time. The water balance accounting procedure with the subtraction of potential evapotranspiration (PET) forms the incoming precipitation (p) in each month. The negative value of (P-PET) indicates the amount by which (P) failed to meet the water need. On the other hand Positive values of (P-PET) refers to amount that 'is in excess of the water need. Accumulated potential water loss (acc) is obtained by a progressively adding all the negative value of (P-PET). But if the soil has never reached the field capacity the first value of ace is obtained by a successive approximation method using the field capacity. The soil moisture decreases when P is lower than PET and increases when P is higher than PET. Change in soil storage (Cst) is obtained by subtracting the soil moisture in any month from that value in the previous month. When Precipitation is equal to or greater than PET, the actual evapotranspiration (AE) will be equal to PET. If P less than PET, AE is obtained by adding P to the magnitude of Cst. The difference of PET and AE gives the values of water deficiency (WD) as: WD = PET-AE (3)

Water surplus occurs only if the soil has been recharged to its field capacity and whenever precipitation is higher than PET and soil is not at the field capacity. The excess first goes to recharge the soil moisture. The water surplus (WS) can be written as

$$WS = (P - PET) - Cst$$

The accuracy of the computation may be tested with the yearly of PET, P, AE, WD and WS in the following manner

P = AE + WS (5)

The connection with elimatic water balance, the term water deficiency (WD) and water surplus (WS) are used. WD represents the amount of water loss through AE, which cannot be met

SOHAM-Nepal

(45)

by precipitation. In this article the seasons are classified as winter - December of the previous year to February (DJF), Pre-monsoon (spring) – March to May (MAM), Monsoon (summer) -June to September (JJAS), Post-monsoon (fall) – October and November (ON). The seasonal effect of precipitation is strongly pronounced with high precipitation input during the monsoon (JJAS) and very little precipitation during (ON) the winter period.

### 4. MODEL AND DATA USED

Monthly average data (1987 - 2008) of minimum temperature, maximum temperature, homidity; precipitation, wind speed and susshine duration is used for calculating the PET. Similarly the CROPWAT 8.0 model is used for calculating the PET. Output from CROPWAT 8.0 PET, precipitation data is used for calculating AE, WS, WD. Water Surplus (WS) is the excess of water from precipitation fall after the soil water is replenished and the domand of PET is met, WD is a general term used to describe a situation where the available water within a region is less than the region's demand. It is the water that is available from precipitation (snow and rain) glacier melt for rivers and recharge of groundwater. The season wise (DJF, MAM, IJAS and ON) water balance is calculated from the equation of temperature and precipitation at Annapuma, Langtang, and Khumbu, Moreover, the season wise climatic water balance is obtained from the Thronthwait climatic balance shown in Figure 5. For the field capacity 50 mm. assumed, due to soil and evaporation routine parameters ranges (50mm - 500mm) are used for the estimation of parameter uncertainty by Monte Carlo simulations (Seibert 1996). In the selected three stations there are not so much of missing data except in few cases. For the missing data in small (one day) gaps linear interpolation is adopted for temperature data and for the long gaps, monthly series are simply

Journal of Hydrology and Meteorology, Vol. 8, No. 1

replaced by the mean values of the respective months. The data are then computed for annual as well as seasonal mean.

# 5. RESULTS AND DISCUSSION Precipitation

Precipitation during the summer multiperiod which is a major component from accumulation of glacier in the Nepul Himaloyas was strongly influenced by mesoscale mountain valley circulation. Remarkable diurnal variation was found in precipitation and had crucial effect on the distribution of precipitation. Especially, from October 1985 to March 1986, the amount of precipitation was large and it was controlled by behaviour of westerly trough (Western disturbances) Precipitation in the cold season is also associated with large scale snow cover. Due to the accumulation of glaciers in Nepal, a is important to determine the behaviour the thermal circulation in mountainscale in the summer monsoon season the behaviour of westerly trough in the remaining seasons. Especially, inter-annual variability of the latter is more important for the accumulation of glacier than was expected (Seko, 1987). The snow line does not always coincide with the temperature 0°C isotherm throughout the year. The relation between snow line and air temperature are greatly changed from season to season (Morinage et.al., 1987). The fluctuation in snow line in Langtang valley was reported by Yamada et al. (1992) and Kappenberger et al (1993). Some studies related to mass balance of glaciers in the valley were evaluated by Ageta et al. [] and Steinegger et al (1993). Seko (1987). and Takahshi (1991), Shiraiwa et al. ( and Ueno et al (1993) evaluate the distribution of precipitation in the valley. Although the altitudinal dependence of precipitation in the

valley was evaluated largely by their analysis, it is still not enough to clarify how the local climate would change glucier area when the global climate inspact. The precipitation up to 64%, 77% and 82% of long term annual total was observed at Annapurna, Langtang and Khumbu respectively during monsoon season (JJAS) in the Nepal Himalayan region which is depicted in Table 1.

From the three reference stations (Annapurna, Langtang and Khumbu) it can be started the total monthly average precipitation (1987 – 2008) varies over space. The average annual total precipitation at Annapurna, Langtang and Khumbu is 2304mm, 653mm and 405mm respectively (Table 1).

Mouth	Ausapurna	STRUCTURE OF STR	Real manage
Jan	47	11	- 0
Fub	83	18.	2
Mar	144	27	17
Apr	197 -	31	8
May	216	31	23
	313		43
Jus Jul	442	158	92.
Aug	463	169	133
Sep	255	91	.64
Aug Sep Oct	99	23	7
Nov	23	5	4

90

504

653

406

Table 1: Comparison, of seasonal cycle of Total Average precipitation (mm) (1987 - 2008)

Temperature

The mean monthly temperatures were calculated at Annapurna, Langtang and Khumbu which is presented at Table 2. The mean monthly maximum was observed to be 10.4°C at Annapurna, 9.9°C Langtang and 5.9°C in July. The average monthly minimum was observed to be -1.3°C in Annapurna area in January, -2.4°C in Langtang and -6.0°C in Khumbu in February. This can be justified by the fact that the temperature decreases with altitude. The similar trends of air temperature

153

147

2.304

Table 2: Maximum, minimum and mean temperature data which was used to derive PET using CROPWAT 8 model.

Der

MAM

JIAS ON

Tetal

2000	-	Annapure	a standing	South State	Langtan	e side di	Contraction of the	Khumite	Addama and	
Nicoth	Min 1	Max T	Mean T	Min T	Max T	Mean T	Min T	Max T	Mean 1	
Jan	-6.0	3.3	+1.3	-7.0	3.1	-1.9	-11.3	0.0	-5.7	
Feb	-5.9	3.7	-1.1	-7.2	2.4	-2.4	-11.4	-0.6	-6.0	
Mar	-3.1	7.1	2.0	-4.2	5.2	0.5	-8.7	1.1	-3.8	
Apr	-0.5	10.5	5.0	-1.3	8,0	3,4	-5.7	, 3.5	-1,1	
May	2.7	13.2	8.0	1.9	10.0	6.0	-2.2	5.6	1.7	
Jun	5.6	14.0	9.8	5.2	11.4	8.3	1.7	7.7	4.7	
Jul	2.3	13.7	10.4	7.5	12.3	9.9	3,6	8.3	5.9	
Aut	6.9	13.5	10.2	6.9	11.9	9.4	3.1	7.9	5.5	
Sep	5.1	13.1	9.1	5.0	10.7	7.9	- 1.1	7.1	4.1	
Oct	0.9	11.8	6.4	0.5	8.5	4.5	-4.2	4.9	0.4	
Non	-2.3	8.8	3.3	-2.8	6.4	1.8	-7.3	3.3	-2.0	
Dec	-3.6	6.4	1.4	-4.8	5.Z	0.Z	-8.7	2.6	-3.0	
Average	0.6	9.9	5.3	0.0	7.9	3.9	-4.2	4.3	0.1	

Journal of Hydrology and Meteorology, Vol. 8, No. 1

cariation are also foted at all three stations. Freezing rain occurs when air temperature is above and ground surface is below 32°F. (0°C). If threshold temperature found to be up to the -2°C temperature the precipitation will fromza (Seibert, 1996). From the temperature precipitation relationship of three Himalaya region stations, the percentage of freezing precipitation in Annapurna is 2%, in Langtang is 4% and in Khumbu is 9%. Above result shows that the freezing precipitation is lower than the melting rate, therefore glaciers are rapidly retreating in these regions. The glacier area loss is about 20% in last 40 years. The subsidence of glacier surface by 0.40m per year in Dudh Koshi basin is also reported since late 1960's due to the melting of the glaciers. Bolch et al. (2008) and Bajracharya et al. (2008) have also reported the glacier retreat rate of 10 to 60m per year in Dudh Koshi basin.

The mass balance of glacier can be divided into a winter and summer season, mainly influenced by freezing precipitation and mean threshold air temperature (Paterson, 1994). At the end of the summer, mow may be accumulating on the higher part of the glacier while ablation continues near the terminus. Thus the accumulation varies from place to place on the glacier (Paterson, 1994). The freezing precipitation is less where accumulation is also less. As Khumbu is in higher elevation as compared to two other stations, the average air temperature is found to be 4.9°C, which is lower than the threshold value, so there is more accumulation of snow in winter season shown in Table 3.

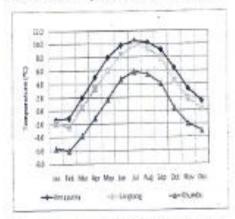
Table 3: Comparison of seasonal average temperature (1987-2008)

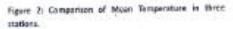
Seuson	Annaparna	Langtang	Khambu
DJF	-0.4	-1.4	-4.9
MAM	5	3.3	-1
JJAS.	0.0	8.8	5
ON	4.8	3.1	-0.8

Journal of Hydrology and Meteorology, Vol. 8, No. 1

# Potential Evapo-transpiration (PET)

The PET is the amount of water that would be evaporated under an optimal set of conditions, among which is an ultimate supply of water. The highest value of PET was found in the month of May in all three stations as shown in Table 4. In Annapurna area, the PET shows quite variable trend in the modelled result (highest values of 96 mm and the lowest value of 49 mm). PET (Figure 3) was also decreased with elevation similar to the temperature shown in Figure 2.





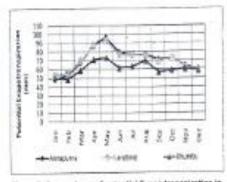


Figure 3: Comparisons of patential Event transpiration in three stations

Table 4: Potential evapotranspiration in three stations (mm)

Month	Amapurpa	Langtang	Khumbu
Jan	49	53	50
Feb	53	55	49
Mar	68	70	59
Арг	88	87	71
May	96	92	73
him	79	76	62
Jul	76	76	63
Aug	76.	75	70
Sep	71	68	57
Oct	72	72	59
Nov	63	62	60
Dec	59	58	59
Total	852	844	732

and transpiring. When the temperature increases, AE also increases as shown in Table 3 and Table 5. In this study AE is compared with temperature only. In Annaporta and Khumba area PET >AE in all season, but in Langtang area PET equals to AE in summer and in other season PET >AE as shown in Table 5. This indicates that the deficit occurs when the soil is completely dried out. Actual evapotranspiration AE in a soil water budget is the actual amount of water delivered to the atmosphere by evaporation and transpiration. In wet months, when precipitation exceeds potential evapotranspiration, setual evapotranspiration is equal to PET. In dry months, when potential evapotranspiration exceeds precipitation, actual evapotranspiration is equal to precipitation plus the absolute value of the change in soil moisture storage.

# Actual evapotranspiration (AE)

The AE is an output of water that is dependent on moisture availability, procipitation, sunshine hour, wind, temperature, and humidity. Think of AE as "water use" that is actually evaporating

# Climatic Water Balance

there is three stations of Nepal Himalaya.

There is less water deficit 40 mm at Annapurna than at other two stations (Langtang and Khumbu). The highest water deficit is 382mm

Table 5: Comparison PET, AL	MD and Ma in cines searching	Ci iniparte i
	CONTRACTOR AND A CONTRACT	

Station Name	Perameter	Dec-Feb (DJP)	Mar-May (MAM)	Jun-Sep (JJAS)	(Oci-Nov (ON)	Total (mm)
Y. Lines	PET	161.0	252.0	303.0	136.0	852.0
Annapurno	AE	135.0	252.0	303.0	123.0	813.0
	WD	27.0	0.0	0.0	* 13.0	40.0
	WS	6,0	294.0	1170.0	27.0	1491.0
	PET	166.0	249.0	295.0	134.0	.844.0
Langtong	AE	38.0	90.0	296.0	71.0	495.0
	WD	129.0	159.0	0.0	63.0	351.0
	WS	0.0	0.0	177.0	0.0	177.0
	PET	158.0	203.0	252.0	119.0	732.6
Khumbu -	AB	20.0	49.0	232.0	55.0	356.4
	WD	144.0	155.0	19.0	64.0	382.0
	WS	0.0	0.0	49.0	0.0	49.0

Journal of Hydrology and Meteorology, Vol. 8, No. 1

at Khumbu and the lowest at Annapuma. Water deficit of 351 mm is found at Langtang as shown in Table 6. Table 6 shows that the water deficit is increased from west to eastern Nepol Himalava.

The highest water surplus of 1491 mm was at Annapurna, 177 mm at Langtang and the lowest 49 mm at Khumbu which is similar to the precipitation distribution, continuously, increased from eastern to western Himalaya due to the altitudinal and monsoonal effect shown in Table 6.

Table 6: Comparisons of climatic water balance in three stations.

Climatology of water Balance	Автерите	Longtong	Khambu
Water Deficiency (mm)	40,0	351.0	382.0
Water Surpla's (mm)	1451.0	170.0	49.0

Devkota (2003) found the highest rainfall pocket of more than 320 cm annually over central mountainous region, particularly along the southern flanks of Anapuma range, whereas the driest part is found over the north of the same range with less than 40 cm annually. The strong rainfall gradient across this range shows the importance of topography on spatial variation of appeal rainfall distribution in Nepal. The second highest rainfall zone of more than 240 cm per year is located over the northeast mountainous region. Tarai belt has rainfall distribution ranging from 160 to 200 cm annually, whereas the western Tarai shows less rainfall in comparison to the rest of the Tarai. While Devkota (2003) noted that highest rainfall zone is located at the middle mountainous region. The precipitation decreases with increase in altitude. The water surplus also shows similar trends as that of precipitation.

Journal of Hydrology and Meteorology, Vol. 8, No. 1

### 6. CONCLUSION

This study shows that the precipitation , increases from eastern to western regions. It may be due to the orographic effect in the precipitation as three stations are located in the different elevations. PET is decreased with elevation similar to the temperature variation. The highest water surplus is found in the Annapurna areas, but less significant amount of water surplus is obtained in Langtang. and Khumbu area Table 6. In Annapurna temperature and precipitation is higher than in comparison to the other two stations (Langtang and Khumbu). Therefore snow accumulation is higher and melting rate is also higher in Annapurna. Water surplus occurs in three seasons of the year (spring, summer and fall) at Annapuma station, but very small quantity of water surplus is found in Langtang and Khumbu in summer (Table 5). Water deficiency is increased from western to eastern regions whereas water surplus is increased from eastern to western regions. Freezing precipitation and elimatic water balance shows that Annapuma area has the highest water surplus. This may be due to the fact that this area is located at the highest rainfall pocket of Nepal. The retreating rate is not similar in three catchments due to the difference in the temperature profile (Table 2) and the freezing precipitation. Snow melting rate is higher in the Annapurna area as the freezing precipitation is only 2%. The melting rate of glaciers is higher in western region as compared to the middle and eastern regions of Nepal Himalaya.

### ACKNOWLEDGEMENTS

The author would like to thank Department of Hydrology and Meteorology (DHM) for , providing the necessary data for this research. Also, the author would like to acknowledge Dr. Sunil Kansakar for reviewing this paper

SOHAM-Nepal

55

and for his valuable feedbacks. Likewise, useful suggestions from Dr. Sunil Adhikary are highly acknowledged.

### REFERENCES

- Ageta, Y.,Iida, H and Watanabe, O. (1984): Glaciological studies on Yada Glacier in Langtang Himal. Glucial Studies in Langtang Valley, report of the Glacier Boring Project 1981-82 in the Nepal Himalaya, 41-47.
- ALLEN, R.G., PEREIRA, L.S., RAES, D., SMITH. M., (1998), Crop evapotranspiration, guidelines for computing crop water requirements, FAO Irrigation and Drainage paper, no. 56, Rome, pp. 17.
- Bajracharyu, SR.; Mool, PK & Shrestha BR. (2008). 'Global climate change and melting of Himolayan glaciers." In Ranade, PS; ed. Melting glaciers and rising sea levels: impacts and implications, Hyderabad, India, Icfai University Press, 28-46
- Barnett, T. P., Adam, J. C & Lettermaier, D. F. (2005) "Potential impacts of a warming climate on water availability an snowdominated regions" Vol 438/17 November 2005/doi:10.1038/pature04141.
- Bolch, T.; Buchroithner, MF.; Peters, J.; Baessler, M. & Bajracharya, S. (2008).Identification of glacier motion and potentially dangerous glacial lakes in the Mt. Everest region/Nepol using spaceborne imagery.' Nat. Hazardy Earth Syst. Sci; 8, 1329-1340.
- Devkota (2003), Climate variability over Neptil observations, forecasting, model evaluation and impact on ogriculture and water resources un published PhD thesis.
- Hall, M. P. and D. B. Fagre. 2003. Modeled climateinduced glucier change in Glacier National Park, 1850-2100. Bioscience 53(2):131-140
- ICIMOD (1996) climatic and hydrological atlan of Nepal, Kathmandu ICIMOD.

Journal of Hydrology and Meteorology, Vol. 8, No. 1

- Journal ogricultural water management 96(2009) 167 - 178, Elsevier science direct (homopoge: www.elsevier.com/locato/ugwat).
- Kappenberger, G., Steinoggar, U., Brown, L.N. and Kostka, R (1993): Rocent changes in glacier tongues in the Longtang Khola basin, Nepul. determine by terrestrial photogrammetry. Snow and glacier hydrology, International Association of Hydrological aciences Publication, 218, 95-101.
- Ma Xing, Xu Jianche, and Qian Jie (2008), Waser Resource Management in a Middle Mountain Watershed. A Case Study in Xialmang. Yunnan, China.
- Mats Eriksson, Xu Jianchu, Arun Bhakta Sheestha, Ramesh Anarda Veidya, Santosh Nepal and Klas Sandstrom (2009), The changing Himalays "Impact of climate change or water resource and livelihoods in the grater Himalayas" Published by ICIMOD.
- Montrith, J.L., 1963. Gas exchange in plant communities. In: Environmental Control of Plant Growth.
- Monteith, J.L., 1965. Evaporation and environment-Symp. Soc. Exp. Biol. 19, 205-234 Penman. H.L., 1948. Natural evaporation from open water, bare and grass. Proc. R. Soc. Lond., Ser. A 193, 120-145.Exp. Biol. 19, 205-234.
- Seko, Katsumoto, and Morinage Yuki, Takahashi,Shahei (1987), Seasonal variation of snow lise in Langtang valley, Nepal Himnioyas, 1985-1986, Balletin of glucier rescarch, 5 (1987) 49-53.
- Paterson W.S.B. (1994), The Physics of glaciers 34 Edition; Elsevier Science Ltd
- Seibert Jan (1996) Estimation of Parameter Uncertainty in the HBV Model Paper presented at the Nurdic Hydrological Conference (Akureyri, Iceland - August 1996).
- Soko,K and Takahashi, S (1991), Characteristicss effect out winter precipitation and it glacier in the Nepal Himplays. Bulletin of Glacier Research 9, 9-16.

- Steinegger, U., Braan, L.N., Kappenberger, G., and Tortari G (1993): Assessment of annual anow accumulation over the past 10 years at high elevation in the Langtang region. Snow and glacter hydrology, International Association of Hydrological sciences Publication, 218, 155-165.
- Thornthwaite, C.W. and Mather, J.R. (1955), The water balance. In publication of elimatology, Vol.5 No.1:1-86.
- Ueno, K. ,Shiraiwa, T and Yamada, T. (1993). Precipitation environment in the Largrang valley, Nepal Himalayas. Snow and glacier hydrology. International Association of Hydrological sciences Publication, 218, 207-219.
- Yamada, T., Shinaiwa, T.,Iida, H., Kadota, T., Watanabe, O., Rana, B., Ageta, Y. and Fushimi,H. (1992): Fluctuations of the glaciers from the 1970s to 1989 in the

Journal of Hydrology and Meteorology, Vol. 8, No. 1



Evolving Water Resources Systems: Understanding, Predicting and Managing Water–Society Interactions

Editors

ATTILIO CASTELLARIN DICIM, Enuversity of Bilegra, Bologna, Indu

SERENA CEOLA DECAME University of Belogna, Belogna, bala

ELENA TOTH DRCHAE University of Belogna, Belogna, Judy

ALBERTO MONTANARI DECEM University of Belogue Bologue, Boly

Proceedings of ICWR53014 Boksgna, taly, Ame 2214

IAHS Publication 364 a heliotisteer of Prosecution and Invent

# Climate change scenarios and its impact on water resources of Langtang Khola Basin, Nepal

### TIRTHA RAJ ADHIKARI<sup>1</sup>, LOCHAN PRASAD DEVKOTA<sup>1</sup> & ARUN BHAKTA SHRESTHA<sup>2</sup>

1 Central Department of Hydrology and Meteorology, Tribhuvan University, Kathmandu, Nepal tirtha43@yshoo.com

2 International Centre for Integrated Mountain Development, Kathmandu, Nepal

Abstract General Circulation Models (GCMs) successfully simulate future climate variability and climate change on a global scale, however, poor spatial resolution constrains their application for impact studies at a regional or a local level. The dynamically downscaled precipitation and temperature data were used for the future climate scenarios prediction for the period 2000–2000s, under the Special Report on Emissions Scenarios (SRES) A2 and A1B scenarios. In addition, rating equation was developed from measured discharge and gauge (stage) height data. The generated precipitation and temperature data from downscale and rating equation was used to run the HBV-Light 3.0 conceptual rainfall-runoff model for the calibration and validation of the model, gauge height was taken in the reference period (1988–2009). In the HBV-Light 3.0, a GAP optimization approach was used to calibrate the observed streamflow. From the precipitation scenarios that SRES A2 and A1B emissions at Kyanging, an increase of precipitation during summer and spring and a decrease during winter and axhum sectors was shown. The model projected annual precipitation for the 2050s of both the A2 and A1B scenarios are 716.4 mm and 703.6 mm, respectively. Such precipitation projections indicate the future increase of precipitation in all seasons except the summer.

Key words water resources; Nepal; climate change

### INTRODUCTION

Climate and water studies play an important role in the protection of the environment. This study attempts to assess the downscaling of GCMs simulated gridded data to high resolution regional gridded or point data models: dynamical climate model, weather typing, transform function and scenario generation (<u>http://www.cics.uvic.ca/scenarios/index.cgi?Scenarios</u>). The Coupled Global Climate Model (CGCM3) of National Centres for Environmental Prediction (NCEP) predictors have been considered as the independent variables for multiple regression analysis for climate observation as a dependent variable. Finally, mean sea level pressure, surface vorticity, surface divergency, 500 hPa geo-potential heights and specific humidity at 500 hPa for temperature downscaling, and meridional velocity, surface zonal velocity and 850 hpa geopotential height for precipitation downscaling were selected as significant predictors. Finally, optimization of the model was completed by applying the ordinary least squares method. In the above analyses, observed and NCEP data sets have a year length of 365 days (366 in leap years). The historical meteorological daily observed climate data are used as a predictor and input in the statistical downscaling method.

### STUDY AREA

The Langtang River catchment (583.41 km<sup>2</sup>) is located approximately 100 km north of Kathmandu, Nepal. In this study, data from Syaprubesi hydrological station at latitude 280.09'30" and longitude 850.20'45", and Langtang Kyanging meteorological station at latitude 280.12'00" and longitude 850.34'00" are used. The elevation of the study area ranges from Syapra besi, 434 m.a.s.l. up to the peak of Langtang Lirung at 7234 m.a.s.l., with an average altitude of 4334 m.a.s.l. In total, 26% (153.14 km<sup>2</sup>) of the catchment is glacierized. The glacier tongues below 5200 m.a.s.l. is 32 km<sup>2</sup> long and are generally debris covered (Immerzeel *et al.* 2011). The main valley is divided by the Langtang Khola River and it is typically U-shaped. The Gandaki River system in central Nepal consists of the Kaligandaki Mustang and converges with the Trishuli at Deoghat in

Copyright @ 2014 IAHS Press

### Tirtha Raj Adhikari et al.

Chitwan, the river is then called the Narayani Langtang Khola and is one of the snow- and glacierfed rivers and is the main tributary of Narayani basin (Trishuli). The extreme daily simulated mean discharge at Syaprubasi hydrological station is 60.5 m<sup>3</sup>/s.

### METHODOLOGY

The daily climate data were collected from the Department of Hydrology and Meteorology (DHM), Government of Nepal. Meteorological data used in this study include daily precipitation, daily maximum temperature and daily minimum temperature of Kyanging Langtang snow and glacier hydrology station temperature. The products of scenarios generated by using CGCM3 temperature and precipitation data were used with the HBV (Hydrologiska Byrans Vattenbalansavdelning) ltpht 3.0 hydrological model for the calculation of future discharge from Langtang Khola catchment at Syaprubesi. Seibert (2005) describes the model as follows: daily discharge is simulated by HBV light 3.0 using daily rainfall, temperature and potential evaporation as input. In this study, seasons in Nepal are classified as: winter (DJF) December of the previous year to February; spring (MAM) March to May; summer (JJAS) June to September; and autumn (ON) October to November. Four applications of computer software programs are applied in this study: (1) SDSM for generating daily climate temperature and precipitation scenarios (SDSM 4.2), developed by Wilby and Dawson (2007) in the UK, is chosen for developing daily climate scenario study, (2) hqrating model (developed by the Department of Hydrology and Meteorology, Government of Nepal) to develop the rating curve, (3) ArcGIS 9.3 for glacier area delineation, and (4) HBV Light 3.0 for discharge modelling (Seibert 2005).

Continuous discharge measurement of a stream is very difficult and costly, but the continuous record of river stage can be easily obtained. Hence to compute the daily flow, there should be an adequate correlation between stage and discharge. Discharge ratings for gauging stations are usually determined empirically using periodic measurements of discharge and stage (Reddy 2005). The discharge measurements are made by current meter. Measured discharges are then plotted against concurrent stages on graph paper to define the rating curve. Hydrological data used in this study are: daily gauge (stage) height (1994–2010) and occasional discharge measurement data of Syaprubesi hydrological station (1979–2009). These unpublished discharge measurement data are available from the Department of Hydrology and Meteorology (DHM). On the basis of this discharge measurement and stage height data the rating equation (1) was developed in Syaprubesi hydrological station of Langtang Khola:

 $\overline{10}$ Gladier Area (Kim<sup>2</sup>) en. 50 -m 3J 20 10 0 4020-4520 4520-5020 5020-5520 5520-6020 6020-6520 6520-7020 7020-7520 7520 Glacier Area 7 7 0 3 21 62 53

Langtang Khola Basin

Fig. 2 Glacier Area in elevation wise.

 $Q = 0.328 \times (H + 2.022)^{3.378}$ 

In this study the watershed is divided into 13 elevation and one vegetation zone by using ArcGIS 9.3 for glacier area delineation. The delineated area histogram of Langtang Khola basin glacier area is shown in Fig. 2. The largest glacier area, 62 km<sup>2</sup>, occurs in the 5520 m elevation

(1)

zone and the lowest glacier area, 3 km<sup>2</sup>, is found in the elevation of 4520 m. HBV light 3.0 is applied on the time period from January 2002 to December 2004, with the discharge data recorded in Syaprubasi station. Firstly automatic Generatic Algorithm Package (GPA) optimization was applied and then manual calibration was done to refine the parameters by "trial and error". In addition to visual inspection of the simulated time series and the observed, several objective criteria were used to assess the best parameter set. Validation was done with the parameter sets from the GPA optimization for comparison. The model was validated for the Langtang Khola Syaprubasi from 2005 to 2009, with the same parameter sets of calibration. At Kyanging, observed daily temperature data are available from 1988 to 2009. Consequently, observed temperature and NCEP data from 1988 to 1995 were used for downscale calibration and data from 1996 to 2003 were used for its validation.

### Modelling calibration and validation

The seasonal and annual values of observed (OBS) and NCEP simulated temperature, including their percentage difference, are presented in Table 1: depicting the highest seasonal percentage of difference in maximum and minimum temperatures were -0.1°C and -1.0°C, respectively, in the calibration. Similarly, the annual percentage of different maximum temperature is 1.3°C and minimum temperature is 1.0°C in the validation. These percentage of difference indicate a degree of reliability of the SDSM temperature calibration and validation process at Langtang Kyanging shown in Table 2. Observed daily precipitation data were available from 1988 conwards. Hence, observed precipitation and NCEP predictor data from 1988 to 1995 were utilized for GCMS calibration and data from 1996 to 2003 were used for its validation. Seasonal and annual values of observed and NCEP simulated total precipitation and their difference are presented in Table 1. The precipitation for NCEP calibrated (NCEP\_Cal) scenarios of spring, summer and autumn are increased whereas it is decreased in winter, showing summer percentage of difference -15% (of observed summer total). But in the NCEP validation (NCEP\_Val) process Table 2, showing the summer percentage of difference 12.7% (of observed summer total). This explains relatively poor reliability of the SDSM precipitation calibration process, which could be due to altitudinal effect of the summer monsoon at Langtang Kyanging.

### Table 1 Calibration of observed data with CGCMB of NCEP data.

Maximum Temp (*C)				Minin	um Temp	(0)	Precipi	Precipitation (mm)			Discharge (m <sup>3</sup> /s)		
Season	OBS	NECP Cal	% of diff	OBS	NECP Cal	% of diff		NECP Cal	% of diff	OBS	NECP Cal	% of diff	
DJF	2.1	2.4	-0.3	-7.7	-6.7	-1.0	12.8	10.9	14.7	17.5	15.5	11.8	
MAM	6.6	6.8	-0.3	-2.4	-1.5	-0.9	29.9	31.2	-4.4	19.6	15.4	21.2	
JIAS	10.5	10.5	0.0	5.3	6.3	-1.0	101.3	116.6	-15.0	58.4	45.9	21.4	
ON	6.5	6.2	4.6	-2.6	-1.6	38.5	1.3	13.6	-946.2	27.4	23.5	14.3	
Annual	6.8	6.9	-0.1	-1.2	-0.2	-1.0	535.0	618.4	-15.6	33.4	26.9	19.5	

### Table 2 Validation of observed data with CGCMB of NCEP data.

Maximum Temp (*C)				Minin	nun Tenn	(0)	Precipitation (mm)			Discharge (m <sup>3</sup> /s)		
Season	OBS	NECP Val	% of diff	OBS	NECP Val	% of diff	OBS	NECP Val	% of diff	OBS	NECP Val	% of diff
DJF	3.7	2.5	1.2	-5.3	-6.6	1.3	8.1	11.1	-36.7	16.5	9.1	44.7
MAM	7.7	7.0	0.8	-0.1	-0.9	0.8	32.1	31.6	1.4	17.8	7.2	59.2
JJAS	12.0	10.5	1.5	7.4	6.4	1.0	130.3	113.8	12.7	49.3	42.0	14.8
ON	8.5	6.7	21.2	0.5	-0.5	200.0	15.6	12.5	19.9	23.8	20.9	12.2
Annal	8.3	7.0	1.3	1.2	0.2	1.0	673.0	608.5	9.6	28.9	21.8	24.6

### Discussion for future climate and discharge scenarios

GCMS-simulated seasonal and annual range of mean of 20 ensembles for temperature scenarios with A2 and A1B emission scenarios at Langtang Kyanging are shown in Table 3. In the maximum temperature of the model simulation feature the autumn temperature is warmer than winter, spring and summer. The Table shows that the model projects warmer days in every season of the entire 2050s for both emissions. The warming is higher in maximum than in minimum temperatures, indicating an increasing trend of future daily temperature range.

Similarly, GCMS-simulated seasonal and annual mean of temperature scenarios with SRES A2 and A1B emission scenarios at Langtang Kyanging are shown in Table 3. According to the Table, the model projects warmer days increased in every season up to the 2050s for both A2 and A1B scenarios. GCMS-simulated seasonal and annual mean for precipitation scenarios with SRES A2 and A1B emissions at Kyanging are shown in Table 3. Where, for both low and high emissions, the model generally projects an increase of precipitation during summer and spring, there is a decrease during winter and autumn seasons. Such precipitation projections indicate that there is sufficient to balance the deficit, indicating drier Langtang Kyanging due to the effects of enhanced greenhouse gas in the 2050s.

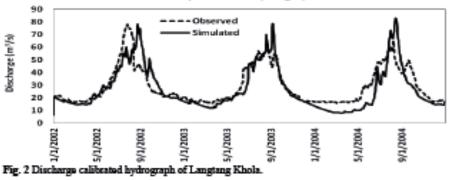
### Table 3 Temperature and Precipitation both A1B and A2 Scenario.

Tmax*					Tmin* A1B	•			Times A1B	****			Precipi	tation (m	m)****	
Sesson	Scenar	ño	A2 54	omario	Some	io-	A2 84	oinanto	Scena	io	A2 80	onario	AIB S	cenario	A2 So	mario
	2020	2050	2020	2050	2020	2050	2020	2050	2020	2050	2020	2050	2020	2050	2020	2050
DJF	1.0	1.5	1.1	1.3	-6.8	-6.0	-6.9	-6.1	-3.1	-2.3	-3.0	-2.5	10.8	10.1	7.4	6.9
MAM	7.1	7.1	73	7.1	-1.2	-0.4	-0.9	-0.1	33	4.0	3.7	4.4	28.6	31.9	28.7	31.3
JJAS	10.5	10.9	10.6	10.8	6.5	69	6.6	6.9	95	9.9	9.6	9.9	142.5	142.1	142.6	142.2
ON	7.6	7.9	7.6	8.0	1.2	1.8	1.2	2.1	4.2	4.8	4.3	5.0	11.9	11.0	9.6	10.0
Annual	6.8	7.1	6.9	7.1	0.4	1.0	0.4	1.1	3.9	4.5	4.1	4.6	711.2	716.4	697.2	703.6

\*Maximum temperature (°C), \*\*Minimum temperature (°C), \*\*\*Mean temperature (°C) and \*\*\*\*Precipitation (mm).

Table 4 Maximum and minimum discharge scenario.

Season.	Maximu A1B Sce	n Discharge nario	A2 Scans	nio		Minimum Discharge (m²/s) A1B Scenario A2 Scenario				
	20205	2050S	20205	2050S	20205	2050S	20205	2050S		
DJF	20.2	21.9	16.8	18.8	7.7	8.6	7.9	8.6		
MAM	35.5	34.2	21.0	21.2	3.7	4.1	3.9	43		
IIAS	55.9	56.4	58.5	57.0	24.9	23.1	25.6	24.7		
ON	27.4	29.0	39.9	43.3	16.3	16.9	16.5	16.9		
Annual	37.3	37.8	35.7	36.2	13.9	13.7	14.3	14.3		



Comparision of Hydrograph

The model is able to accurately simulate the daily discharge data at Syaprubasi hydrological station at the outlet of Langtang Khola (2002–2004). The observed and simulated hydrograph during the calibration period is shown in Fig 2. Downscale simulated results from temperature and precipitation in a daily scenario data were applied in HBV *light 3.0* for a hydrological model. The seasonal and annual range of mean of the 2020s and 2050s ensembles for discharge scenarios with A2 and A1B at Syaprubasi hydrological station are shown in Table 4. The table shows that the model A1B projects maximum discharge increased in every season, except in the spring seasons of the entire 2050s century for the emission. By the end of the 2020s, simulation projects an increase of discharge in winter, summer and autumn, but a decrease in spring by the maximum (minimum) discharge of 37.3 m<sup>3</sup>/s (13.9 m<sup>3</sup>/s). Similarly, by the end of the 2050s winter, spring and autumn will increase but in summer there will be a decrease of maximum (minimum) discharge of 37.8 m<sup>3</sup>/s (14.3 m<sup>3</sup>/s) and maximum (minimum) 36.2 m<sup>3</sup>/s (14.3 m<sup>3</sup>/s) for the A2 scenario. The overall scenario shows a decreasing discharge in Langtang Khola, which may be due to the decreasing glacier area, and as a result the glacier melt contribution is less.

### CONCLUSION

Performance of SDSM downscaling based on NCEP and GCMs predictors at Langtang, Kyanging are evaluated using statistical properties of daily climate data. It was found that the application of SDSM for statistical downscaling is suitable for developing daily climate scenarios. To demonstrate the procedure of developing scenarios, SDSM is applied, based on daily outputs of common climate variables from GCMs simulation, which has been widely used in the development of daily climate scenarios, and the results can be used in many areas of climate change impact studies. According to this study, the autumn temperature is much warmer compared to winter, spring and summer. The precipitation is increased for NCEP calibrated scenarios for spring, summer and autumn, whereas in winter it is decreased. The model generally projected an increase of precipitation during summer and spring, and a decrease during winter and autumn seasons. However, maximum projected discharge will increase for all seasons except for spring compared to a minimum projected discharge in summer.

Acknowledgments The author(s) would like to acknowledge the Data Access Integration (DAI, see http://quebec.ccsn.ca/DAI/) Team for providing the data and technical support. The DAI data download gateway is made possible through collaboration among the Global Environmental and Climate Change Centre (GEC3), the Adaptation and Impacts Research Division (AIRD) of Environment Canada, and the Drought Research Initiative (DRI). The Ouranos Consortium (in Quebec) also provides IT support to the DAI team. We show appreciation to the Department of Hydrology and Meteorology (DHM), Government of Nepal for providing necessary data for this study.

### REFERENCES

Immerzeel, W. W. et al. (2011) Hydrological response to climate change in a glacierized catchment in the Himalayas. Climatic Change DOI 10.1007/s10584-011-0143-4.

Reddy P. Jaya Rami (2005) A Text Book of Hydrology. Laxmi Publications 7/21, Ansari road, Daryaganj, New Delhi 110002.
Seibert, J. (2005) HBV light version 2, User's Manual, Uppsala University, Institute of Earth Sciences, Department of Hydrology, Uppsala, Sweden.

Wilby, R. L. and Dawson, C. W. (2007) Statistical Downscaling Model (SDSM) Version 4.2 user manual.